國 立 交 通 大 學

電信工程研究所

博 士 論 文

異質性無線網路之干擾管理技術

Interference Management for
Heterogeneous Wireless Networks

研 究 生： 蔡 昂 勳

指導教授： 王 蒞 君

中 華 民 國 一 百 零 一 年 六 月

異質性無線網路之干擾管理技術

Interference Management for Heterogeneous Wireless Networks

研究生：蔡昂勳　　Student: Ang-Hsun Tsai

指導教授：王蒞君　博士　　Advisor: Dr. Li-Chun Wang

國立交通大學

電信工程研究所

博士論文

A Dissertation
Submitted to Institute of Communications Engineering
College of Electrical and Computer Engineering
National Chiao Tung University
in Partial Fulfillment of the Requirements
for the Degree of Doctor of Philosophy
in
Communication Engineering
Hsinchu, Taiwan

2012 年 6 月

異質性無線網路之干擾管理技術

研究生：蔡昂勳　　指導教授：王蒞君　博士

國立交通大學

電信工程研究所

摘要

本論文主要在探討異質無線網路之干擾管理技術，包括正交分頻多重接取之毫微微細胞網路、機器型態通訊毫微微細胞網路以及裝置間通訊毫微微細胞網路。此外，本論文也提出了相對應的解決方案，用以確保對用戶的服務品質。本論文之主要研究課題如下所述。

在第一個部份中，我們在正交分頻多重接取之毫微微細胞系統下，提出了一個位置知曉機制，同時結合一個低成本、四區段的切換式波束方向性天線，以提高頻譜效率。這個切換式波束方向性天線安裝在毫微微細胞基地台上，用以減輕來自毫微微細胞的干擾。而且，我們提出利用調整使用的子載波數量來控制毫微微細胞與巨細胞之間的干擾，以確保所有用戶的鏈結可靠度。隨著知道戶外用戶的位置資訊，並藉著調整每個毫微微細胞所使用的正交分頻多重接取子載波數量，我們提出的位置知曉之毫微微細胞結合四區段的切換式波束方向性天線可以有效地避免毫微微細胞與巨細胞之間的干擾。此外，我們提供了一個設計原則，用以決定合適的頻譜分配方案以及毫微微細胞的接取方式。

在第二個部分中，我們在正交分頻多重接取之多用戶毫微微細胞系統下，提出一個低複雜度且分散式的穩定子通道分配演算法，使得在系統容量、用戶間公平性以及服務延遲等系統效能之間可以取得一個最佳的權衡。我們建議毫微微細胞可以結合低成本可重置的切換式多波束方向性天線，更進一步地降低干擾去改善系統容量。同時，我們發展一個天線輻射方位暨子通道分配法則，讓系統容量的最佳化、用戶間公平性之確保以及服務延遲效能之改善得以實現。以系統容量，用戶間公平性以及延遲效能為目標，相較於現有的方案，包括（1）通道導向的子通道分配方案、（2）使用者導向的子通道分配方案、（3）比例式公平的子通道分配方案、（4）指數法則的子通道分配方案、以及

（5）排隊等候基準之指數法則的子通道分配方案，我們提出的穩定子通道分配結合切換式多波束方向性天線方案會是一個最佳的選擇。

在第三個部分中，我們在機器型態通訊毫微微細胞系統下，提出分群控時機制以改善因大量機器型態通訊裝置同時上傳資訊所造成的網路壅塞以及訊息延遲等問題。該分群控時機制將所有機器型態通訊裝置分成多個小群組，並指定每個群組一段可以上傳資訊的允傳時段。透過分群控時機制，就可以將大量機器型態通訊裝置所造成的巨大流量隨著時間而緩和其峰值流量。於是，該機制有能力同時減輕無線接取網路及核心網路過載的發生。然而，如果過度地分群會使得群組數量大量增加，於是每個群組在等候其允傳時段的時間就會過長，導致訊息傳遞所需要的時間大幅地增加，造成無法容忍的訊息延遲情況發生。因此，我們分析了機器型態通訊毫微微細胞系統下的網路過載機率以及訊息延遲的關係，並探討如何分群控時以達到同時解決網路壅塞並確保訊息延遲效能的最佳權衡。

在最後一個部分中，我們在裝置間通訊毫微微細胞系統下，提出了一個智慧型資源管理機制以改善系統容量與服務品質。藉由巨細胞基地台與毫微微細胞基地台所廣播之特定訊息，每對裝置間通訊用戶能夠有效地及自主地選擇合適的資源並調整適當的傳輸功率，以減輕複雜的三階層式之干擾。同時，我們建議透過調整正交分頻多重接取之毫微微細胞系統的資源使用率，以控制毫微微細胞系統對巨細胞系統及裝置間通訊系統的干擾，進一步保護所有用戶之鏈結可靠度。我們提供了一個設計原則，用以決定進入裝置間通訊模式之適合的距離，並選擇最佳的毫微微細胞系統資源使用率，以改善系統容量並確保鏈結可靠度。

總而言之，本論文之主要貢獻在於解決異質無線網路中所可能造成複雜的干擾問題以及網路壅塞情形。而且，本論文所提出的解決方案能顯著地改善系統容量及網路過載情況發生，並確保鏈結可靠度及延遲效能等服務品質。

Interference Management for Heterogeneous Wireless Networks

A Dissertation

Presented to

The Academic Faculty

By

Ang-Hsun Tsai

In Partial Fulfillment

of the Requirements for the Degree of

Doctor of Philosophy in Communication Engineering

Institute of Communications Engineering

College of Electrical and Computer Engineering

National Chiao Tung University

June, 2012

Interference Management for

Heterogeneous Wireless Networks

Student: Ang-Hsun Tsai Advisor: Dr. Li-Chun Wang

Institute of Communications Engineering
National Chiao Tung University

Abstract

In this dissertation, we investigate interference management techniques in heterogeneous wireless networks, including orthogonal frequency-division multiple access (OFDMA)-based femtocell networks, machine type communications (MTC) femtocell networks, and device-to-device (D2D) femtocell networks.

In the first part, we propose a location-aware mechanism combined with a low-cost four-sector switched-beam directional antenna to enhance the spectrum efficiency of OFDMA femtocell systems. The switched-beam directional antenna is installed for femtocell base stations to mitigate the interference from femtocells. Moreover, the subcarrier number adjustment method is developed to control the interference among femtocells and macrocells, and ensure all users' link reliability. With the knowledge of the locations of outdoor users, the proposed four-sector switched-beam antenna in a femtocell can effectively avoid the interference among femtocells and macrocells by adjusting the number of OFDMA subcarriers used at each femtocell. Furthermore, we provide a design principle to decide the suitable spectrum allocation scheme and access method for femtocells.

In the second part, we propose a low-complexity distributed stable subchannel allocation algorithm to improve the tradeoff of capacity, users' fairness, and head

of line (HOL) delay for OFDMA-based multi-user femtocell systems. The stable subchannel allocation scheme can optimize the capacity by repeatedly rearranging the subchannel allocation, and guarantee the fairness and delay performance by limiting the maximum allowable number of subchannels for a user. In addition, we suggest applying the low-cost reconfigurable switched multi-beam directional antennas on femtocells to further reduce the two-tier interference and improve the system capacity. Furthermore, we develop a joint antenna pattern selection and subchannel allocation method to optimize the system capacity, guaranteeing the fairness among users, and improving the HOL delay. Compared to the existing method (i.e., the channel-oriented subchannel allocation scheme, user-oriented subchannel allocation scheme, proportional fair subchannel allocation scheme, exponential rule subchannel allocation scheme, and queue-based exponential rule subchannel allocation scheme), the proposed stable subchannel allocation scheme with the switched multi-beam antenna is the optimal option to achieve the highest femtocell capacity, while guaranteeing the fairness and HOL delay.

In the third part, we propose the group-based time control method to improve the network congestion and message delay caused by the massive concurrent data transmission from MTC devices in femtocell systems. By dividing the MTC devices into several groups and dedicating each group with a granted time interval for access, the heavy traffic load of massive MTC devices can be spread over the time to alleviate the traffic peak, which mitigates both the radio access network (RAN) and the core network (CN) overloads simultaneously. However, excessively dividing the groups may incur the intolerable message delay because of the immoderate increase on the cycle time. Accordingly, we analyze the overload probability and message delay of the MTC femtocell system to achieve the optimum tradeoff.

In the final part, we propose the intelligent resource management mechanism to enhance the system throughput and link reliability for D2D femtocell systems. Based on the specific information broadcast by the macrocell and femtocell base stations, the D2D pairs can jointly select the suitable resource blocks and adjust the appropriate power to alleviate the complicated three-tier interference in an effective

manner. In addition to joint resource block selection and power adjustment for D2D communications, we suggest adjusting the utility rate of resource blocks for the OFDMA femtocells to guarantee the link reliability of all users. The design principle provided in this part can determine the suitable D2D distance to enter the D2D mode, and select the optimal resource utility rate of femtocells to improve the system throughput subject to the link reliability requirement.

In summary, the main contribution of this dissertation is to solve the complicated issues of interference and network congestion in the heterogeneous wireless networks. The proposed solutions significantly improve the system capacity and the network overload, while guaranteeing the quality of services.

Acknowledgements

First of all, I would like to express my deeply gratitude to my advisor, Prof. Li-Chun Wang. Not only the important insights to research problems, encouragement, and support, he also showed me a way of being optimistic to face difficulties. Without his advice, guidance, comments, and all that, this work could not have been done. He indeed opened a door to the future for me.

Special thanks to my mates of Mobile Communications and Cloud Computing Laboratory in National Chiao Tung University (NCTU), Taiwan. They gave me kindly help and suggestions in my study. Drs. Jane-Hwa Huang, Wei-Cheng Liu, Meng-Lin Ku, and I-Cheng Shen gave me many valuable suggestions and ideas in my research. My dear mates, Chung-Wei Wang, Chu-Jung Yeh, Hsien-Wen Chang, Wai-Chi Li, Chiao Lee, Chien-Cheng Tien, Ssu-Han Lu, Tsung-Chan Hsieh, Yen-Ming Chen, Gen-Hen Liu, Chen-Hsiao Chou, Wen-Pin Lai, Yu-Jung Liu, Tsung-Ting Chiang, Kai-Ping Chang, Rebaca, Shu-Hau Yang and Jr-Ling Jang, always encouraged me when I felt frustrated. I was so lucky to have all these lab mates.

I also want to express my sincere gratitude to my friends, Yu-Hsien (Shyan) Lu, Chin-Fu (Roger) Shih, Kuo-Fu Chiu, Chia-Chin (Albert) Chang, Yu-Cheng Chang and Zi-Yang Yang. They gave their time and assistance in helping me work out my problems during the difficult course of the dissertation.

I would like to acknowledge and extend my heartfelt gratitude to Master Der-Jing Shih and Master Der-Shin Shih in Shian-Feng Temple, Nantou, Taiwan. They always warmly back me up from their deeply inside mind. Most especially to my deceased Father, Fu-Yu Tsai, and my Mother, Jing-Yu Hsu, words alone can not express what I owe them for their encouragement. Their patient and unselfish love

enabled me to complete this dissertation. In addition, I am grateful to my father-in-law, Shu-Chi Ho, and my mother-in-law, A-Chie Ho Chen, for their kindness.

Finally, my thanks would go to my beloved wife, Shu-Hui Ho, and my dear sons, Yi-An (Ryan) Tsai and Fong-Chuan (Hank) Tsai, for their loving considerations and great confidence in me all through these years. I hope that my achievement can be an example to my sons.

Ang-Hsun Tsai

NCTU, Taiwan
June 2012

Contents

List of Tables

List of Figures

Chapter 1

Introduction

Recently, the traffic demand in mobile communications rapidly increase because of the widespread use of intelligent terminals, such as tablet personal computers and smart phones. In the predicament of data explosion, operators have to extensively deploy macrocell base stations to supply sufficient data transmission rate and improve the quality of service for customers' desires. However, the dense deployment of the macrocell base stations requires a lot of space and money for the power consumption and maintenance cost. Alternately, the heterogeneous wireless network technologies, such as femtocells, machine type communications (MTC), and device-to-device (D2D) communications, can not only provide reliable data service for customers, but also significantly improve the system capacity in a cost-effective way for operators.

Femtocells, which are low power and low cost, can improve system capacity and indoor coverage [1–4]. As shown in Fig. 1.1, femtocells are connected to the network center through the broadband wirelines inside the customers' homes. Unlike base stations in conventional cellular systems, femtocells require very low transmission power due to the short transmission distance. From the operator's viewpoint, deploying femtocells can significantly improve the system capacity because the same spectrum can be repeatedly used by a huge number of other femtocells. In addition, femtocells can offload the traffic of the outdoor macrocell users toward the indoor

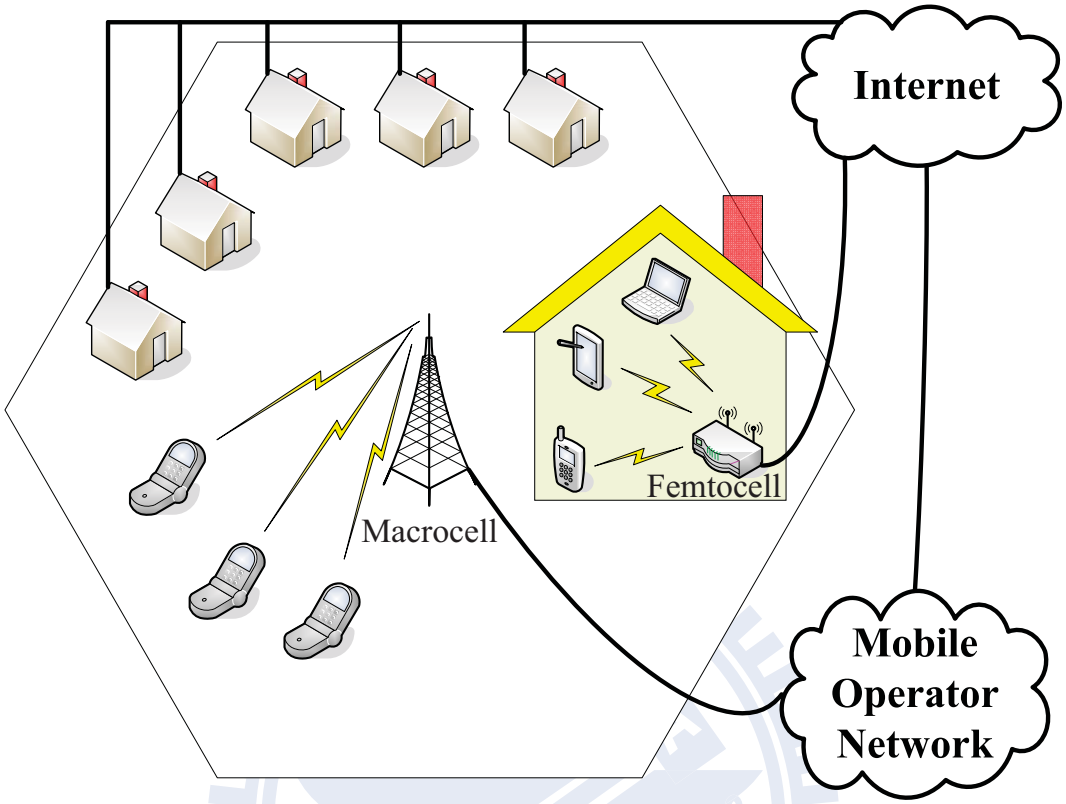

Figure 1.1: The concept of femtocells.

femtocell base station (fBS). From the customers' perspective, the fBS is much closer than the outdoor macrocell base station, which improves the indoor signal quality.

Machine-type communications (MTC), or machine-to-machine (M2M) communications, is an emerging technology that permits devices to communicate with MTC servers or with each other without human intervention or interaction [5], as shown in Fig. 1.2. It was said that over 50 billion machines are expected to communicate at the year 2020 while there are total 6 billion people in the world [6]. Some use cases such as metering, road security, and consumer electronic and devices are considered in the Third Generation Partnership Project (3GPP) [7]. Moreover, some features of MTC are categorized by 3GPP [5], including low mobility, time controlled, small data transmissions, group based MTC features, etc. In the future, the MTC devices will be more and more popular and be installed extensively.

Device-to-device (D2D) communications is the proximity communications [8]

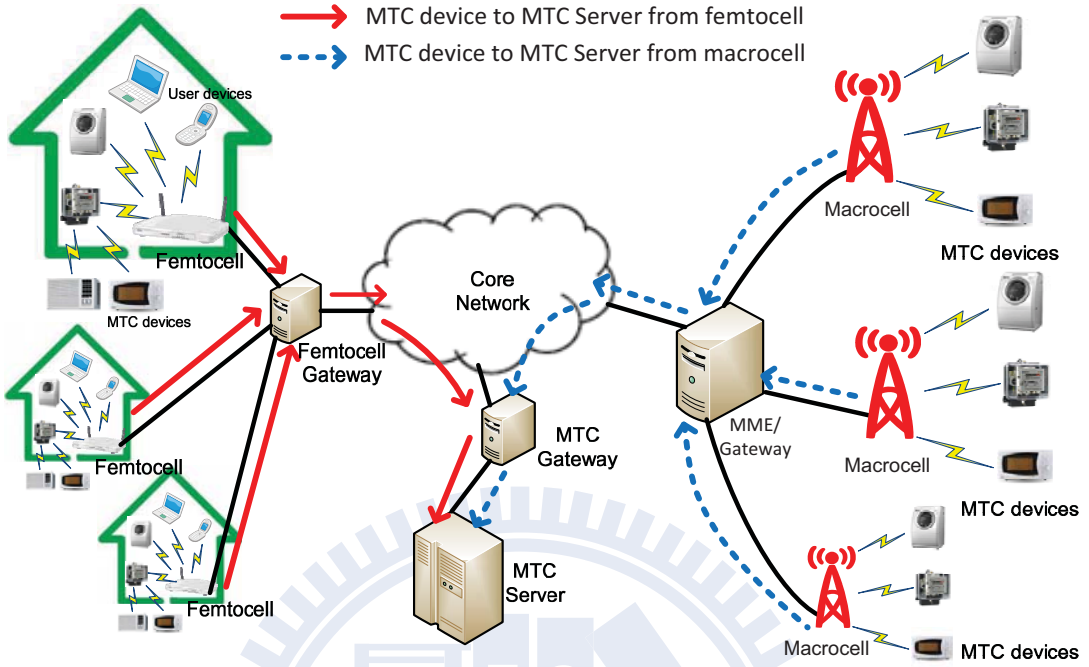

Figure 1.2: The concept of machine-type communications (MTC) femtocell networks.

which would enable the direct communications between proximate devices using the licensed band, as shown in Fig. 1.3. With the short distance between the proximate devices, D2D pairs need only very low transmission power to reliable communication. Because the same resource is reused by D2D pairs, D2D communications can enhance the spectrum efficiency. In addition, the device can directly communicate with the others without the assistance of the macrocells, which can offload the traffic from macrocell systems. Therefore, the D2D communications can offload the macrocell, improve the spectrum efficiency, and benefit both mobile users and operators.

In this dissertation, we mainly focus the impacts of the heterogeneous wireless network technologies on the system capacity and service quality.

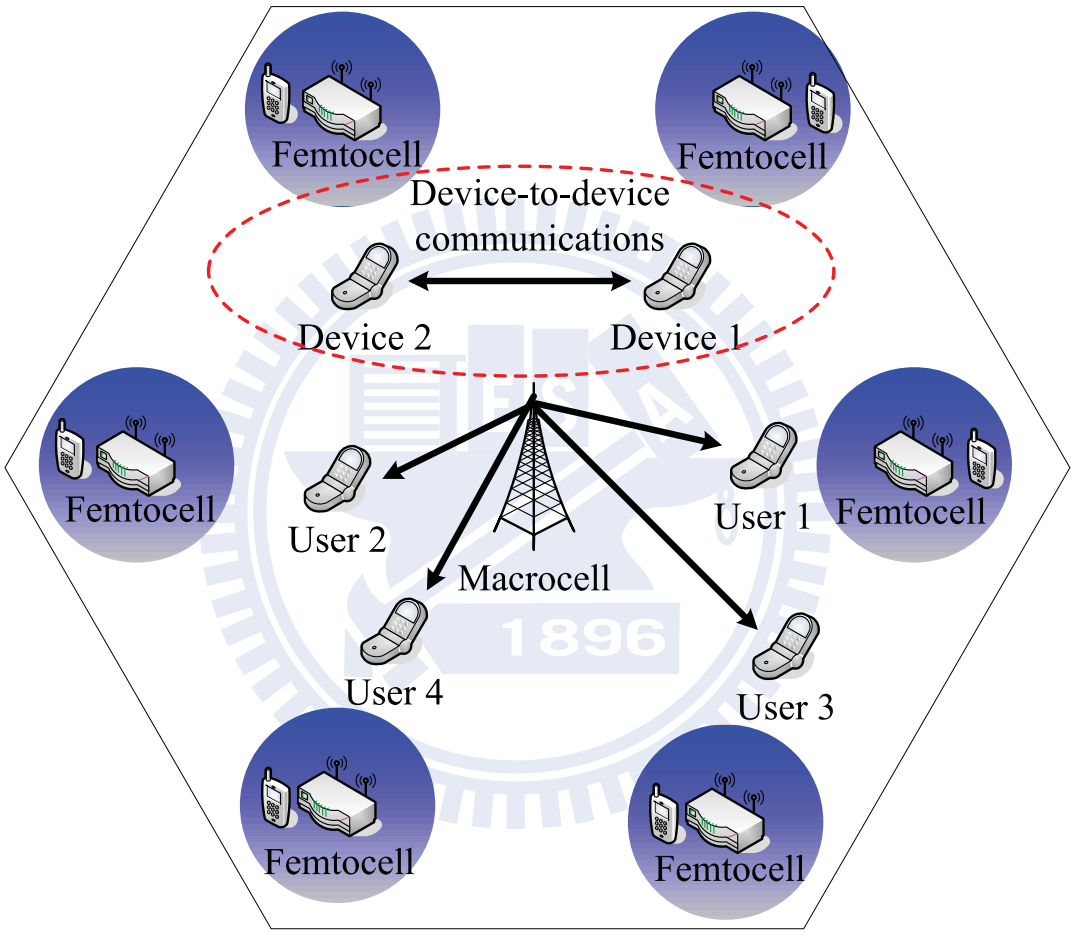

Figure 1.3: The concept of device-to-device (D2D) communications femtocell networks.

1.1 Challenges

Although the heterogeneous wireless network technologies benefit operators and customers, there are some challenges, such as interference, congestion, etc., existing in the heterogeneous wireless networks. In this section, we will briefly describe the challenges for the heterogeneous wireless networks (i.e., femtocell, MTC, and D2D).

1.1.1 Femtocells

The key challenge in improving system capacity for femtocells is reducing the strong two-tier interference [2–4, 9]. As shown in Fig. 1.4, when femtocells are densely deployed, the femtocell user suffers the femto-to-femto and macro-to-femto interference, while the macrocell user are affected by the femto-to-macro and macro-to-macro interference. Meanwhile, the macrocell users also experience the interference from the femtocells and macrocells as well. The severe two-tier interference significantly degrades the system capacity because the subcarriers available for the femtocells are reduced. Therefore, efficiently managing the two-tier interference can improve the system capacity.

In general, interference management and resource allocation are often jointly addressed in the orthogonal frequency-division multiple access (OFDMA)-based femtocell system with multiuser. Adaptively allocate subchannels to suitable users can efficiently control the interference between macrocells and femtocells, thereby improve the system throughput. Because of the channel variations, the greater the multi-user diversity, the higher the system throughput. Nevertheless, in addition to system throughput, the fairness and service delay are two additional important issues for the system. Basically, a user is desirable to be treated as fairly as other users in terms of receiving service, and to experience the delay-sensitive services without any lag time. Hence, the subchannel allocation scheme should simultaneously consider the achieved throughput, fairness among users, and delay performance for the OFDMA-based multiuser femtocell system.

Generally, there are traditional channel-oriented and user-oriented subchannel

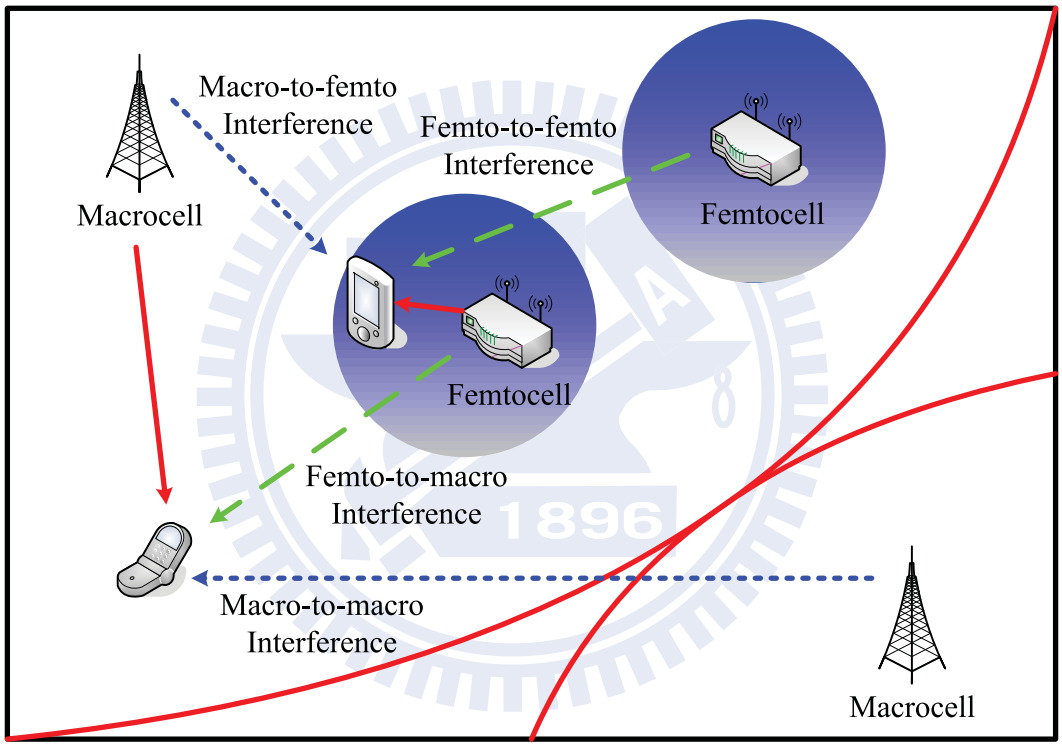

Figure 1.4: Two-tier interference in the femtocell network.

allocation schemes [10]. The channel-oriented subchannel allocation scheme is from the subchannel's viewpoint to allocate the user which can achieve the best throughput for the subchannel. However, this scheme may be unfair for users, and the users with poor link gain may have the long service delay. On the contrary, the user-oriented subchannel allocation scheme is from the user side to in turn select the subchannel with higher link gain, and therefore the fairness and the service delay can be ensured. Nevertheless, the selection sequence for users significantly affects the throughput because the subchannel selected by the preceding user can not be reassigned to another user, even if the overall throughput may be improved after rearrangement. Therefore, the user-oriented subchannel allocation scheme sacrifices the overall throughput to achieve better throughput fairness and delay performance. Both the channel-oriented and user-oriented subchannel allocation schemes are unstable assignment for users and subchannels.

The subchannel assignment problem is similar to the college admissions problem. In [11], the authors proved that the college admissions can achieve a stable and optimal assignment by using the deferred acceptance algorithm [12]. Therefore, we apply the deferred acceptance algorithm to the subchannel assignment. A desirable subchannel assignment should simultaneously takes the throughput, fairness, and service delay into account, and achieve the tradeoff among these elements. We consider that an assignment is stable if the throughput for an arbitrary user pair can not be improved after the exchange of subchannel allocations, under the fairness and delay requirement. Therefore, we propose a stable subchannel allocation scheme to achieve the tradeoff among the throughput, fairness, and head of line (HOL) delay. In the stable subchannel allocation scheme, the overall throughput can be improved by *repeatedly* rearranging the channel assignment of users, while the fairness and HOL delay can be guaranteed by limiting the maximum allowable number of subchannels used by a user. Consequently, the goals of throughput improvement, fairness and HOL delay performance can be fulfilled by using the developed stable subchannel allocation method.

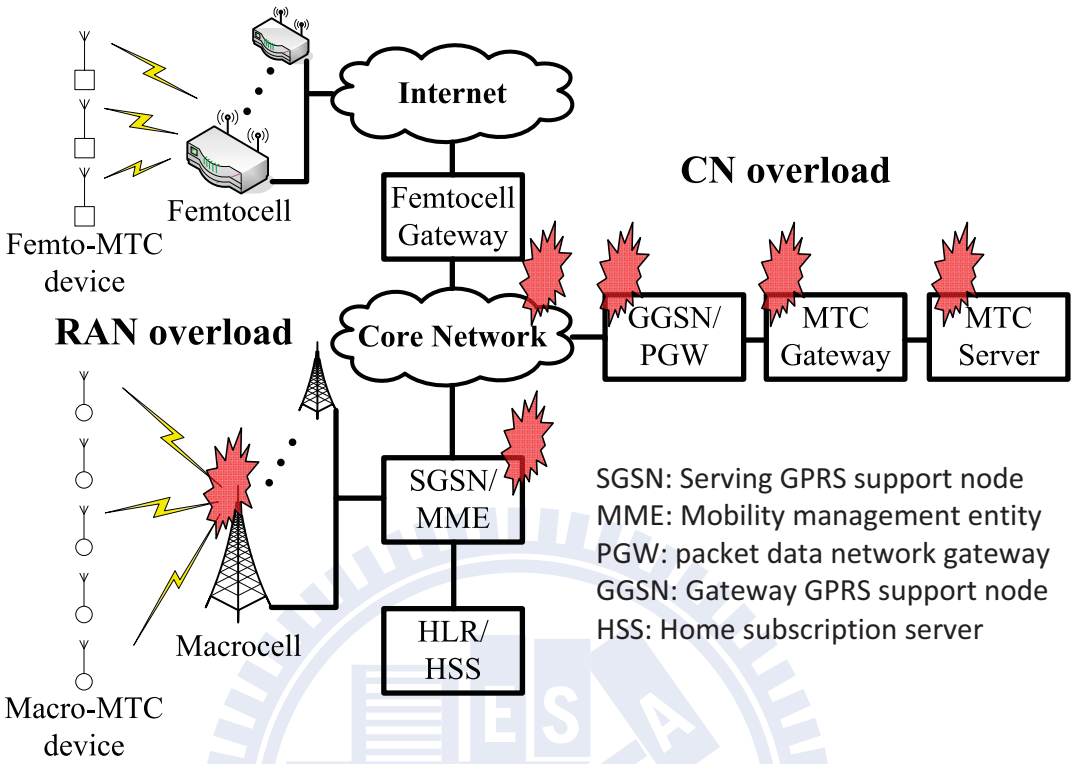

Figure 1.5: Radio access network (RAN) congestion and core network (CN) congestion.

1.1.2 Machine type communications (MTC)

The network congestion may take place because of massive concurrent data transmission from MTC devices in the MTC femtocell network, as shown in Fig. 1.5. Generally, there are radio access network (RAN) and core network (CN) congestions [5, 13] in the MTC network. The RAN congestion usually occurs in a specific cell coverage when a lot of MTC devices concurrently access the same base station. When a huge number of MTC devices transmit the message from a mass of base stations to a single MTC server, the CN congestion may happen. Nevertheless, the serious CN congestion may result in intolerable delays, packet loss, and service unavailability.

Femtocell can be a key to the success of the MTC network. Femtocells can improve system capacity and indoor coverage with low power and low cost, and will be

deployed extensively in the future [2,4]. Unlike base stations in conventional cellular systems, femtocells connect to the network center through the broadband wire-lines inside the customers' homes. Due to short transmission distance, femtocells require very low transmission power, and can extend battery life of MTC devices. In addition, femtocells can off-load the traffic from macrocell and ease the RAN congestion problem if MTC traffics are shared among the femtocell base stations. Nevertheless, there will be CN overload problems even if RAN congestion situation is eased. The CN congestion will get more serious because huge MTC messages pass radio access and are pumped into the core network for numbers of base stations.

To guarantee that MTC devices can reliably send their messages to the MTC server, the CN overload is a real challenge. The best way to solve the congestion problem may be to expand the capacity of the CN, so as to support more traffic load. However, the cost for capacity expansion may be too high, and the network planner may not know how much the additional system capacity should be expand. Another cost-effective way is to appropriately control the traffic load into the CN, such as overload control. If the overload can be effectively controlled by the MTC server, not only the CN congestion can be improved, but also the messages from MTC devices can be reliably transferred to the MTC server.

1.1.3 Device-to-device (D2D) communications

The complicated three-tier interference is the key issue in the heterogeneous D2D femtocell networks, as shown in Fig. 6.1. For both the uplink and downlink phases, the received device suffers the macro-to-device, femto-to-device, and device-to-device interference, while the transmitted device interferes with the macrocell users, femtocell users and the other devices. The system capacity and service quality may decline because of the strong three-tier interference. Accordingly, intelligently managing the three-tier interference is the crucial necessity of the success of D2D communications.

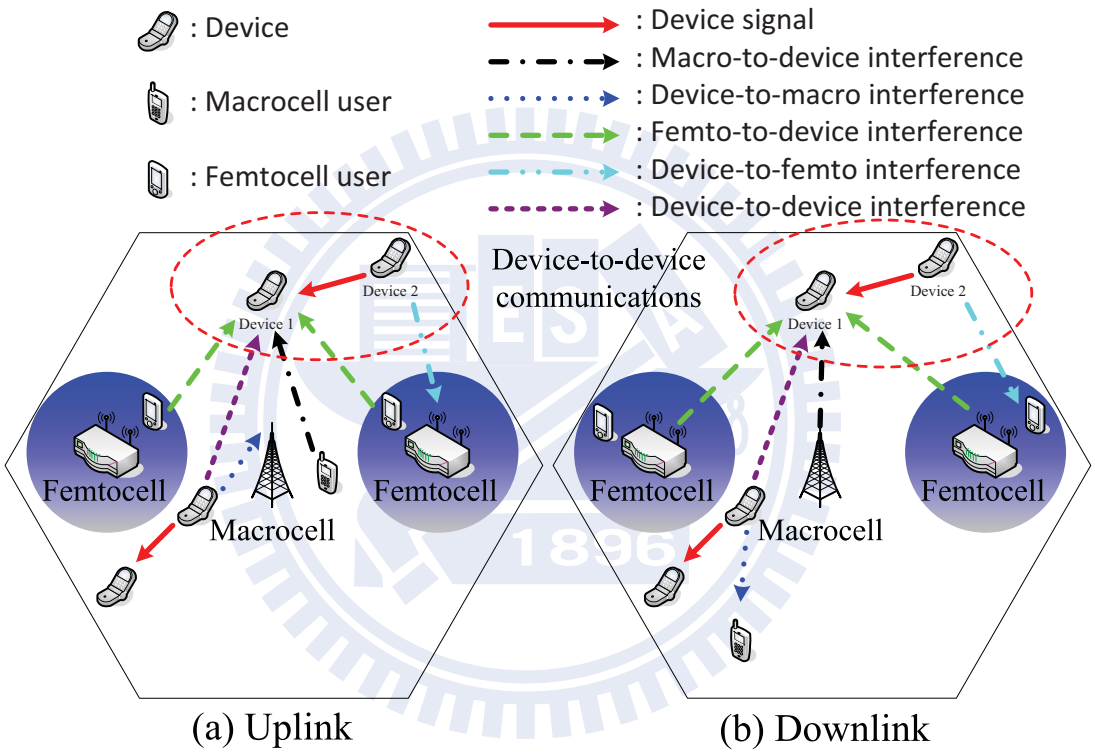

Figure 1.6: Three-tier interference in the Macro/Femto/D2D heterogeneous network.

1.2 Problems and Solutions

In this section, we will briefly describe our problem formulations and the corresponding solutions, including the capacity evaluation and enhancement in the OFDMA femtocell network, overload control in the MTC femtocell networks, and intelligent resource management in the D2D femtocell networks.

1.2.1 Capacity Evaluation for OFDMA Femtocells by Location Awareness and Directional Antennas

In this part, we propose a location-aware mechanism combined with a low-cost four-sector switched-beam directional antenna to enhance the spectrum efficiency of the OFDMA-based femtocell systems. The considered location-awareness capability is specified in the current IEEE 802.16m WiMAX standard, but has not been applied to avoid the interference between indoor femtocells and outdoor macrocells. With the knowledge of the locations of outdoor users, the proposed four-sector switched-beam antenna in a femtocell can effectively avoid the interference among femtocells and macrocells by adjusting the number of OFDMA subcarriers used at each femtocell. Numerical results show that the proposed approach can significantly improve spectrum efficiency compared to the existing methods.

1.2.2 Subchannel Allocation for Multi-Beam OFDMA Femtocells

In this part, we propose a low-complexity distributed stable subchannel allocation algorithm to improve the throughput, fairness, and head of line (HOL) delay for the orthogonal frequency-division multiple access (OFDMA)-based femtocell systems. By repeatedly rearranging the subchannel allocation, the proposed stable subchannel allocation scheme can achieve a better tradeoff among the throughput, fairness, and HOL delay performance. We combine the subchannel allocation with a low-cost reconfigurable switched multi-beam directional antenna to further improve

the throughput. We compare our stable subchannel allocation scheme with the existing methods, including the channel-oriented, user-oriented, proportional fair, exponential rule, and queue-based exponential rule subchannel allocation methods in terms of throughput, fairness index and HOL delay performance. Numerical results show that the proposed stable subchannel allocation scheme with the switched multi-beam antenna is the optimal option to achieve the better femtocell throughput while guarantee the fairness and HOL delay performance.

1.2.3 Overload Control for Machine Type Communications (MTC) Femtocell Networks

In this part, we analyze the propose group-based time control mechanism to improve the network overload and delay performance in the femtocell-based machine type communications (MTC) networks. The MTC network may be congested if numerous MTC devices concurrently deliver messages to the MTC server. Femtocells can solve the radio access network (RAN) congestion, however the core network (CN) congestion becomes more difficult to handle. The proposed group-based time control method can spread the traffic load of MTC devices over the time, and thereby mitigate the RAN overload and CN overload simultaneously. Moreover, with the developed adaptive joint access probability adjustment and group rearrangement method, the network can rapidly repeatedly rearrange the suitable group size for the MTC devices to mitigate the CN overload. Numerical results show that the proposed approach can significantly improve the network congestion and message delay compared to the existing methods.

1.2.4 Intelligent Resource Management for Device-to-Device (D2D) Femtocell Networks

Device-to-device (D2D) communications and femtocell systems are the key technology in the 4G LTE-A. Both D2D and femtocell systems can offload the traffic from macrocell systems, improve the spectrum efficiency, and benefit both mobile users

and operators. However, the complicated three-tier interference (i.e., macro-to-device/device-to-macro, femto-to-device/device-to-femto, and device-to-device interference) is the challenging issue in the heterogeneous macro/femto/D2D networks. In this paper, we propose a network-assisted device-controlled method to intelligently manage the devices' resource in the D2D femtocell network. Based on the specific information broadcast by macrocell and the femtocell base stations, the D2D pairs can effectively and autonomously jointly select the suitable resource blocks and adjust the power to guarantee the signal quality of all users. Simulation results show that the proposed method can simultaneously improve the system throughput and service quality.

1.3 Dissertation Outlines

This dissertation consists of three themes as shown in Fig. 1.7. The first part including Chapters 3 and 4 considers the location awareness capability, directional antenna, and subchannel allocation to manage the two-tier interference in the OFDMA femtocell network. In the second part, i.e. Chapter 5, we investigate the network congestion issue when the MTC system is consider in the femtocell network . Chapter 6 is the final part which is mainly to develop a intelligent resource management scheme for the D2D femtocell network with the complicated three-tier interference.

The remaining chapters of this dissertation are organized as follows. Chapter 2 introduces the background and literature survey of this dissertation. Chapter 3 evaluates the system capacity and link reliability for the OFDMA femtocells by the location awareness and directional antennas. The capacity enhancement for the multi-beam OFDMA femtocells by various subchannel allocation methods is investigated in Chapter 4. In Chapter 5, a congestion control mechanism for the MTC femtocell network is developed to improve the network overload and delay performance. Chapter 6 is the final part to investigate a efficient resource management scheme for the D2D femtocell network. Finally, the concluding remarks and some suggestions for future research topics are given in Chapter 7.

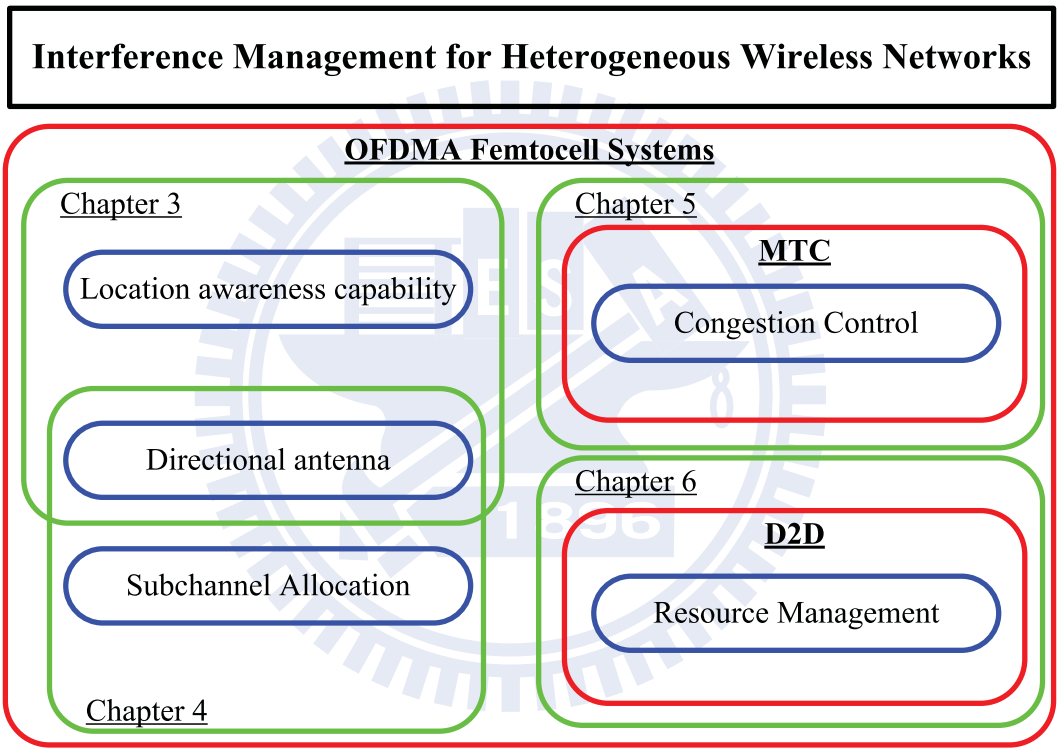

Figure 1.7: Outline of this dissertation.

Chapter 2

Background and Literature Survey

In this chapter, we survey the related works for the four considered issues in this dissertation, including the capacity evaluation of the OFDMA femtocells, subchannel allocation schemes of the multi-beam OFDMA femtocells, congestion control of the MTC networks, and the resource management of the D2D networks.

2.1 Capacity Evaluation for OFDMA Femtocells by Location Awareness and Directional Antennas

In the literature, most studies on femtocells considered the omnidirectional femtocells and can be categorized into three kinds: power control, access method, and spectrum allocation.

1. In [1, 14], the power control method for femtocells with omnidirectional antenna were discussed. In [1] an autoconfiguration method of transmit power was proposed for the code division multiple access (CDMA)-based femtocells with the shared spectrum allocation scheme. In [14], the authors proposed a distributed femtocell uplink power control to achieve higher SINR performance on the condition that the link quality of the macrocell users can be

guaranteed.

2. Access methods for femtocells were discussed in [3, 15, 16]. In [3], the authors compared the closed subscriber group (CSG) and open subscriber group (OSG) femtocell systems, where the CSG femtocell base stations only serve the authorized users, and the OSG femtocell base stations can serve any users. Because the OSG users can select the base station with best signal quality among the femtocells and macrocells, the OSG scheme has better coverage than the CSG scheme. In [15], the authors studied different access methods for femtocells and proposed a hybrid access approach to improve the average throughput. In [16], the authors investigated the effects of access methods in the uplink femtocell systems. They suggested that the access method depend on the cellular user density in the TDMA/OFDMA network, and showed that open access is the optimal choice in the CDMA network.

3. In [17–22], spectrum allocation schemes for femtocells with omnidirectional antenna were discussed. In [17], the channel selection issues in the WiMAX-based femtocell systems was investigated by taking into account of the femto-to-femto interference. Paper [19] developed the distributed channel selection schemes for femtocells to improve the capacity by adjusting the number of used subcarriers. In [18], the authors analyzed the optimal fraction of spectrum allocated to macrocell and femtocell systems, in which the macrocell and femtocell systems are assigned with different frequency bands. In [20], the authors designed an on-demand two-tier resource allocation mechanism to improve the system throughput. In [21], the authors proposed the cognitive radio resource management scheme for femtocell networks to achieve the higher capacity with ensuring the delay requirement. Afterward, they further proposed the strategic game based radio resource management scheme for femtocells to alleviate the severe femto-to-femto interference as well as improve the system capacity with the delay guarantee [22].

Fewer papers have examined the femtocell systems with directional antennas, such as [23–27]. Intuitively, directional antennas can increase signal strength due to higher antenna gain and decrease the interference due to the narrow-beam patterns. In [23], the uplink capacity in CDMA-based femtocell networks using sector antennas and time-hopping techniques were analyzed. The multiple antennas in CDMA-based femtocell systems were applied to reduce the unnecessary handover and enhance the indoor coverage [24]. However, the main focus of [23,24] was on the shared spectrum allocation scheme in the CDMA-based femtocell systems.

The receive antenna diversity was applied to mitigate the uplink co-channel interference and improve the signal reception quality for femtocells [25,26]. In [27], the authors proposed power control method using switched parasitic array antenna in OFDMA-based femtocell networks to avoid the co-channel interference to macrocell users. Nevertheless, the works of [25–27] aimed to alleviate the co-channel interference by the antenna diversity. Three of them did not investigate the impacts of the location of outdoor users and they also did not apply the partial usage of femtocell subcarriers approach to reduce the femto-to-macro interference. In our previous work [28], the capacity and link reliability of low-cost E-plane horns based reconfigurable directional antenna for the OFDMA-based femtocell systems were investigated. The major research in [28] was to investigate the impact of directional antenna on the link reliability and capacity of indoor users. However, the impact of femtocells on the outdoor users was not considered in [28].

2.2 Subchannel Allocation for Multi-beam OFDMA Femtocells

In the literature, most femtocell papers investigated the resource allocation methods and interference management of the femtocell systems with the omnidirectional antennas. In [29], the authors proposed the power loading technique and proportional fair resource allocation to maximize the femtocell throughput, to mitigate the interference to macrocell users, and maintain the fairness among users. In [30], the

authors proposed the Lagrangian dual method to maximize the femtocell throughput by jointly adjusting the subchannel allocation and power in the OFDM-based femtocell network with the two-tier interference. In [31], the authors proposed a cognitive radio (CR)-based resource allocation scheme to control the two-tier interference and improve the system throughput. In [32], the authors managed the resource by proportional fair resource allocation for OFDMA-based femtocell system. In [33], the authors suggested the proportional fair scheduling and frequency reuse to improve the spectrum efficiency in the femtocell system. In [19], the authors developed the distributed channel-gain oriented and interference-avoidance oriented channel selection schemes to maximize the throughput under the link reliability requirement for the OFDMA-based femtocell network. However, the works in [19, 29–33] focused on the system throughput only, but did not discuss the fairness and delay issues.

In [34], the authors provided a QoS-oriented intercell fairness metric and spectrum splitting strategy to maximize the system throughput in the macrocell-femtocell networks. In [35], the authors employed the proportional fair scheduling and power control to maximize the system throughput and improve the intercell fairness in femtocell networks. In [18], the authors proposed a decentralized spectrum allocation policy to maximize the area spectral efficiency, and to guarantee the quality of service requirement for macrocell and femtocell networks. Nevertheless, the fairness among users and delay performance were not considered in [18, 34, 35].

In [20], the authors proposed a resource allocation mechanism and applied the game theory to improve the overall system throughput in the two-tier OFDMA femtocell networks. In [21, 22], the authors proposed the strategic game based radio resource management mechanism with the CR technique to improve the system throughput and ensure the delay performance. However, the fairness issue was not considered in [20–22].

To our knowledge, fewer papers consider the femtocell systems with directional antennas, such as [23, 24]. Intuitively, directional antennas can increase signal strength due to higher antenna gain and decrease the interference due to the narrow-beam patterns. In [23], the uplink throughput in the code-division multiple access

(CDMA)-based femtocell networks using sector antennas and time-hopping techniques were analyzed. The work in [24] took advantage of multiple antennas to reduce the unnecessary handover and enhance the indoor coverage. However, the main focus of [23, 24] was on the CDMA-based femtocell systems. In our previous work [28], the throughput and link reliability of low-cost E-plane horns based reconfigurable directional antenna for the OFDMA-based femtocell systems were investigated. However, the impact of subchannel allocation schemes for femtocells was not studied in [28].

2.3 Overload Control for Machine Type Communications (MTC) Femtocell Networks

In the literature, most papers investigated the overload probability and delay in the RAN congestion. In [36], the authors proposed an media access mechanism with the access class barring (ACB) method to improve the RAN throughput and average access delay. In [6], a concentrator-based congestion avoidance algorithm is proposed to reduce RAN traffic. Furthermore, a cluster formation algorithm to minimize the installation of concentrator and communications costs in [37]. The studies in [38, 39] handled massive QoS access issue with a call admission control mechanism. However, the proposed methods are too complicated to solve the RAN congestion problem from system perspective.

2.4 Intelligent Resource Management for Device-to-Device (D2D) Femtocell Networks

The technical challenges of D2D networks have recently been investigated in [40–44]. In [40], the authors introduced some functionalities, such as interference management, link adaptation, channel measurements, etc., to facilitate the D2D communications underlay the cellular networks. In addition, the effect of the largest permis-

sible D2D distance for reliable communications on the cellular SINR was discussed in [40]. Some management mechanisms of the connection setup for D2D communications were provided in [41]. The authors [41] also described that the maximum transmission power and resource allocation should be controlled to limit the interference to the cellular network. In [42], the authors proposed the Aura-Net system to facilitate the proximal discovery and autonomously manage the proximity communications by a wireless technology (FlashLinQ) without the assistance of the macrocells. In [44], the authors described that the network can help D2D pairs to discover with each other to mitigate the overhead, and appropriately switching cellular/D2D mode and power control are two important issues for the proximity communications in the cellular networks. More discovery issues of proximity communications were discussed in [40–46].

In the literature, most studies on proximity communications investigated the impacts of resource management on the system throughput and link reliability for the cellular macrocell networks with proximity communications systems. The resource allocation for proximity communications were discussed in [47–52]. In [47–49], the authors provided three resource allocation modes for the cellular macrocell networks with the D2D communications, and analyzed the optimum power for these modes. The authors [47–49] showed that the system throughput can be improved by properly selecting the resource allocation mode with the corresponding optimum transmission power in the macrocell systems with D2D communications. In [50], the authors proposed a greedy heuristic algorithm to allocate the resource blocks with lower channel gain for macrocell and D2D users. Because the lower channel gain causes the less interference, the system throughput can be improved. In [51], the authors proposed four resource allocation modes to improve the sum throughput by proper mode selection for cellular and D2D communications. The fractional frequency reuse technique was applied to the radio resource allocation of the D2D communications underlay the macrocells [52]. By appropriately allocating the resource, the interference between macrocell and D2D can be reduced, therefore the overall system throughput was improved. However, these works [47–52] were focused

on the macrocell and D2D coexistent network systems. The complicated three-tier interference of the heterogeneous Macro/Femto/D2D wireless networks was not considered.

Chapter 3

Capacity Evaluation for OFDMA Femtocells by Location Awareness and Directional Antennas

In this chapter, we develop a subcarrier number adjustment method combining with location-aware capability to mitigate the two-tier interference in OFDMA-based femtocell systems. We consider a four-sector switched-beam OFDMA-based femtocell system and utilize the location awareness capability in the IEEE 802.16m WiMAX system [53]. When an outdoor user is close to a femtocell, the number of occupied subcarriers is reduced to lower the interference. If an outdoor user is far away from the femtocells, the subcarriers can be fully utilized by the femtocell's users. We show that the proposed location-aware switched-beam femtocell system can improve its spectrum efficiency due to its capability of avoid interference to the outdoor users.

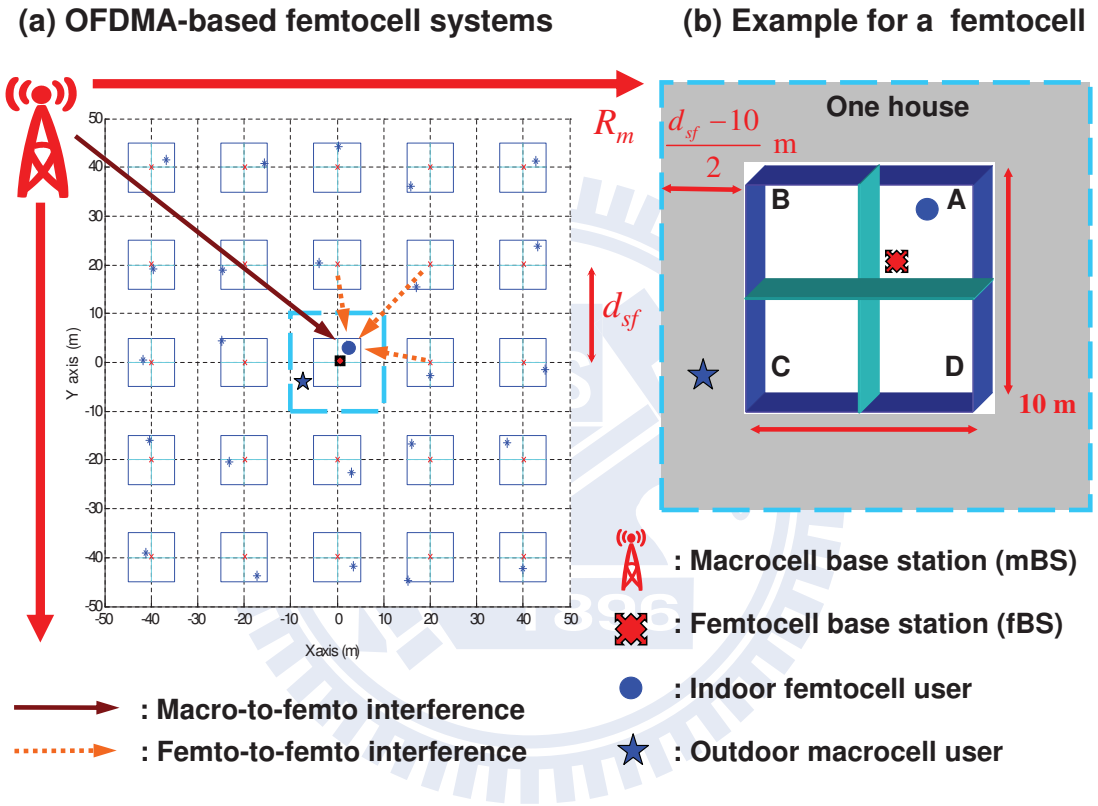

Figure 3.1: An illustrative example of the two-tier interference scenario in femtocells: (a) a cluster of 25 femtocells, each of which faces femto-to-femto and macro-to-femto interference; (b) each 4-sector femtocell is surrounded by the streets with $(d_{sf}-10)/2$ (m) and one macrocell user is appeared in the street area of 25 femtocells.

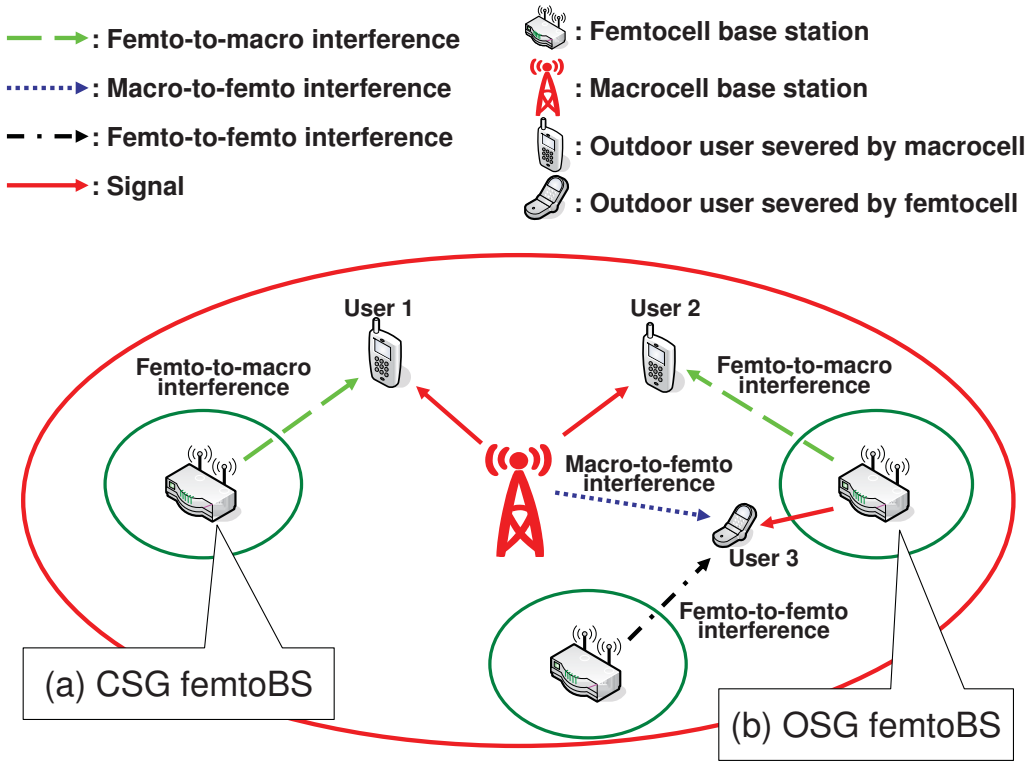

Figure 3.2: Two-tier interference for outdoor users with two access methods: (a) closed subscriber group (CSG) access method; (b) open subscriber group (OSG) access method.

3.1 System Model

3.1.1 System Architecture

We consider the OFDMA-based femtocell systems in the campus or community environment. Fig. 3.1(a) shows a cluster of 25 femtocells and a macrocell with a radius of R_m (m). Assume that each house covers an area of 100 (meter^2) and has four 5×5 (meter^2) rooms. Let the fBS be deployed at the center of each house with a shift of (0.1m, 0.1m), and denote d_{sf} (m) as the separation distance between two neighbouring fBSs. It is assumed that the femtocell user's locations are uniformly distributed within the house, and one outdoor user is located in the shadowed region with width of $(d_{sf} - 10)/2$ (m) surrounding the house, as shown in Fig. 3.1(b).

Both the exclusive and shared spectrum allocation schemes in OFDMA-based femtocells are considered in our model. The former scheme allocates different frequency bands to the macrocell and femtocell system, and the later scheme allows the same spectrum shared by both the marcocell and femtocell system. Compared with the shared spectrum allocation schemes, the exclusive spectrum allocation scheme can reduce the mutual interference, but may have lower spectrum efficiency. On the contrary, the shared spectrum scheme can increase the spectrum efficiency at the cost of higher two-tier interference.

In the shared spectrum scheme, two spectrum management schemes are further considered and compared in this chapter: CSG and OSG access methods. According to the CSG method, the outdoor macrocell user cannot access the femtocell. By contrast, if the OSG method is adopted, the macrocell users can access the femtocell. In principle, the CSG method can ensure privacy and security better than the OSG method. However, the interference issue of CSG is more severe than the OSG method because the outdoor user can be arranged to use the idle subcarriers of femtocells. Fig. 3.2 shows the two-tier interference scenario for an outdoor user in the OSG and CSG schemes.

3.1.2 Location Awareness

If the appearance of an outdoor macrocell user can be detected by the nearby femtocells, the usage of subcarriers in the femtocell system can be adjusted in order to reduce the interference to the macrocell system. Furthermore, location capability combined with network level signalling can support location-based services (LBS), and emergency E911 calls. The locations of outdoor macrocell user can be estimated by many kinds of techniques, e.g., the network-managed, MS-managed, femtocell-assisted, and GPS-based methods [53]. For the network-managed location estimation method, the time of arrival (TOA) and the angle of arrival (AOA) in the uplink transmissions are used to locate the outdoor user. For the MS-managed method, a mobile user can calculate the location information with fewer interactions with the network compared with the network-managed location estimation method. The femtocell-assisted location determination method relies on mobile users which are not connected to any femtocells to collect the information of neighboring fBSs. Based on the collected information, the network can determine the macrocell user's location.

In the following we discuss the subcarrier usage adjustment procedures to reduce interference for the location-aware femtocell systems. During the registration processes of femtocells, a cellular operator can obtain the location information of the femtocells [1], which is stored in the location database of femtocell gateways at the network center. After positioning an outdoor user, cellular networks inform the corresponding femtocell gateway to look up its location database, and notify the femtocells close to that particular outdoor user. By reducing the used subcarriers in femtocells, the link reliability of outdoor users can be ensured even with the shared spectrum allocation scheme. Location-aware femtocells need not reduce the subcarrier usage if an outdoor user is far away from them. By contrast, conventional femtocells without location awareness shall use fewer subcarriers to guarantee the link quality of the outdoor users. Hence, the location-aware femtocells can achieve higher femtocell capacity compared with the conventional femtocells. Usually, only

the approximate location of the outdoor user is required by the location-aware femtocells to make decision about the subcarrier usage. If it is necessary to reduce more interference and estimate the macrocell user location more accurately, femtocell gateways can instruct more femtocells near that macrocell user to adjust subcarriers usage.

3.1.3 Channel Models

To evaluate the two-tier interference in the OFDMA-based hybrid macrocell and femtocell systems, we consider the following radio propagation effects, including path loss, wall penetration loss, shadowing, and frequency-selective multipath fading.

Path Loss

According to [54], the path loss between transmitter and receiver with the propagation distance d (m) is defined as:

$$L(d)\ (\text{dB}) = \begin{cases} 20\log_{10}(\frac{4\pi d}{\lambda})\ , & d \leq d_{BP} \\ 20\log_{10}(\frac{4\pi d_{BP}}{\lambda}) + 35\log_{10}(\frac{d}{d_{BP}})\ , & d > d_{BP}\ , \end{cases} \tag{3.1}$$

where λ is the wavelength, d_{BP} is the break-point distance, and $d_{BP} = 5$ meters and 30 meters for indoor links and outdoor links at the 2.5 GHz carrier frequency, respectively.

Wall Penetration Loss

The wall penetration attenuation is assumed to be 5 dB per wall for indoor links, and 10 dB per wall for the outdoor-to-indoor links. We denote $\widetilde{PL}_i$ as the total penetration loss between the i-th femtocell and the considered user, and $\widehat{PL}$ as the wall penetration loss between the macrocell and the considered user.

Shadowing

The log-normally distributed shadowing random variable $10^{\xi/10}$ is considered in our model, where ξ is a Gaussian distributed random variable with zero mean. The

shadowing standard deviations for the indoor links, the macrocell-to-femtocell links, and the femtocell-to-femtocell links are $\sigma = 5$ dB, 8 dB and 10 dB , respectively.

Frequency-selective Multi-path Fading

To model the received link quality in the OFDMA system, the Stanford University interim-3 (SUI-3) channel model [55] is adopted in this chapter. The SUI-3 channel model considers a 3-tap channel with non-uniform delays .

3.2 Performance Metrics

In this chapter we consider the following performance metrics, including carrier to interference-and-noise ratio (CINR), link reliability, femtocell capacity, and spectrum efficiency.

3.2.1 Carrier to Interference-and-noise Ratio (CINR)

For the femtocell users, the two-tier interference comes from the macrocell and the other neighboring femtocells. Suppose that $\widehat{G}(\theta)$ is the antenna gain of the macrocell and $\widetilde{G}(\theta_i)$ is that of the i-th femtocell. Due to the frequency selective fading, $|\widehat{H}_m|^2$ represents the link gain between the macrocell and the femtocell user; and $|\widetilde{H}_{i,m}|^2$ is that between the i-th femtocell and the femtocell user. Therefore, the CINR of the m-th subcarrier for the considered femtocell user is defined as

$$\gamma_{F,m} = \frac{\frac{\widetilde{P}_t \widetilde{G}(\theta_i) 10^{\frac{\widetilde{\xi}_i}{10}} |\widetilde{H}_{i,m}|^2}{L(d_i)\widetilde{PL}_i}}{\frac{\widehat{P}_t \widehat{G}(\theta) 10^{\frac{\widehat{\xi}}{10}} |\widehat{H}_m|^2}{L(D)\widehat{PL}} + \sum_{k=1,k\neq i}^{K} \frac{\widetilde{P}_t \widetilde{G}(\theta_k) 10^{\frac{\widetilde{\xi}_k}{10}} |\widetilde{H}_{k,m}|^2}{L(d_k)\widetilde{PL}_k} + N_0}, \tag{3.2}$$

where the first term of the denominator is the interference from the macrocell, and the second term is that from the neighboring femtocells. $\widehat{P}_t$ is the transmission power of macrocell and $\widetilde{P}_t$ is that of femtocells. $\widehat{\xi}$ is the shadowing between the macrocell and the femtocell user, and $\widetilde{\xi}_i$ is that between the i-th femtocell and the considered femtocell user. D is the separation distance between the macrocell and the considered femtocell user. d_i is the separation distance from the i-th femtocell

to the considered femtocell user. N_0 is the noise power and K is the total number of femtocells.

For the macrocell users, the interference comes from all the adjacent femtocells. The CINR of the m-th subcarrier for the considered macrocell user is expressed as

$$\gamma_{M,m} = \frac{\frac{\widehat{P}_t \widehat{G}(\theta) 10^{\frac{\widehat{\xi}}{10}} |\widehat{H}_m|^2}{L(D)\widehat{PL}}}{\sum_{k=1}^{K} \frac{\widetilde{P}_t \widetilde{G}(\theta_k) 10^{\frac{\widetilde{\xi}_k}{10}} |\widetilde{H}_{k,m}|^2}{L(d_k)\widetilde{PL}_k} + N_0} \ . \tag{3.3}$$

According to the exponential effective SIR mapping (EESM) method [56], we can map a vector of CINRs for multiple subcarriers to a single effective CINR. Suppose that the femtocell uses N_d subcarriers for transmission. The CINR for each subcarrier is γ_m, $m = 1, 2, \ldots, N_d$. Then, the effective CINRs for the N_d used subcarriers can be calculated by

$$\gamma_{eff}(\gamma_1, \gamma_2, ..., \gamma_{N_d}) = -\beta \cdot \ln(\frac{1}{N_d} \sum_{m=1}^{N_d} \exp[-\gamma_m/\beta]) \ , \tag{3.4}$$

where β is the calibration factor for the selected modulation coding scheme (MCS) [56]. Table 3.1 lists the considered MCSs, the corresponding effective CINR thresholds, and the EESM parameter β. With the information of effective CINR, the MCS and the corresponding theoretical spectrum efficiency η can be determined according to Table 3.1.

3.2.2 Link Reliability, Capacity and Spectrum Efficiency

Link reliability P_{rel} is defined as the probability that the effective CINR of the considered user is higher than a predefined effective CINR threshold γ_{th}, that is,

$$P_{rel} = \Pr[\gamma_{eff} \geq \gamma_{th}] \ . \tag{3.5}$$

Capacity in this chapter is defined as the total throughput of an OFDMA-based femtocell. Consider that each femtocell uses N_d subcarriers for transmission. For bandwidth B, M-point FFT, and the theoretical spectrum efficiency η, the corresponding an OFDMA system capacity can be calculated by

$$C = \frac{B}{M} \frac{N_d}{1+G} \cdot \eta \ , \tag{3.6}$$

Table 3.1: **Modulation and coding schemes (MCS)**

Modulation	**Code Rate**	**Theoretical Spectrum Efficiency η (bps/Hz)**	**Minimum CINR (dB)**	**EESM β (dB)**
QPSK	1/2(4)	0.25	γ_{th}= -2.5 dB	2.18
QPSK	1/2(2)	0.5	0.5 dB	2.28
QPSK	1/2	1	3.5 dB	2.46
QPSK	3/4	1.5	6.5 dB	2.56
16-QAM	1/2	2	9 dB	7.45
16-QAM	3/4	3	12.5 dB	8.93
64-QAM	1/2	3	14.5 dB	11.31
64-QAM	2/3	4	16.5 dB	13.8
64-QAM	3/4	4.5	18.5 dB	14.71

where G is the guard fraction defined in [57] .

Next, we discuss the spectrum efficiency of femtocells with the exclusive and shared spectrum allocation schemes corresponding to 90% link reliability. In the exclusive spectrum scheme with the total bandwidth B, the femtocells and macrocells are allocated with non-overlapping $B/2$ bandwidth. Denote C_{ex} as the femtocell capacity with link reliability $P_{rel} \geq 90\%$ for the required γ_{th}. In this case, the spectrum efficiency of one femtocell in the exclusive spectrum scheme is defined as

$$SE_{ex} = \frac{C_{ex}}{B} \ . \tag{3.7}$$

In the shared spectrum scheme, the femtocells use the same frequency band of bandwidth B as the macrocells. Let C_{sh} be the capacity of a femtocell with the link reliability $P_{rel} \geq 90\%$ for the required γ_{th}. Therefore, the spectrum efficiency for the shared spectrum scheme is defined as

$$SE_{sh} = \frac{C_{sh}}{B} \ . \tag{3.8}$$

Indeed, SE_{ex} and SE_{sh} defined in (3.7) and (3.8) are the measurements of spectrum efficiency improvement for one single femtocell. The spectrum efficiency SE_{ex} and SE_{sh} are for only one single femtocell. Although it is not equal to the spectrum efficiency of a heterogeneous macrocell/femtocell system, the considered spectrum efficiency can be used to quantitatively compare the spectrum efficiency of the exclusive and shared allocation schemes. Intuitively, with the two times of bandwidth, the exclusive spectrum allocation scheme may have less spectrum efficiency than the shared allocation scheme. However, in the shared spectrum scheme, femtocells must decrease the used subcarriers to ensure the link reliability of all the users, and thus significantly reduce the spectrum efficiency. Hence, we suggest exploiting the location awareness capability of the femtocell system to improve the spectrum efficiency of shared spectrum allocation scheme.

As discussed in Section 3.1.2, the location-aware femtocell system can adaptively determine the number of subcarriers used by a femtocell depending on the separation distance to an outdoor user. Therefore, only the femtocells close to the outdoor user

should decrease the used subcarriers to reduce the interference. In this situation, the femtocell capacity is C_{sh1}. On the contrary, the femtocells far away from the outdoor user can still use all subcarriers with capacity C_{sh0}. Suppose that the probability that there is an outdoor user around the considered femtocell is p. With the location awareness, the average spectrum efficiency for the shared spectrum allocation scheme can increase to

$$SE_{LA} = \frac{pC_{sh1} + (1-p)C_{sh0}}{B} \ . \tag{3.9}$$

The existence probability p of an outdoor user around a femtocell can be measured by the femtocell [24] from the long-term statistics depending on the population density, femtocell density, femtocell transmission power, and so on.

To achieve higher spectrum efficiency, the location-aware femtocell system need to adaptively operate in the suitable spectrum allocation scheme and access method according to the existence probability p of an outdoor user and the probability threshold p^*. The probability threshold p^* for selecting the spectrum sharing scheme can be obtained as follows. Since SE_{LA} is the average spectrum efficiency for a location-aware femtocell system, as defined in (3.9). In the condition that using the shared spectrum scheme in the location-aware femtocell system can have higher spectrum efficiency than using the exclusive spectrum scheme. We have

$$SE_{LA} = \frac{pC_{sh1} + (1-p)C_{sh0}}{B} \geq SE_{ex} = \frac{C_{ex}}{B} \ . \tag{3.10}$$

Then, by rearranging (3.10), we can find the probability threshold p^* as

$$p \leq p^* = \frac{C_{sh0} - \frac{1}{2}C_{ex}}{C_{sh0} - C_{sh1}} \ . \tag{3.11}$$

Accordingly, for the location-aware femtocell system, the shared spectrum allocation scheme can achieve higher spectrum efficiency than the exclusive spectrum allocation scheme as $p < p^*$. The location-aware femtocell need to periodically report the existence probability of outdoor users to the femtocell gateway at the network center. Then, femtocell gateway can calculate the probability threshold by (3.11) in advance, and adaptively instruct the location-aware femtocells to switch the suitable

spectrum allocation and access method. For a given environment, the the location-aware femtocells can operate in the shared spectrum allocation scheme if $p < p^*$. Otherwise, the location-aware femtocells should work in the exclusive spectrum allocation scheme to achieve the best spectrum efficiency.

3.3 Directional Antennas for Femtocells

Directional antennas can decrease the two-tier interference and thus improve femtocell capacity. For now, most of the femto base stations are equipped with only omnidirectional antennas, which have lower antenna gain. In addition, each user will be easily interfered by neighboring femtocells. On the contrary, directional antennas can reduce the interference to adjacent femtocells and achieve the better CINR due to high main lobe gain and narrow beam pattern . In this section, we compare the four-sector switched-beam antenna and the IEEE 802.16m sector antenna.

3.3.1 IEEE 802.16m Sector Antenna

We consider the sector antenna in the IEEE 802.16m system [58] which has the radiation pattern $A(\theta)$ as follows:

$$A(\theta) = -\min[12(\frac{\theta}{\theta_{3dB}})^2, A_m] \quad \text{(dB)} \tag{3.12}$$

where θ_{3dB} is the 3 dB beamwidth (corresponding to $\theta = 70°$), and $A_m = 20$ dB is the maximum attenuation. The sector antenna pattern in the IEEE 802.16m is mainly designed for outdoor environments. We consider a four-sector femtocell base station that follows the above antenna pattern. In such a four-sector femtocell requires four radio transceivers, yielding higher implementation cost.

3.3.2 Four-sector Switched-beam Directional Antenna

To resolve the high implementation cost issue of the four-sector femtocell using the IEEE 802.16m sector antenna, we designed a low-cost E-plane horns based reconfigurable directional antennas, which required only one single radio transceiver by

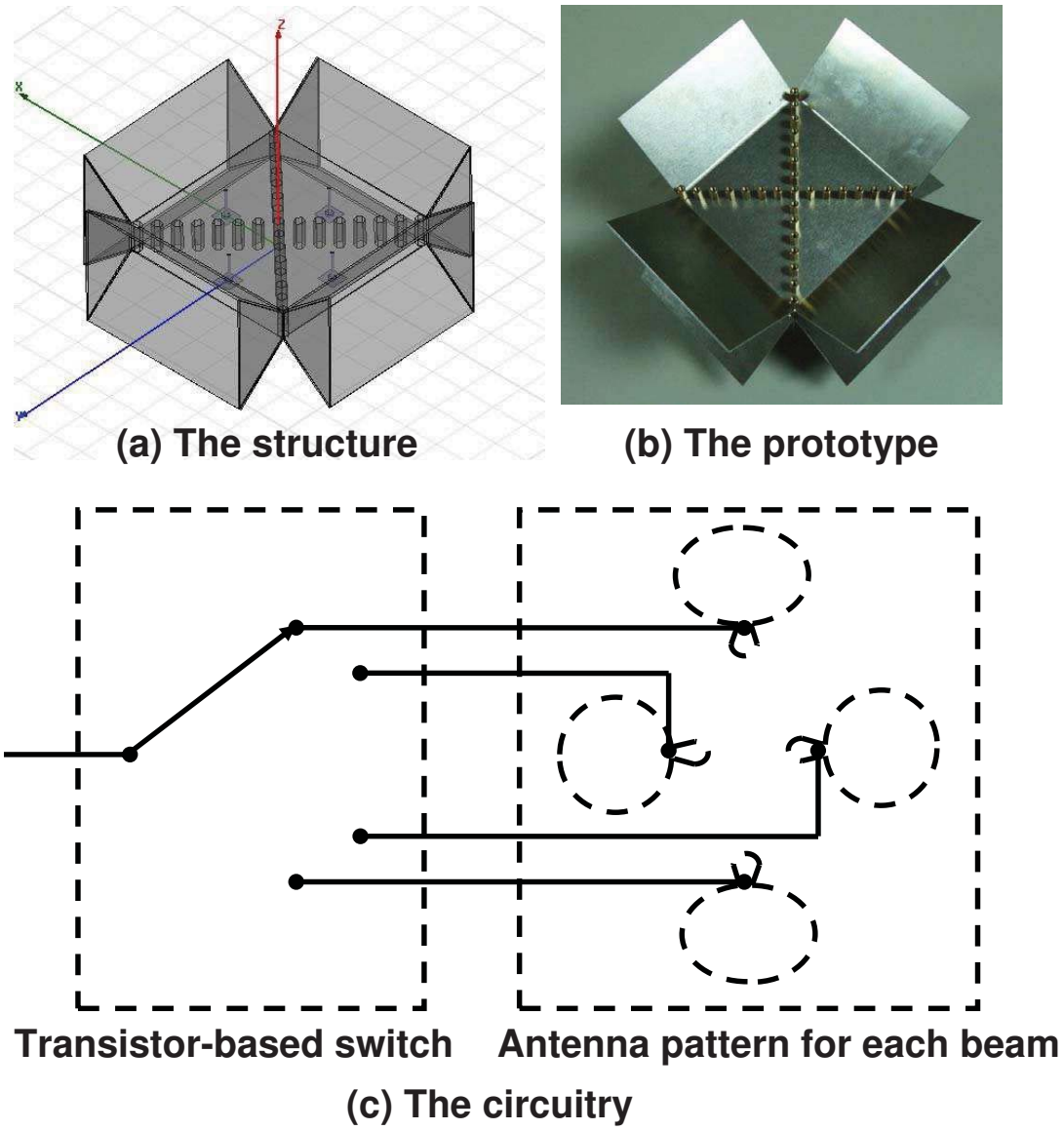

Figure 3.3: (a) The structure of four-sector switched-beam directional antenna and (b) the prototype. (c) The circuitry for the four-sector switched-beam directional antenna with the transistor-based switch.

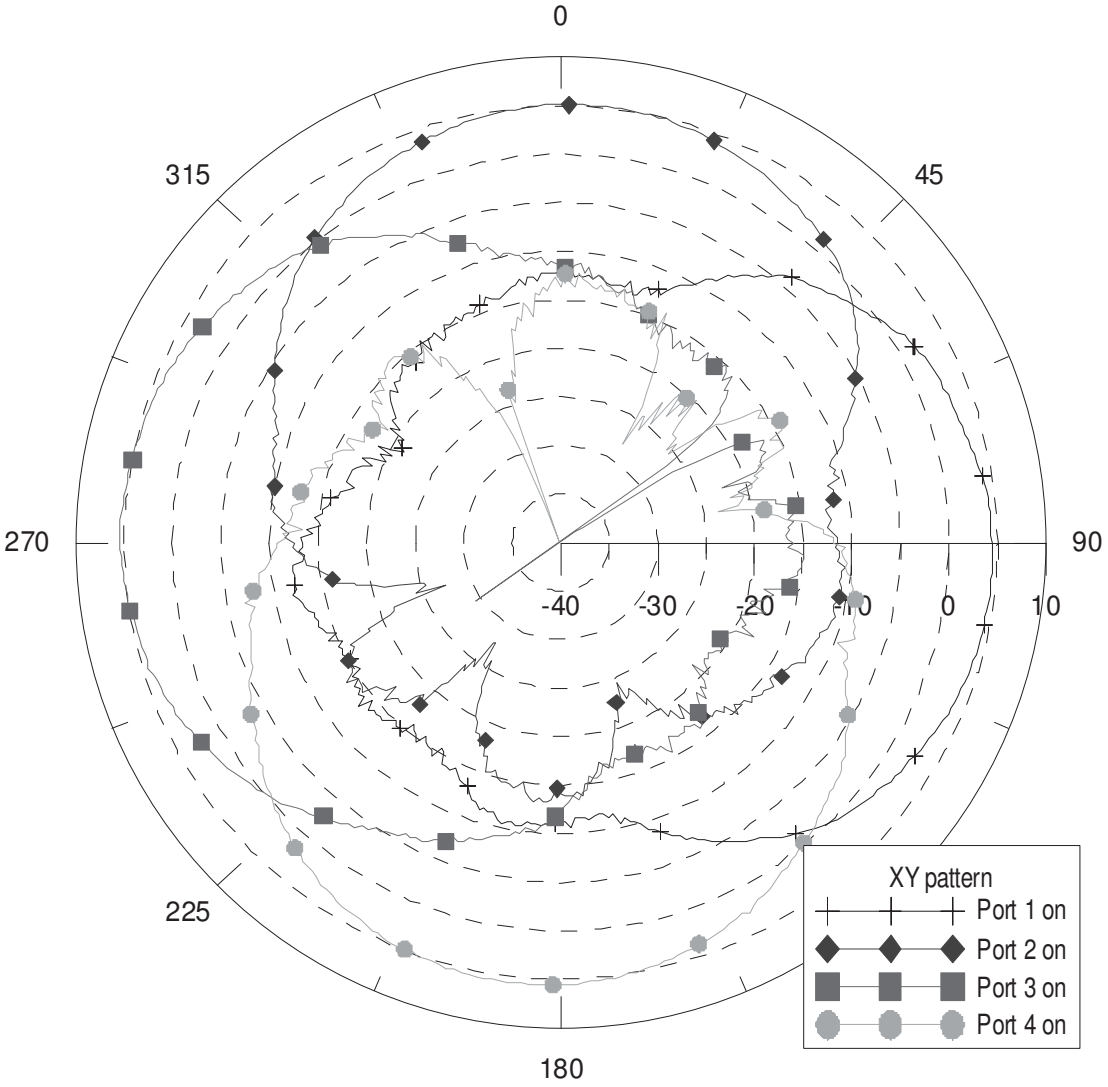

Figure 3.4: Each beam pattern of four-sector switched-beam directional antenna.

adopting the switched-beam antenna techniques. Next, we detail the structure of the switched-beam antenna as follows. Figure 3.3 shows the structure and prototype of the reconfigurable four-sector switched-beam antenna. This antenna system consists of a transistor-based switch, and post-wall E-plane horns. According to the location of the femtocell user, the switched-beam antenna dynamically alters the beam pattern to the desired user. The low-cost switched-beam antenna needs only one radio transceiver. The beam pattern is shown in Fig. 3.4. Due to the excellent isolation among E-plane horns, this antenna system also has very low side-lobe level. The size of this antenna prototype is about $19.2 \times 19.2 \times 9.5$ (cm), which can be downsized further for femtocell applications.

3.3.3 Effects of Antenna Azimuth on Interference

The azimuth of directional antenna of the neighboring home base station remarkably affects the interference of a user. If a user is within the main-lobe of neighboring femtocell's antenna, the user suffers from a strong interference. We explain the effects of antenna azimuth on the interference by the example in Fig. 3.5. In Case I, the main interference of the considered user comes from the neighboring femtocell fBS_B as shown in Fig. 3.5(a). In Case II (Fig. 3.5(b)), the neighboring femtocell fBS_A has a strong interference to the considered user. Obviously, compared with Case I, the user in Case II has a higher interference due to a shorter propagation distance. Figure 3.5(c) shows the random antenna azimuth case. In practice, the users arbitrarily deploy the fBSs without coordination. Hence, the home base stations have random antenna azimuths. We consider three antenna azimuth cases as shown in Fig. 3.5(a) $\sim$ (c) to investigate the effects of azimuth on the link reliability of femtocells.

3.4 Simulation Results

In this section, we show performance improvements of integrating directional antennas, location awareness, and subcarrier usage ratio adjustment for the OFDMA

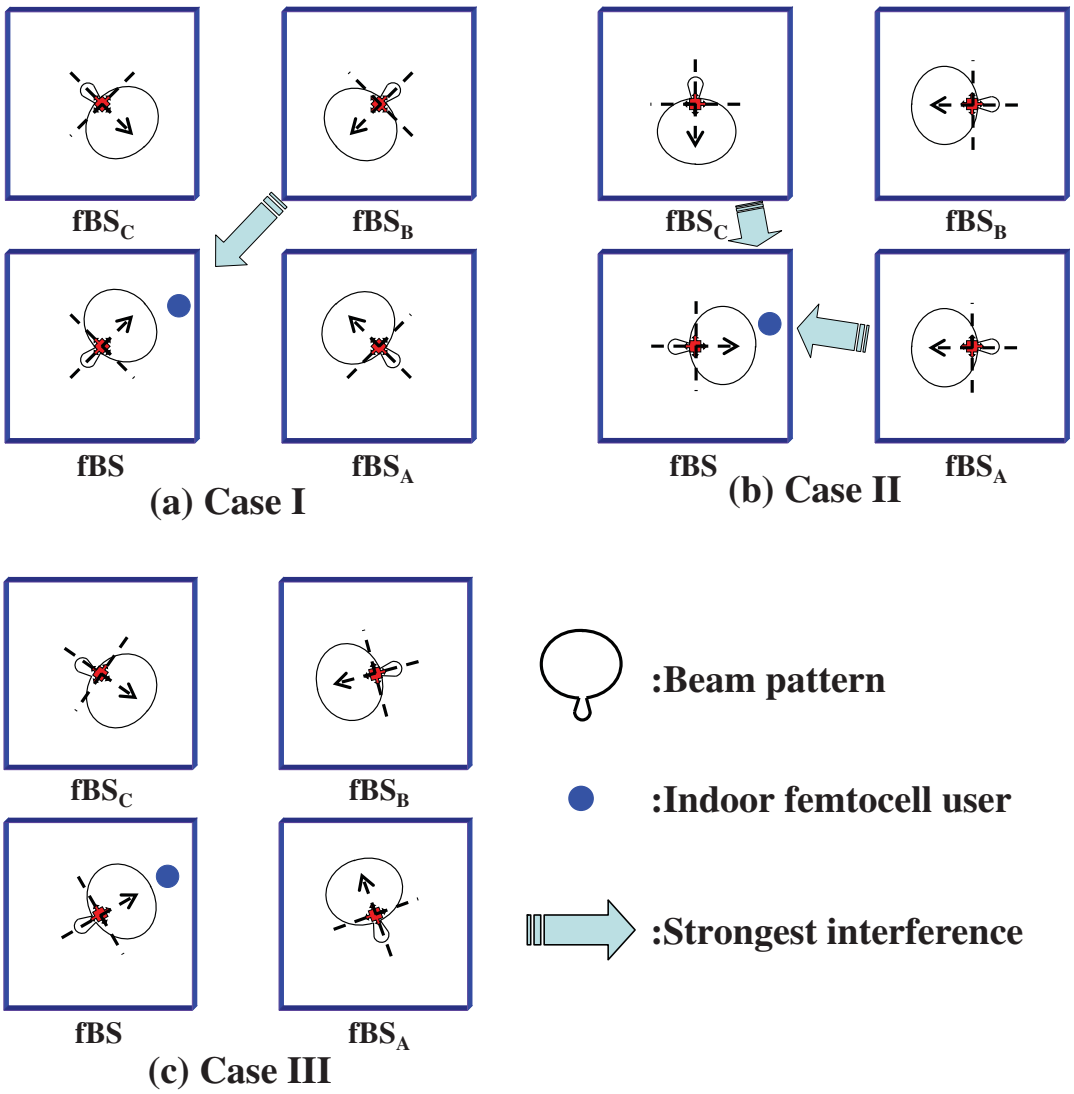

Figure 3.5: The effects of antenna azimuth on the interference.

femtocell systems subject to the femto-to-macro, macro-to-femto and femto-to-femto interference. We compare our designed four-sector switched-beam antenna with the IEEE 802.16m sector antenna and the 0-dB omnidirectional antenna in both the exclusive and shared spectrum allocation schemes. Macrocells and femtocells in the exclusive spectrum allocation scheme are allocated with non-overlapping 5 MHz frequency bands. In the shared spectrum allocation scheme, femtocells and macrocells share the total 10 MHz frequency band. We assume that the macrocell system is fully loaded, i.e., all the subcarriers are occupied by the macrocell users. In the meanwhile, it is assumed that macrocell users request one subchannel (i.e., 18 subcarriers) for voice calls. In this fully loaded situation, all the femtocells are interfered by the macrocell system.

Our simulation environment is shown in Fig. 3.1, where there are 25 femtocells separated by $d_{sf} = 20$ m. These are also covered by a macrocell with a radius of $R_m = 500$ m, and the mBS's transmission power is $\widehat{P}_t = 20$ dBm. Each fBS is deployed at the center of each house with a shift of (0.1 m, 0.1 m), and all fBSs have the same transmission power $\widetilde{P}_t = 20$ dBm. The indoor femtocell users are uniformly distributed within the house. The outdoor users are uniformly located in the shadowed region with width of $(d_{sf} - 10)/2 = 5$ m surrounding the house, as shown in Fig. 3.1(b). The channel models and the performance metrics are described in Sections 3.1.3 and 3.2, respectively. All results are simulated by MATLAB. Table 3.2 [59] lists the related system parameters for the considered OFDMA-based femtocell, including the predefined effective CINR threshold $\gamma_{th} = -2.5$ dB, link reliability requirement $P_{rel} = 90\%$, etc. In the OFDMA-based femtocell systems, the more the OFDMA subcarriers used by a femtocell, the higher the femto-to-femto and femto-to-macro interference. Thus, appropriately adjusting the number of used subcarriers can lower the interference. The total number of OFDMA subcarriers for the use of data payload is $N_{ds} = 720$. Denote N_d as the used subcarriers and define the subcarrier usage ratio as $\rho = \frac{N_d}{N_{ds}}$.

Table 3.2: **The OFDMA-based femtocell system parameters**

Downlink OFDMA Parameters	**Values**
Carrier Frequency	2.5 GHz
Macrocell BS (mBS) Transmit Power	43 dBm
Femtocell BS (fBS) Transmit Power	20 dBm
Macrocell BS Antenna Gain $G(\theta)$	8 dB
Macrocell radius (R_m)	500 m
Noise Figure (mBS/fBS/MS)	5 dB / 5 dB / 7 dB
System Bandwidth (B)	10 MHz
Sampling Frequency	11.2 MHz
FFT Size (M)	1024
Subcarrier Bandwidth	10.9375 kHz
Null Subcarriers	184
Pilot Subcarriers	120
Data Subcarriers (N_{ds})	720
Guard Fraction (G)	1/8
Predefined Effective CINR Threshold for Link Reliability (γ_{th})	-2.5 dB
Minimum Link Reliability Requirement	$P_{rel} = 90\%$

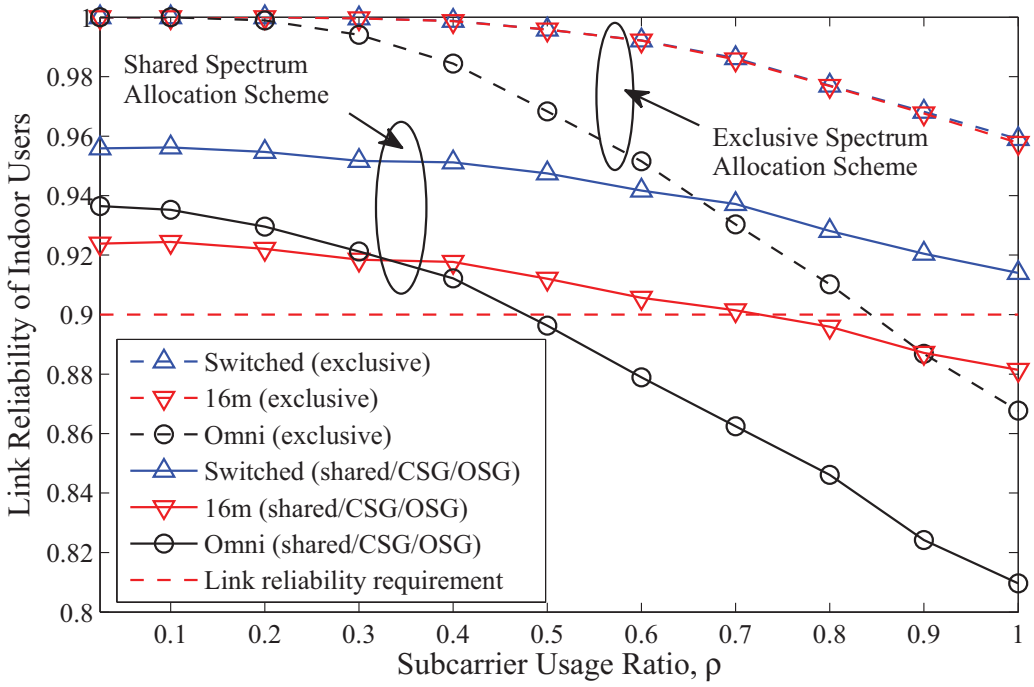

Figure 3.6: Link reliability of indoor femtocell user versus the subcarrier usage ratio ρ of the femtocells, for the exclusive and shared spectrum allocation schemes. The switched-beam directional antenna, IEEE 802.16m sector antenna and 0-dB omnidirectional antenna are compared.

3.4.1 Impact of Directional Antenna on Link Reliability

Figure 3.6 shows the link reliability performance of indoor femtocell users against the subcarrier usage ratio ρ using the pattern of the switched-beam directional antenna, the IEEE 802.16m sector antenna, and the omnidirectional antenna in both the exclusive and shared spectrum allocation schemes. From the figure, we have the following observations:

- In the shared spectrum scheme, the switched-beam directional antenna has the best indoor user's link reliability performance because of better capability to overcome the femto-to-femto inter-cell interference and higher antenna gain. Note that a higher subcarrier usage ratio ρ yields higher femto-to-femto

interference. The sector antenna pattern specified in the IEEE 802.16m outperforms the omnidirectional antenna pattern when the subcarrier usage ratio $\rho > 0.33$. The directivity of the IEEE 802.16m sector antenna can help reduce the femto-to-femto inter-cell interference at the range of large value of ρ. For $\rho < 0.33$, however, the IEEE 802.16m sector antenna has worse indoor user's link reliability than the omnidirectional antenna because its antenna gain $A(\theta) < 0$ dB in the azimuth angle $\theta \neq 0^o$ (referring to (3.12)) and the gain of the omnidirectional antenna is equal to 0 dB in all azimuth angle.

- Compared with the shared spectrum allocation scheme, the exclusive spectrum allocation scheme has better indoor user's link reliability performance because the macro-to-femto cross-tier interference does not exist. In such a femto-to-femto interference-limited case, the switched-beam directional antenna even with the higher antenna gain yields the similar indoor user's link performance as the IEEE 802.16m sector antenna. Nevertheless, both the switched-beam antenna and the IEEE 802.16m sector antenna perform better than the omnidirectional case.

- To provide high sucarrier usage ratio in femtocell systems, it is important to control the femto-to-femto interference. For the link reliability requirement $P_{rel} = 90\%$, the switched-beam antenna can support $\rho = 1$ in both shared and exclusive spectrum allocation scheme. However, the IEEE 802.16m sector antenna can support subcarrier usage ratio $\rho = 1$ in the exclusive spectrum allocation scheme, but can only support $\rho = 0.73$ at most in the shared spectrum allocation scheme. For omnidirectional antenna scheme, the largest permissible subcarrier usage ratio $\rho = 0.85$ and $\rho = 0.48$ in the exclusive and shared spectrum allocation schemes, respectively.

Figure 3.7 shows the link reliability performance of outdoor user against the subcarrier usage ratio ρ of the femtocells, in the shared spectrum allocation scheme with the CSG and OSG access methods. We assume that in the CSG method the outdoor user around the considered femtocell is served by the macrocell, while the

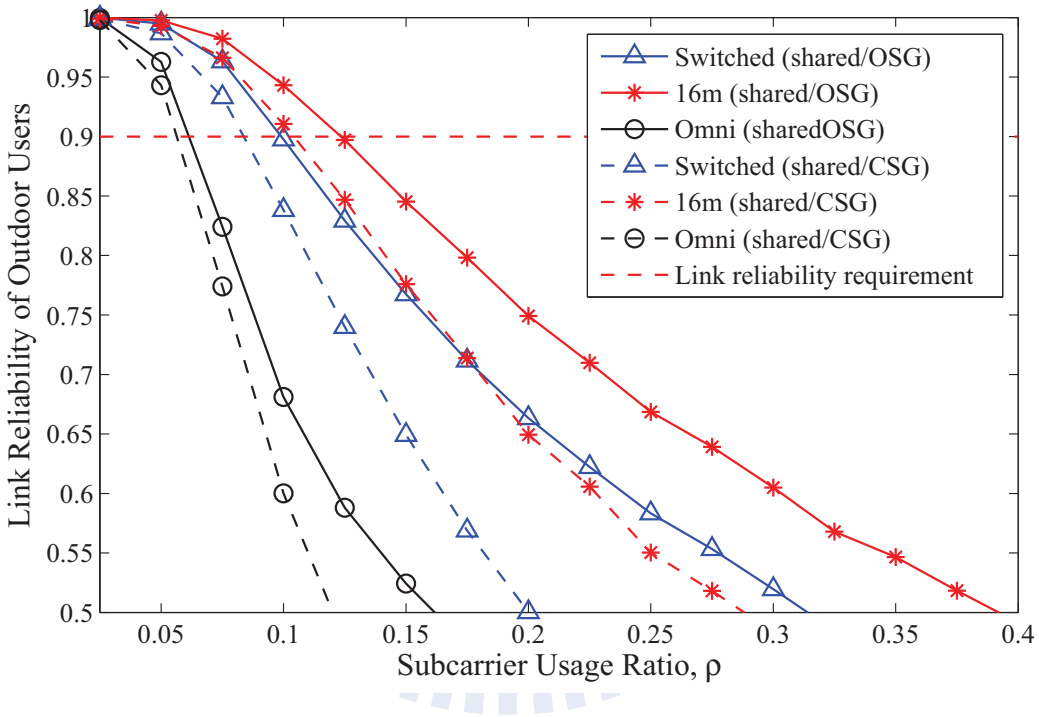

Figure 3.7: Link reliability of outdoor user versus the subcarrier usage ratio ρ of the femtocells, in the shared spectrum allocation scheme with the CSG and OSG access methods.

outdoor users can select the base station with the stronger signal strength among the mBS and the fBSs in the OSG method. Besides, the outdoor user need only one subchannel for voice calls. We have the following observations:

- The IEEE 802.16m sector antenna can yield better link reliability of outdoor user than the switched-beam antenna for both CSG and OSG methods. Though the higher-gain switched-beam antenna can enhances the signal strength, it also increases the interference from femtocells to lower the link reliability of the outdoor user. Nevertheless, both the switched-beam antenna and the IEEE 802.16m sector antenna perform better than the omnidirectional case.

- To ensure the link reliability of the outdoor users, it is also important to control the femto-to-macro and femto-to-femto interference in the shared spectrum allocation scheme. For the link reliability requirement $P_{rel} = 90\%$, the IEEE 802.16m sector antenna can support subcarrier usage ratio $\rho = 0.12$ at most in the OSG method, and $\rho = 0.11$ at most in the CSG method. However, the switched-beam antenna can support subcarrier usage ratio $\rho = 0.10$ at most in the OSG method, and $\rho = 0.09$ at most in the CSG method. For omnidirectional antenna scheme, the largest permissible subcarrier usage ratio $\rho = 0.065$ and $\rho = 0.06$ in the OSG and CSG methods, respectively.

Figure 3.8 shows the spectrum efficiency against the subcarrier usage ratio ρ, for the femtocells with the exclusive and shared spectrum allocation schemes. We have the following observations:

- It is shown that as the OSG access method and the switched-beam antenna are used to reduce the interference in the shared spectrum scheme, the spectrum efficiency compared with the omnidirectional antenna with the CSG access method is improved from 0.11 bps/Hz at $\rho = 0.06$ to 0.21 bps/Hz at $\rho = 0.1$. Therefore, the switched-beam antenna with the OSG method can improve 91% spectrum efficiency compared with the omnidirectional antenna with the CSG method.

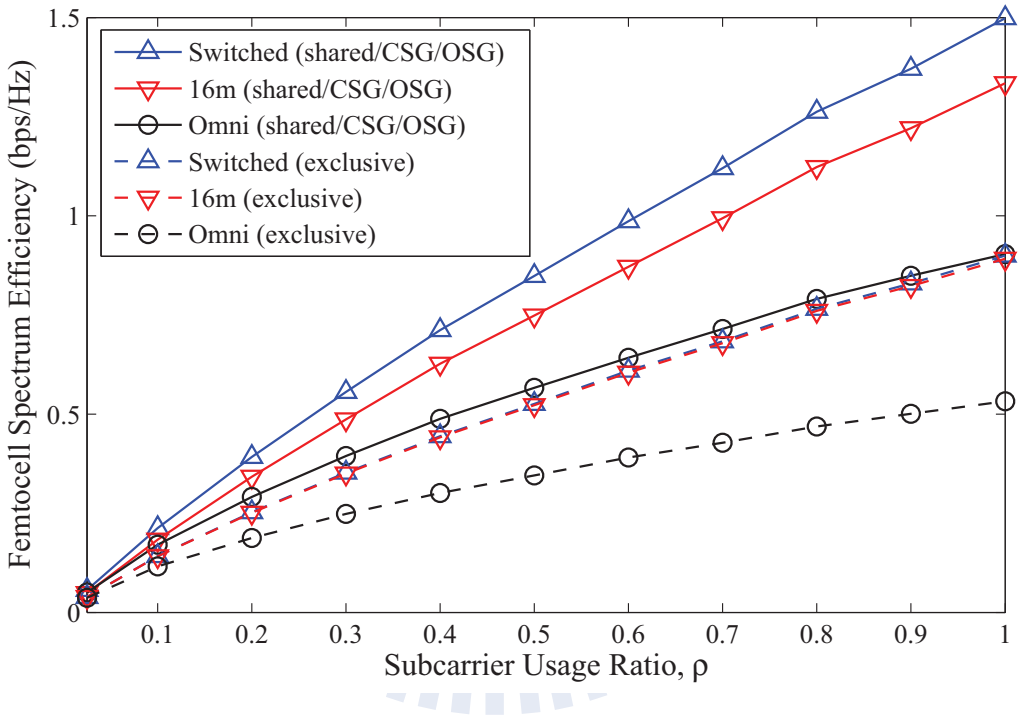

Figure 3.8: Femtocell spectrum efficiency versus the subcarrier usage ratio ρ, for the exclusive and shared spectrum allocation schemes with the CSG and OSG access methods.

- With a link reliability requirement, the shared spectrum allocation scheme may not always have better spectrum efficiency, even if the macrocells and femtocells share the same spectrum. As far as the switched-beam antenna with link reliability requirement $P_{rel} = 90\%$ is concerned, the maximum allowable subcarrier usage ratio $\rho = 1.0$ in the exclusive spectrum allocation scheme, and $\rho = 0.1$ in the shared spectrum allocation scheme with the OSG method. The corresponding spectrum efficiency is 0.9 bps/Hz and 0.21 bps/Hz in the exclusive spectrum allocation scheme and in the shared spectrum allocation scheme with the OSG method, respectively.

- It is also shown that with a link reliability requirement, the improvement of the spectrum efficiency is higher than that of the largest permissible subcarrier usage ratio. Compared with the omnidirectional antenna, the directional antenna can improve the link reliability of indoor users to increase the largest permissible subcarrier usage ratio, and thereby improve the spectrum efficiency. As far as the link reliability of indoor users is concerned, in the shared spectrum allocation scheme, the switched-beam antenna can support the largest permissible subcarrier usage ratio $\rho = 1.0$ and achieve 1.5 bps/Hz spectrum efficiency, while the omnidirectional antenna can support $\rho = 0.48$ and achieve 0.55 bps/Hz spectrum efficiency. Therefore, the switched-beam antenna can not only improve 108% maximum allowable subcarrier usage ratio but also improve 173% spectrum efficiency, compared with the omnidirectional antenna.

3.4.2 Impact of Location Awareness on Spectrum Efficiency

Figure 3.9 shows the average spectrum efficiency of the location-aware femtocell systems against the existing probability p of a nearby outdoor user. We assume that if there is an outdoor user around the considered femtocell (referring to Fig 3.1), the considered femtocell and all 24 neighboring femtocells should use fewer subcarriers

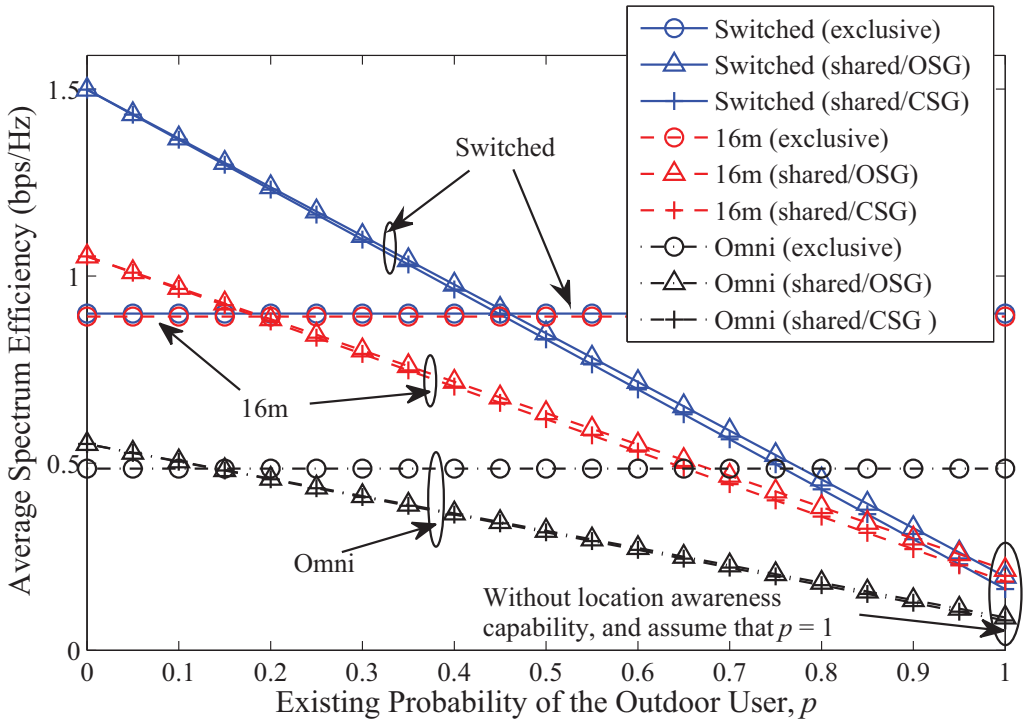

Figure 3.9: Average spectrum efficiency of the location-aware femtocell systems versus the existing probability of the outdoor user, under the link reliability requirement $P_{rel} \geq 90\%$.

to reduce the interference for this outdoor user. We have the following observations:

- If the location awareness capability is not available, it is usually assumed that an outdoor user will appear with probability $p = 1$ and thus the maximum allowable subcarrier ratio for femtocell can be set up to $\rho = 0.1$. When the OSG and CSG shared spectrum scheme is used and $p = 1$, the femtocell can achieve spectrum efficiency about 0.2 bps/Hz for the switched-beam and the IEEE 802.16m sector antennas, but has only 0.1 bps/Hz for omnidirectional antenna. However, when the femtocell can be aware of the appearance of the outdoor user under the condition $p = 0.4$, the spectrum efficiency can be improved to 1.0 bps/Hz, 0.7 bps/Hz, and 0.38 bps/Hz for the switched-beam antenna, the IEEE 802.16m sector antenna and omnidirectional antenna, respectively. It implies location awareness can improve the spectrum efficiency of femtocells by at least two times for different antenna patterns.

- If the exclusive spectrum allocation scheme is used, location awareness cannot help resolve the interference between femtocells and macrocells, resulting in the same spectrum efficiency for different appearance probabilities of macrocell users.

- One can observe that location awareness capability can also affect the choice of spectrum sharing schemes for different antenna patterns. When the switched-beam antenna is used, the shared spectrum schemes provide higher spectrum efficiency than the exclusive scheme when $p < 0.46$. The shared spectrum schemes can result in higher spectrum efficiency than the exclusive spectrum scheme only for $p < 0.19$ when the IEEE 802.16m sector antenna is used and for $p < 0.15$ when the omni-directional antenna is use, respectively.

3.4.3 Impacts of Femtocell Density and Existing Probability of Outdoor Users on Spectrum Efficiency

Figure 3.10 shows the impact of femtocell density on the the maximum allowable subcarrier usage ratio ρ for the location-aware femtocells with the shared spectrum

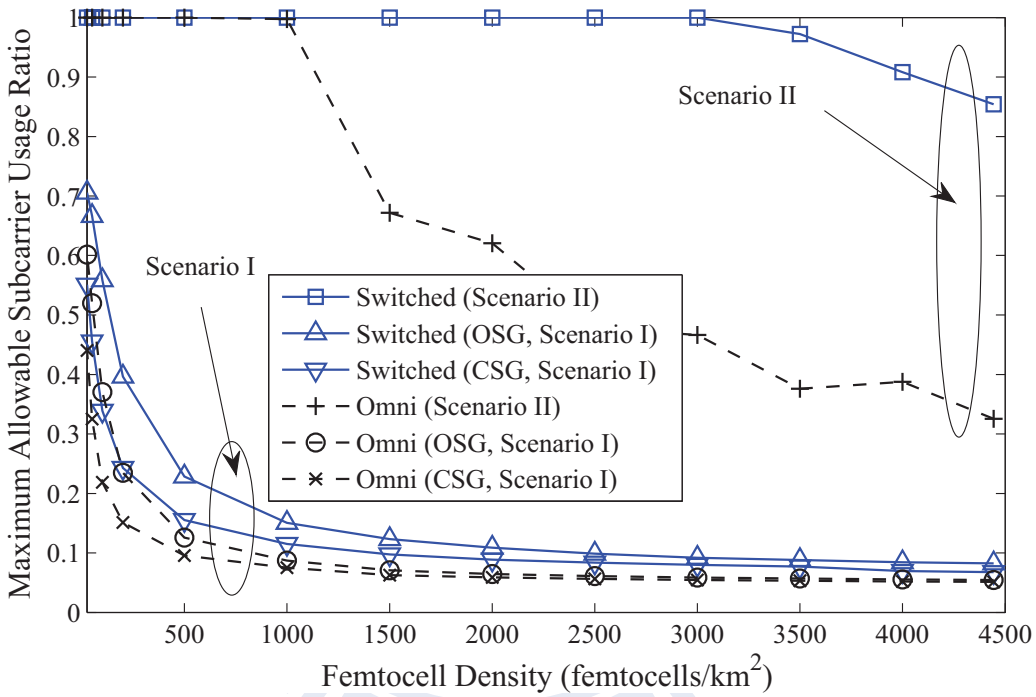

Figure 3.10: Maximum allowable subcarrier usage ratio of the location-aware femtocell versus the femtocell density in the shared spectrum allocation scheme subject to the link reliability requirement $P_{rel} \geq 90\%$. Scenario I: an outdoor user appears near the considered central femtocll; Scenario II: there is no outdoor user around the considered central femtrocell.

location scheme subject to the link reliability requirement $P_{rel} \geq 90\%$. We consider two scenarios. Scenarios I represents the situation that an outdoor user appears near the considered central femtocell, and Scenario II represents the situation that an outdoor user does not appear near the considered central femtocell. From the figure, we have the following observations:

- In Scenario I, the femtocell density significantly affects the maximum allowable subcarrier usage ratio ρ when an outdoor user appears near the considered central femtocell. When the femtocell density is higher than 500 femtocells/km^2 (the corresponding nearest separation distance between two femtocells is $d_{sf} \approx 45$ m), the maximum allowable subcarrier usage ratio ρ shall be smaller than 0.25 to ensure the link reliability of outdoor users.

- In Scenario II, the maximum allowable subcarrier usage ratio ρ can be increased since the outdoor user does not exist. For example, when the femtocell density reaches 4500 femtocells/km^2 (the corresponding nearest separation distance between two femtocells is $d_{sf} \approx 15$ m), a location-aware femtocell system has the potential to improve $\rho = 0.05$ to $\rho = 0.33$ even with onmidirectional antenna. If the switched-beam antenna is used, a location-aware femtocell system has the potential to improve $\rho = 0.08$ to $\rho = 0.85$.

Figure 3.11 shows the achieved spectrum efficiency of the location-aware femtocells against the femtocell density for various existing probability p of an outdoor user near the considered femtocell. We consider the location-aware femtocell using the switched-beam antenna and the OSG access method with $P_{rel} \geq 90\%$ in the shared spectrum allocation scheme. We have the following observations:

- The existing probability p of an outdoor user significantly affects the achieved spectrum efficiency of the location-aware femtocell system in the shared spectrum allocation scheme. The higher the existing probability p, the lower the achieved spectrum efficiency of the location-aware femtocell system. In this case, if the femtocell density is 1000 femtocells/km^2, the achieved spectrum efficiency of $p = 0$, 0.2, 0.46, 0.6, and 0.8 can be improved by 470%, 373%,

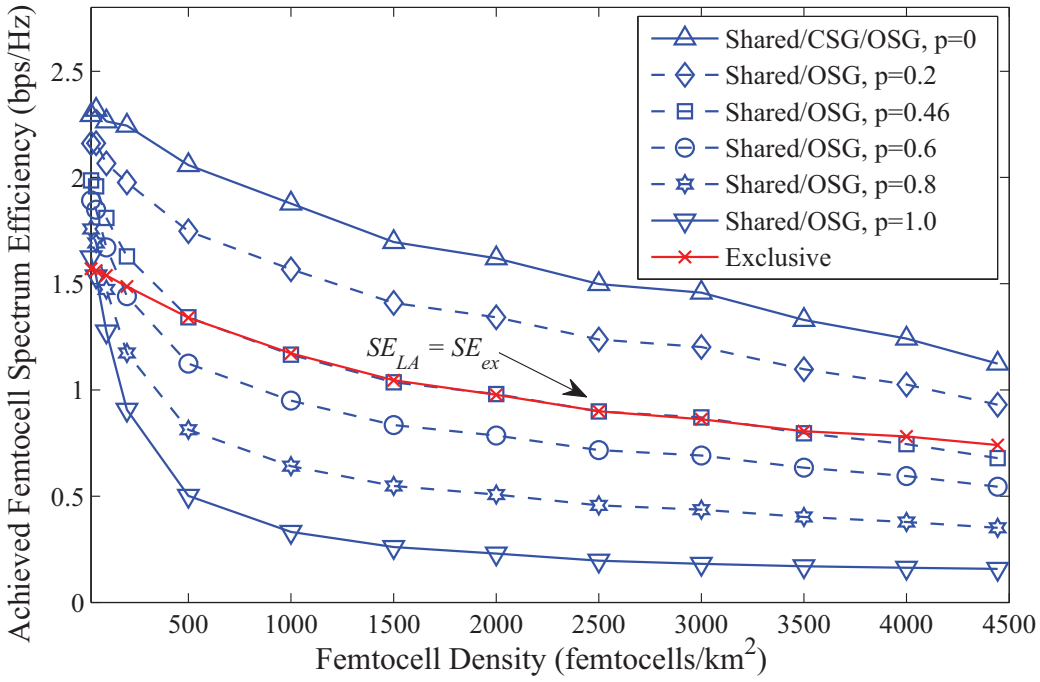

Figure 3.11: Achieved spectrum efficiency of the location-aware femtocell versus the femtocell density for different existing probability of an outdoor user under the link reliability requirement $P_{rel} = 90\%$ in the shared spectrum allocation scheme, where the switched-beam antenna is used.

255%, 188%, and 94% compared to that of $p = 1.0$. If the femtocell density is 4000 femtocells/km^2, the spectrum efficiency can be improved by 675%, 544%, 369%, 269%, and 138% for $p = 0$, 0.2, 0.46, 0.6, and 0.8.

- For the exclusive spectrum allocation scheme with a given femtocell density, the achieved femtocell spectrum efficiency does not fluctuate according to the existing probability p of an outdoor user. This is because the femtocell and macrocell systems are allocated with different frequency bands. For instance, the achieved spectrum efficiency in the exclusive spectrum scheme is 1.2 bps/Hz and 0.8 bps/Hz for the femtocell density of 1000 and 4000 femtocells/km^2, respectively.

- With the information of the existing probability p of a nearby outdoor user and the femtocell density, the location-aware femtocell system can properly choose the spectrum allocation scheme to achieve a better spectrum efficiency. From (3.11), one can calculate the probability threshold p^* for any given femtocell density. For example, the probability threshold is $p^* = 0.46$ when the femtocell density is 2500 femtocells/km^2. If the existing probability of a nearby outdoor user $p > p^*$, the femtocell system should adopt the exclusive spectrum allocation scheme to achieve a higher spectrum efficiency. If $p \leq p^*$, the location-aware femtocell system can select the shared spectrum scheme to improve the spectrum efficiency.

3.4.4 Impact of Antenna Azimuth of Femtocells on Link Reliability

Figure 3.12 shows the link reliability of the indoor femtocell users against the subcarrier usage ratio ρ. We consider three antenna azimuth scenarios of the switched-beam femtocells in Fig. 3.5.However, in this example, the largest difference in link reliability among the three considered cases is only 2.3%. This result implies that the antenna azimuth of switched-beam femtocell has insignificant effects on the link reliability of the femtocell users. Thus it is implied that femtocells can be deployed

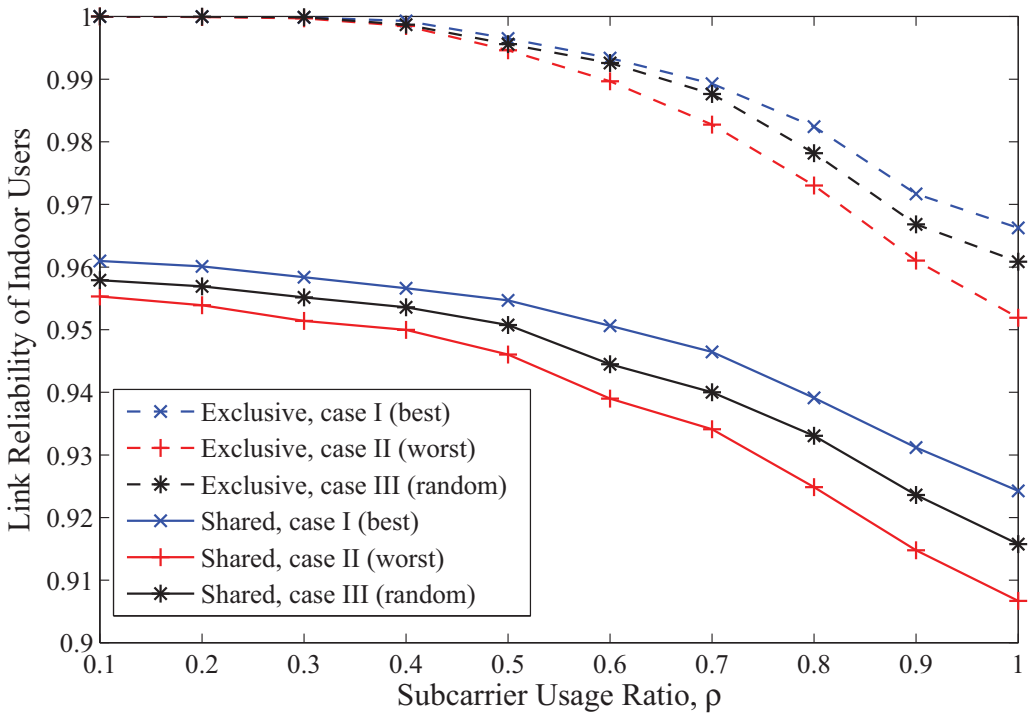

Figure 3.12: Link reliability of indoor users versus the subcarrier usage ratio ρ of the femtocells, considering three antenna azimuth cases for the switched-beam antenna.

with random antenna azimuth.

3.4.5 Summary

The proposed design principle aims to help decide the suitable spectrum allocation and access method for femtocells. Actually, without location awareness, it is usually assumed that the existing probability of outdoor user is $p = 1$. In this situation, to guarantee the link reliability of all indoor and outdoor users, the conventional femtocell can only use fewer subcarriers in the shared spectrum allocation scheme or can operate in the exclusive spectrum allocation to alleviate the interference to the other users. Neither the shared spectrum allocation scheme nor the exclusive spectrum allocation scheme is a good option for the conventional femtocell system. On the one hand, spectrum efficiency is too low even if the directional antennas are used to mitigate the interference to the outdoor users in the shared spectrum allocation scheme. On the other hand, the cost for the two times of bandwidth in the exclusive spectrum allocation scheme is too high. On the contrary, if location awareness is available, the shared spectrum allocation scheme can achieve higher spectrum efficiency than the exclusive spectrum allocation scheme as the existing probability of outdoor users is smaller than the probability threshold. The probability threshold can be calculated by (3.11) in this chapter, and the existing probability of outdoor users is decided by the environment.

For a given environment, the location-aware femtocells can operate in the shared spectrum allocation scheme if the existing probability of outdoor users is smaller than the probability threshold, or the location-aware femtocells should work in the exclusive spectrum allocation scheme to achieve better spectrum efficiency. In our example, when the switched-beam antenna is used, the shared spectrum scheme can provide higher spectrum efficiency than the exclusive scheme when the existing probability of outdoor user is $p < 0.46$. We also take some practical environments into account as example. Firstly, according to [60], the population densities in Europe are 3000, 1000, 500, 100 and 25 citizen/km^2 in the dense urban areas, urban areas, suburban areas, rural areas, and wilderness, respectively. In addition, the

document [60] also showed that only 8 percent of the voice calls originate in the busy/peak hour in case the whole population are voice users. In [2, 4, 27], it was mentioned that 50 percent of all voice calls and 70 percent of data traffic occur indoors. In other words, only 50 percent of all voice calls originate outdoors. When the femtocell density is 2500 femtocells/km^2, the region where the cluster of 25 femtocells covers is 0.01 km^2. The probability p_x that there is not any active outdoor voice user in the region is

$$p_x = \left(1 - (0.1)^2\right)^{(\mathrm{D_p} \times 0.08 \times 0.5)} \tag{3.13}$$

, where D_p is the corresponding population density. Therefore, the existing probability of outdoor users is the probability that there is at least one outdoor user exists in the region is

$$p = 1 - p_x = 1 - \left(1 - (0.1)^2\right)^{(\mathrm{D_p} \times 0.08 \times 0.5)} \tag{3.14}$$

Finally, we can determinate the existing probability of outdoor users are $p = 0.70$, $p = 0.33$, $p = 0.18$, $p = 0.04$ and $p = 0.01$ for the dense urban areas, urban areas, suburban areas, rural areas and wilderness, respectively.

Table 3.3 shows the comparison of various antennas for location-aware femtocells in terms of the average spectrum efficiency. Five environments are considered in the table, and they are the dense urban areas, urban areas, suburban areas, rural areas, and wilderness of Europe [60], respectively. We make a summary of the table.

- It can be seen that the switched-beam antenna has the best spectrum efficiency performance for the location-aware femtocells compared with the IEEE 802.16m and the omnidirectional antennas.

- To have better average spectrum efficiency performance, the location-aware femtocell with the switched-beam antenna should operate in the exclusive spectrum allocation scheme for the dense urban areas, where the existing probability of outdoor users is $p = 0.70$. However, the location-aware femtocell with the switched-beam antenna can operate in the shared spectrum

allocation scheme for the urban areas, suburban areas, rural areas and wilderness, where the existing probabilities of outdoor users are $p = 0.33$, $p = 0.18$, $p = 0.04$ and $p = 0.01$, respectively.

Table 3.3: **Comparison of various antenna for location-aware femtocells**

Antenna Category	Average Spectrum Efficiency (bps/Hz) of the Location-Aware Femtocell					
	Spectrum Allocation Schemes and Access Methods	Dense Urban Areas ($p = 0.70$)	Urban Areas ($p = 0.33$)	Suburban Areas ($p = 0.18$)	Rural Areas ($p = 0.04$)	Wilderness ($p = 0.01$)
Switched	Shared/OSG	0.59	1.07 (Best)	1.27 (Best)	1.45 (Best)	1.49 (Best)
	Shared/CSG	0.56	1.06	1.26	1.44	1.48
	Exclusive	0.9 (Best)	0.9	0.9	0.9	0.9
16m	Shared/OSG	0.47	0.78	0.90	1.02	1.04
	Shared/CSG	044	0.77	0.89	1.02	1.04
	Exclusive	0.89	0.89	0.89	0.89	0.89
Omni	Shared/OSG	0.22	0.40	0.47	1.53	0.55
	Shared/CSG	0.22	0.40	0.47	1.53	0.55
	Exclusive	0.48	0.48	0.48	0.48	0.48

The population densities are 3000, 1000, 500, 100 and 25 citizen/km^2 in the dense urban areas, urban areas, suburban areas, rural areas, and wilderness of Europe, respectively [60].

Chapter 4

Subchannel Allocation for Multi-Beam OFDMA Femtocells

In this chapter, we investigate the impacts of subchannel allocation schemes and directional antenna on femtocell throughput, fairness, and HOL delay performance among users in the OFDMA-based multiuser femtocell systems. We adopt the switched multi-beam directional antenna to reduce the two-tier interference, and further apply the subchannel allocation to control the fairness and HOL delay. We suggest combining the subchannel allocation with the antenna pattern selection to optimize the system throughput and guarantee the fairness and HOL delay. We formulate an optimization problem to jointly select the antenna radiation pattern and allocate the subchannels for multiple users to maximize the femtocell throughput, subject to the constraint of the maximum allowable number of subchannels used by each user. The objective of limiting the maximum allowable number of subchannels is to ensure the throughput fairness and HOL delay performance. In addition, we compare our proposed stable subchannel allocation scheme with various schemes, including the channel-oriented, user-oriented, proportional fair, exponential rule, and queue-based exponential rule subchannel allocation methods in terms of throughput, fairness index and HOL delay performance. Because the stable subchannel allocation scheme can repeatedly rearrange the channel allocation according

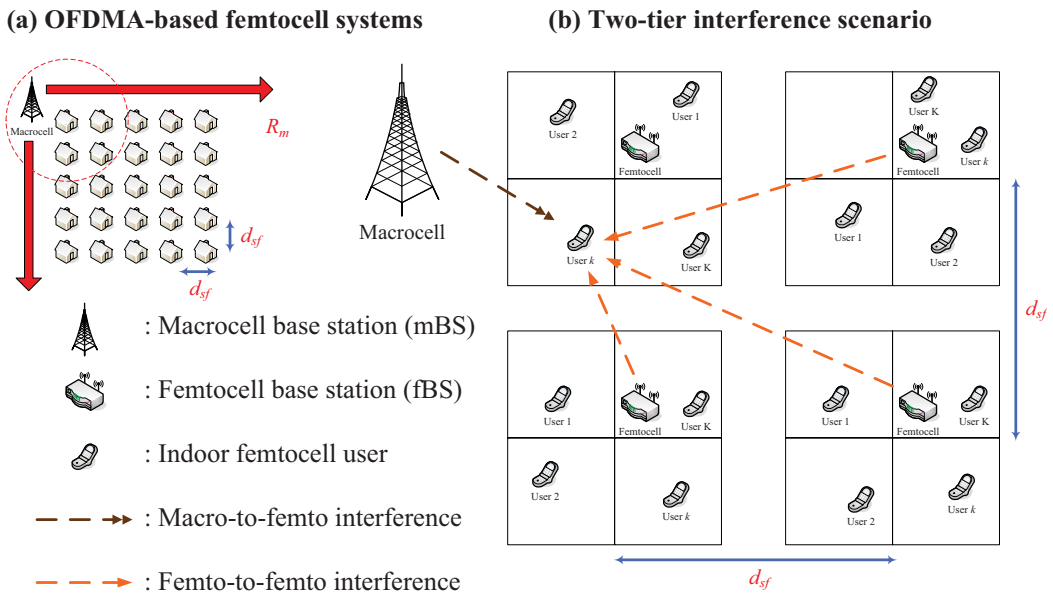

Figure 4.1: An illustrative example of the two-tier interference scenario in femtocells: (a) a cluster of 25 femtocells; (b) each femtocell user faces femto-to-femto and macro-to-femto interference.

to the channel state information of users, the OFDMA-based femtocell system can achieve the optimal throughput, fairness, and delay performance. Simulation results show that the proposed stable subchannel allocation scheme combined the switched multi-beam antenna can achieve the tradeoff among throughput, fairness and HOL delay, compared to the other methods.

4.1 System Model

4.1.1 System Architecture

We consider the OFDMA-based femtocell systems in the campus or community environment. Figure 4.1(a) shows a cluster of 25 femtocells and a macrocell with a radius of R_m (m). Assume that each house covers an area of 100 (meter^2) and has four 5×5 (meter^2) rooms. Let the femtocell base station (fBS) be deployed at the center of each house with a shift of (0.1m, 0.1m), and denote d_{sf} (m) as the

separation distance between two neighbouring fBSs. It is assumed that there are K users in each house, and the femtocell users' locations are uniformly distributed within the house, as shown in Fig. 4.1(b).

In this chapter, we consider the shared spectrum allocation scheme, where the femtocell and the macrocell systems use the same frequency band. With the shared spectrum allocation scheme, the femtocell users suffer the serious two-tier interference that comes from the macrocells and femtocells, as shown in Fig. 4.1(b).

4.1.2 Switched Multi-beam Directional Antenna

This switched multi-beam directional antenna can reduce the two-tier interference to the adjacent femtocells and achieve the better signal quality because of the narrow-beam pattern and the higher main-lobe gain. Due to the excellent isolation among E-plane horns, this antenna system can have low side-lobe level. In addition, the low-cost switched multi-beam antenna needs only one radio transceiver. This switched multi-beam antenna system consists of the one-to-four transistor-based switch for the four antenna ports. By switching on/off the antenna ports, the antenna system can use either one of the four antenna ports, or any antenna port combination at the same time. Therefore, this antenna can flexibly provide various radiation patterns as shown in Fig. 4.2. There are total 15 possible antenna patterns. Noteworthily, the transmission power is evenly distributed by a power divider and fed into the antenna ports. Therefore, the effective antenna gain should be divided by a factor κ, and κ is the number of adopted antenna ports. This antenna can simultaneously serve multiple femtocell users. According to the locations of these users, the switched multi-beam antenna will adaptively select a proper antenna pattern for these users.

4.1.3 Channel Models

We consider the impacts of path loss, wall penetration loss, shadowing, and multi-path fading as follows.

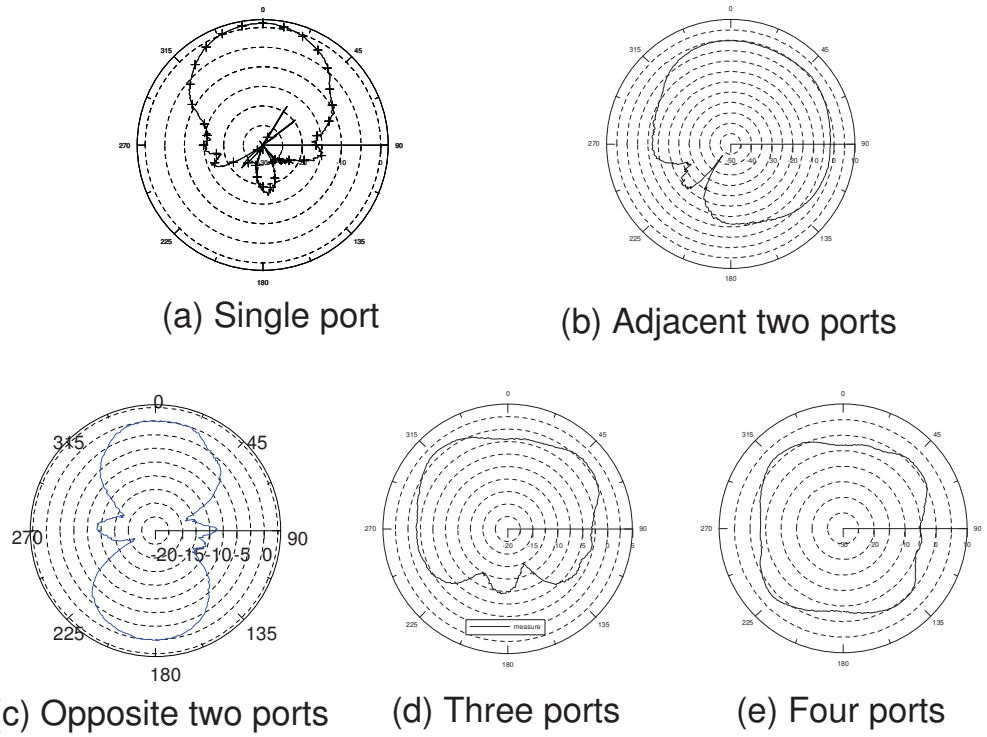

Figure 4.2: Typical radiation patterns of the switched multi-beam directional antenna. This antenna system has four antenna ports controlled by the one-to-four transistor-based switch. Therefore, this antenna can use any antenna port or any antenna port combination at the same time by switching on/off the antenna ports.

Path Loss

According to the 3GPP LTE technical report [61], as the transmitter and the receiver are in the same house, the path loss between the transmitter and the receiver with the propagation distance d (km) is defined as

$$L(d)\ (\text{dB}) = 127 + 30 \log_{10} d\ . \tag{4.1}$$

As the transmitter and the receiver are not in the same house, the path loss is defined as

$$L(d)\ (\text{dB}) = 128.1 + 37.6 \log_{10} d\ . \tag{4.2}$$

Wall Penetration Loss

We assume that the penetration attenuation is 20 dB per wall for outdoor-to-indoor links [61]. Besides, let $W_{F,i,k}$ be the total penetration loss between the i-th femtocell and the considered user k, and $W_{M,k}$ be that between the macrocell and the considered user k.

Shadowing

Shadowing is modeled by a log-normal random variable $10^{\xi/10}$, where ξ is a Gaussian distributed random variable with zero mean. The shadowing standard deviation for the indoor links is $\sigma = 10$ dB; that for the links between the neighboring femtocells and the considered user is $\sigma = 10$ dB; and that for the links between the macrocell and the considered user is $\sigma = 8$ dB [61].

Multi-path Fading

We take the frequency-selective fading channel into account. The multipath fading is described by the Stanford University interim-3 (SUI-3) channel model assuming 3 taps with non-uniform delays [55].

4.1.4 Effective Carrier to Interference-and-noise Ratio (CINR)

To calculate the effective CINR for a subchannel comprising multiple subcarriers in the OFDMA-based femtocell system, we first evaluate the CINR of a subcarrier as follows. The received signal power of m-th subcarrier for the indoor femtocell user k in the i-th femtocell can be expressed as

$$S_{F,i,m,k} = \frac{p_{_{F,i,m}} G_{F,j}(\theta_{i,k}) \cdot 10^{\frac{\xi_{F,i,k}}{10}} |h_{F,i,m,k}|^2}{10^{\frac{L(d_{F,i,k})+W_{F,i,k}}{10}}} . \tag{4.3}$$

$p_{_{F,i,m}}$ is the transmission power of the subcarrier m in the i-th femtocell. $G_{F,j}(\theta_{i,k})$ is the antenna gain for the user k in the i-th femtocell using the j-th antenna pattern. $\xi_{F,i,k}$ is the shadowing between the i-th femtocell and the user k. $|h_{F,i,k,m}|^2$ represents the link gain between the i-th femtocell base station and the user k on the subcarrier m. $d_{F,i,k}$ is the separation distance from the i-th femtocell base station to the user k.

For this indoor femtocell user k, the two-tier interference comes from the macrocell and the other neighboring femtocells. On the subcarrier m of the user k in the i-th femtocell, the total interference from the neighboring femtocells is $I_{F,i,m,k}$, and that from the macrocell is $I_{M,i,m,k}$. Suppose that there are Ψ femtocells. Consider that the neighboring femtocell u uses the j'-th antenna pattern. Then, $I_{F,i,m,k}$ and $I_{M,i,m,k}$ can be expressed as

$$I_{F,i,m,k} = \sum_{u=1,\, u\neq i}^{N_F} \delta_{u,m} \cdot \frac{p_{_{F,u,m}} G_{F,j'}(\theta_{u,k}) \cdot 10^{\frac{\xi_{F,u,k}}{10}} |h_{F,u,m,k}|^2}{10^{\frac{L(d_{F,u,k})+W_{F,u,k}}{10}}} \tag{4.4}$$

and

$$I_{M,i,m,k} = \delta_{M,m} \cdot \frac{p_{_{M,m}} G_M(\theta_k) \cdot 10^{\frac{\xi_{M,k}}{10}} |h_{M,m,k}|^2}{10^{\frac{L(d_{M,k})+W_{M,k}}{10}}} . \tag{4.5}$$

$\delta_{u,m}$ and $\delta_{M,m}$ are the indicator functions for the subcarrier allocation in the u-th femtocell and macrocell, respectively. If the subcrrier m is used in the u-th femtocell (macrocell), $\delta_{u,m} = 1$ ($\delta_{M,m} = 1$); otherwise, $\delta_{u,m} = 0$ ($\delta_{M,m} = 0$). $p_{_{M,m}}$ is the

transmission power for the subcarrier m of the macrocell. $G_M(\theta_k)$ is the macrocell antenna gain for the user k. $\xi_{M,k}$ is the shadowing between the macrocell and the user k. $|h_{M,m,k}|^2$ is the link gain between the macrocell base station and the user k on the subcarrier m. $d_{M,k}$ is the separation distance from the macrocell base station to the user k. Therefore, the CINR of m-th subcarrier for the user k in the i-th femtocell is defined as

$$\gamma_{F,i,m,k} = \frac{S_{F,i,m,k}}{I_{M,i,m,k} + I_{F,i,m,k} + \frac{B}{M}N_0} \ . \tag{4.6}$$

N_0 is the power spectrum density of AWGN. B is the system bandwidth, and M is the FFT size.

According to the exponential effective SIR mapping (EESM) method [56], we can map a vector of CINRs for multiple subcarriers of a subchannel to a single effective CINR. Suppose that a subchannel includes N_d subcarriers, and the corresponding CINR for each subcarrier is $\gamma_{F,i,m,k}$. Then, the effective CINR of the subchannel n for the user k in the i-th femtocell can be calculated by

$$\gamma_{eff,i,n,k} = -\beta \cdot \ln(\frac{1}{N_d} \sum_{m=(n-1)N_d+1}^{nN_d} \exp(-\frac{\gamma_{F,i,m,k}}{\beta})) \tag{4.7}$$

where β is the calibration factor for the selected modulation coding scheme (MCS) [56]. Table 3.1 lists the considered MCSs, the corresponding effective CINR thresholds, and the EESM parameter β. After we obtain the effective CINR of the subchannel n for the user k in the i-th femtocell, we can determine the MCS and the corresponding theoretical spectrum efficiency $\eta_{i,n,k}$, according to Table 3.1.

4.2 Performance Metrics

System throughput, fairness and head of line (HOL) delay are essential factors in the distributed subchannel allocation with the shared spectrum allocation scheme for the multi-user OFDMA-based femtocell system. From the throughput perspective, assigning a subchannel to the user with the best CINR can maximize the system throughput. However, some users with the worse CINR may be allocated with only

few subchannels. This results in throughput unfairness among the users. Therefore, from the fairness viewpoint, it is preferred to constrain the number of subchannels used by a user. Nevertheless, for some delay-sensitive services, such as streaming video, the subchannel allocation also takes account of the latency performance. In this chapter, we consider the following performance metrics, including femtocell throughput, fairness, and delay.

4.2.1 Femtocell Throughput

The achieved throughput is defined as the total throughput of an OFDMA-based femtocell. Let $\varepsilon_{i,n,k}$ be the indicator function for the subchannel allocation. In the i-th femtocell, if the subchannel n is allocated to the user k, $\varepsilon_{i,n,k} = 1$; otherwise, $\varepsilon_{i,n,k} = 0$. Let $\chi_{i,n,k}$ be the achieved throughput of the subchannel n for the user k in the i-th femtocell if the subchannel n is allocated to the user k. Denote the achieved throughput of the subchannel n for the user k in the i-th femtocell and the achieved throughput for the user k in the i-th femtocell as $C_{i,n,k}$ and $C_{i,k}$, respectively. Suppose that there are N data subchannels, and K users in each of the N_F femtocells. Then, the average achieved throughput of the OFDMA-based femtocell can be calculated by [57]

$$\begin{aligned} C =& \frac{1}{N_F} \sum_{i=1}^{N_F} \sum_{k=1}^{K} \sum_{n=1}^{N} \varepsilon_{i,n,k} \cdot \frac{B}{M} \frac{N_d}{1+G} \eta_{i,n,k} \\ =& \frac{1}{N_F} \sum_{i=1}^{N_F} \sum_{k=1}^{K} \sum_{n=1}^{N} \varepsilon_{i,n,k} \cdot \chi_{i,n,k} \\ =& \frac{1}{N_F} \sum_{i=1}^{N_F} \sum_{k=1}^{K} \sum_{n=1}^{N} C_{i,n,k} \\ =& \frac{1}{N_F} \sum_{i=1}^{N_F} \sum_{k=1}^{K} C_{i,k} \end{aligned} \tag{4.8}$$

where G is the guard fraction.

4.2.2 Fairness Index

Multi-user diversity can help increase the system throughput by taking advantage of short-term channel variations of each user terminal, however, this may results in throughput unfairness among the users. Therefore, fairly allocating the resource is important, especially in the case of multi-type services. To our knowledge, the fairness index has two types: Jain's fairness index FI_{Jain} and Wang's fairness index FI_{Wang}. Jain's fairness index is mainly to determine the fairness in the long-term viewpoint. However, Wang's fairness index can be used to determine the fairness in the short-term perspective. The Jain's fairness index is defined as [62]

$$FI_{Jain} = \frac{1}{N_F} \sum_{i=1}^{N_F} \frac{(\sum_{k=1}^{K} C_{i,k}/\alpha_k)^2}{K \sum_{k=1}^{K} (C_{i,k}/\alpha_k)^2} \tag{4.9}$$

where α_k is the weight of the flow for the user k in the multi-type services. The Jain's fairness index is with the range between 0 and 1. Under the perfect fairness situation, all users achieve the same throughput and $FI_{Jain} = 1$.

The Wang's fairness index is defined as [63]

$$FI_{Wang} = \frac{1}{N_F} \sum_{i=1}^{N_F} \frac{1}{\binom{K}{2}} \sum_{\mu=1}^{K-1} \sum_{\nu=\mu+1}^{K} \left| \frac{C_{i,\mu}}{\alpha_\mu} - \frac{C_{i,\nu}}{\alpha_\nu} \right| \tag{4.10}$$

where α_μ and α_ν are the weight of the flow for the user μ and ν in the multi-type services, respectively. The smaller the Wang's fairness index, the fairer is the system. In addition, $FI_{Wang} = 0$ for the perfect fairness situation.

4.2.3 Head of Line (HOL) Delay

The head of line (HOL) delay is defined as the period from the time of receiving service to the next time of receiving service for users.

4.3 Joint Subchannel Allocation and Antenna Pattern Selection

In addition to subchannel allocation, the selection of antenna patterns also significantly affects the user throughput, fairness, and delay of the OFDMA-based femtocell system when using switched multi-beam directional antennas in femtocells. It is better to select the antenna pattern according to the users' locations so that all the intended users are within the main-lobe of serving femtocell's antenna. Thus, we should jointly select the antenna pattern and allocate the subchannels for multiple users with considering these two important factors.

The joint antenna pattern selection and subchannel allocation is formulated as a mixed-integer nonlinear programming problem as follows. The objective is to maximize the femtocell throughput by properly selecting the antenna pattern $\phi_{i,j}$, and determining the indicator function $\varepsilon_{i,n,k}$ for allocating the subchannels for multiple users.

$$\max_{\varepsilon_{i,n,k},\, \phi_{i,j}} \; C \tag{4.11}$$

subject to

$$\phi_{i,j} = \{0, 1\}, \quad \forall i, \forall j \; . \tag{4.12}$$

$$\varepsilon_{i,n,k} = \{0, 1\}, \quad \forall i, \forall k, \forall n \tag{4.13}$$

$$\sum_{k=1}^{K} \varepsilon_{i,n,k} = \{0, 1\}, \quad \forall i, \forall n \tag{4.14}$$

In the following, we explain the above constrains. In the constraint (4.12), $\phi_{i,j}$ is the indicator function for antenna selection. If the antenna pattern j is used by the i-th femtocell, $\phi_{i,j} = 1$; otherwise, $\phi_{i,j} = 0$. In the constraint (4.13), $\varepsilon_{i,n,k}$ is the indicator function to indicate if the subchannel n is allocated to user k in the i-th femtocell. The constraint in (4.14) states the condition that in a femtocell each subchannel can be allocated to at most one user.

We propose a low-complexity joint antenna pattern selection and subchannel allocation method because of the difficulty in solving the mixed-integer nonlinear

optimization problem with integer decision variables in (4.11). With N data subchannels for K users in the femtocell system, there are K^N possible subchannel allocations. Besides, the antenna pattern selection complicates the optimal subchannel allocation problem. It takes much time to calculate the optimal solution. The femtocell base station can not determine the optimal antenna pattern and subchannel allocations in realtime. Therefore, we develop a low-complexity algorithm, by which the femtocell base station can distributedly select the antenna pattern and allocate the subchannels for multiple users.

The main principle of the joint antenna pattern selection and subchannel allocation method is to adaptively determine the optimal antenna pattern and subchannel allocation according to the sets of users' effective CINRs of subchannels on a closed-loop fashion. In a low-mobility femtocell environment, because the wireless channel changes slowly, it is reasonable to assume that the sequential two down links have the similar fading characteristics. Therefore, the femtocell base station can utilize the information to determine the selection of antenna patterns and the allocation of subcarriers for users. In addition, we also consider that the femtocell base station uses the equal power over each subchannel. The procedures of the joint antenna pattern selection and subchannel allocation method are described in the following:

1. The femtocell base station collects all the channel information (e.g., effective CINRs) from users.

2. For each possible antenna radiation pattern, do the following steps.

   (a) Allocate subchannels to multiple users by the predefined subchannel allocation scheme (e.g., channel-oriented, user-oriented, proportion fair, exponential rule, queue-based exponential rule, and stable subchannel allocation schemes) according to all the channel information collected from users in Step 1.

   (b) Estimate the femtocell throughput by (4.8) according to the assignment result in Step 2(a).

3. According to the estimated throughput performance from Step 2(b), select the antenna pattern and the corresponding subchannel allocation which can achieve maximal femtocell throughput.

4.4 Compared Subchannel Allocation Schemes

In this section, we detail some subchannel allocation schemes such as channel-oriented, user-oriented, proportion fair, exponential rule, and queue-based exponential rule subchannel allocation schemes. Firstly, we assume that $\varepsilon_{i,n,k} = 0,\ \forall i, \forall n, \forall k$, before allocating subchannels to users. Then, if the subchannel allocation scheme assigns the subchannel $\hat{n}$ to the user $\hat{k}$, we indicate that $\varepsilon_{i,n,k} = 1$, where $n = \hat{n}$, and $k = \hat{k}$ for each of femtocells. Therefore, the subchannel allocation scheme in this chapter is mainly to pair the subchannel $\hat{n}$ and the user $\hat{k}$ for the better system throughput, fairness, and latency performance.

4.4.1 Channel-oriented Subchannel Allocation Scheme

The channel-oriented subchannel allocation scheme assigns a subchannel to the user with the best effective CINR for the subchannel, thereby enhancing the throughput. This scheme can maximize the throughput due to achieving the maximum multi-user diversity. However, the channel-oriented subchannel allocation scheme is unfair among users and has worse delay performance because users who are with lower effective CINR or who are located far from the base station may be assigned only fewer subchannel. The procedure of channel-oriented subchannel allocation scheme is depicted as fellows.

1) Initialization

   a) $\varepsilon_{i,n,k} = 0,\ \forall i, \forall n, \forall k$

2) For $\hat{n} = 1$ to N

   a) $\hat{k} = \arg_{1 \le k \le K} \max\{\gamma_{eff,i,\hat{n},k}\}$

b) $\varepsilon_{i,\hat{n},\hat{k}} = 1$

4.4.2 User-oriented Subchannel Allocation Scheme

For the user-oriented subchannel allocation scheme, the user select the subchannel with the best effective CINR by turns, therefore, this scheme can achieve better fairness among users and has better delay performance. Nevertheless, the selection sequence for users significantly affects the femtocell throughput because the subchannel selected by the preceding user can not be reassigned to another user, even if the overall throughput may be improved after rearrangement. Therefore, the user-oriented subchannel allocation scheme sacrifices the overall throughput to achieve better throughput fairness and delay performance. The procedure of user-oriented subchannel allocation scheme is depicted as fellows.

1) Initialization

   a) $\varepsilon_{i,n,k} = 0,\ \forall i, \forall n, \forall k$

   b) $\Omega = \{1, 2, \cdots, N\}$

   c) $k = 1$

2) While $\Omega \neq \emptyset$

   a) $\hat{k} = \text{mod}\{(k-1), K\} + 1$

   b) $\hat{n} = \max\{\gamma_{_{eff,i,\ell,\hat{k}}}\}, \forall \ell \in \Omega$

   c) $\varepsilon_{i,\hat{n},\hat{k}} = 1$

   d) $\Omega = \Omega - \{\hat{n}\}$

4.4.3 Proportional Fair Subchannel Allocation Scheme

The proportional fair subchannel allocation scheme assigns a subchannel to a user with the biggest ratio of the short-term throughput over the long-term averaged throughput value. This scheme takes the advantage of the temporal variations of the effective CINR to increase the system throughput, while maintaining a certain

level of fairness among all active users. However, the proportional fair subchannel allocation scheme does not consider the delay issue in each user's service queue and thus has poor delay performance. The procedure of proportional fair subchannel allocation scheme is depicted as fellows.

1) Initialization

   a) $\varepsilon_{i,n,k} = 0,\ \forall i, \forall n, \forall k$

   b) Set the instantaneous throughput $R_{i,k} = 0,\ \forall i, \forall k$.

   c) Let $\varpi_{i,k}$ be the average throughput of user k, where $k = 1, \cdots, K$. The average throughput of users can be measures by femtocell systems.

2) For $\hat{n} = 1$ to N

   a) $\hat{k} = \arg_{1 \le k \le K} \max\{\frac{R_{i,k}+\chi_{i,\hat{n},k}}{\varpi_{i,k}}\}$

   b) $\varepsilon_{i,\hat{n},\hat{k}} = 1$

   c) $R_{i,\hat{k}} = R_{i,\hat{k}} + \chi_{i,\hat{n},\hat{k}}$

4.4.4 Exponential Rule Subchannel Allocation Scheme

The exponential rule subchannel allocation scheme is a modified version of the proportional fair subchannel allocation scheme, and takes the delay issues into account. Namely, the scheme considers the effects of both effective CINRs and service delay, and aims to further improve the performance compared to the proportional fair subchannel allocation scheme. The procedure of exponential rule subchannel allocation scheme is depicted as fellows.

1) Initialization

   a) $\varepsilon_{i,n,k} = 0,\ \forall i, \forall n, \forall k$

   b) Set the instantaneous throughput $R_{i,k} = 0,\ \forall i, \forall k$.

   c) Let $\varpi_{i,k}$ be the average throughput of user k, where $k = 1, \cdots, K$. The average throughput of users can be measures by femtocell systems.

d) Let $\tau_{i,k}$ be the delay time for user k, where $k = 1, \cdots, K$. The delay time also can be measures by femtocell systems.

2) For $\hat{n} = 1$ to N

a) $\hat{k} = \arg_{1 \le k \le K} \max\{\frac{R_{i,k}+\chi_{i,\hat{n},k}}{\varpi_{i,k}} \exp(\frac{\alpha_k \tau_{i,k} - \overline{\alpha\tau}}{1+\sqrt{\overline{\alpha\tau}}})\}$, where $\alpha_k > 0$, $k = 1, \cdots, K$, are selected weights to characterize the desired quality of service, and $\overline{\alpha\tau} = \frac{1}{K}\sum_{k=1}^{K} \alpha_k \tau_{i,k}$.

b) $\varepsilon_{i,\hat{n},\hat{k}} = 1$

c) $R_{i,\hat{k}} = R_{i,\hat{k}} + \chi_{i,\hat{n},\hat{k}}$

d) $\tau_{i,\hat{k}} = 0$

4.4.5 Queue-based Exponential Rule Subchannel Allocation Scheme

Compared to the exponential rule subchannel allocation scheme, the queue-based exponential rule subchannel allocation scheme further considers the queue length of all active users to achieve better fairness. The procedure of queue-based exponential rule subchannel allocation scheme is depicted as fellows.

1) Initialization

a) $\varepsilon_{i,n,k} = 0, \ \forall i, \forall n, \forall k$

b) Set the instantaneous throughput $R_{i,k} = 0, \ \forall i, \forall k$.

c) Let $\varpi_{i,k}$ be the average throughput of user k, where $k = 1, \cdots, K$. The average throughput of users can be measures by femtocell systems.

d) Let $\tau_{i,k}$ be the delay time for user k, where $k = 1, \cdots, K$. The delay time also can be measures by femtocell systems.

2) For $\hat{n} = 1$ to N

a) $\hat{k} = \arg_{1 \le k \le K} \max\{\frac{R_{i,k}+\chi_{i,\hat{n},k}}{\varpi_{i,k}} \exp(\frac{\alpha_k \tau_{i,k} - \overline{\alpha\tau}}{1+\sqrt{\overline{\alpha\tau}}}) \cdot \exp(\frac{\psi_{i,k} - \overline{\psi}}{1+\overline{\psi}})\}$, where $\alpha_k > 0$, $k = 1, \cdots, K$, are selected weights to characterize the desired quality of service, $\overline{\alpha\tau} = \frac{1}{K}\sum_{k=1}^{K} \alpha_k \tau_{i,k}$, and $\overline{\psi} = \frac{1}{K}\sum_{k=1}^{K} \psi_{i,k}$.

b) $\varepsilon_{i,\hat{n},\hat{k}} = 1$

c) $R_{i,\hat{k}} = R_{i,\hat{k}} + \chi_{i,\hat{n},\hat{k}}$

d) $\tau_{i,\hat{k}} = 0$

e) $\psi_{i,\hat{k}} = \psi_{i,\hat{k}} - (\chi_{i,\hat{n},\hat{k}} \cdot \text{TTI})$, where TTI is the transmission time interval.

4.5 Stable Subchannel Allocation

The main principle of the stable subchannel allocation scheme is to optimize the system throughput by the deferred acceptance algorithm [12] which can repeatedly rearrange the subchannel allocation according to the SINRs of all the active users in OFDMA-based femtocell systems. The deferred acceptance algorithm can yield an optimal and stable assignment for the college admissions problem [11]. Because the relationship between subchannels and users is similar to that between students and colleges, the deferred acceptance algorithm can also find an optimal and stable assignment for the subchannel allocation. By properly limiting the maximum allowable number of subchannels used by each user, this scheme can achieve better throughput fairness among users and delay performance. Therefore, the stable subchannel allocation scheme can assign a set of subchannels to a set of users with the maximum number of subchannels who can use, according to the sets of both subchannels' and users' choice lists. The choice list can provide the user's (subchannel's) list of the priorities among the set of subchannels (users) for the deferred acceptance algorithm, so as to get a stable assignment in which the femtocell system has the maximum throughput. In a user's (subchannel's) choice list, the priorities among subchannels (users) are sorted in the decreasing order according the set of effective CINRs. By the deferred acceptance algorithm, we can find a stable assignment which can achieve the optimal femtocell throughput for each user with the maximum allowable number of used subchannels. A stable assignment can be specified by the following two definitions.

Definition 1. *An assignment will be called unstable if there are two subchannels* α

Users \ Subchannels	ch_1	ch_2	ch_3	ch_4	ch_5
u_1	5.1	5.3	5.5	5.7	5.9
u_2	11.5	10.7	12.5	10.1	13.1
u_3	13.5	13.7	10.7	12.5	13.3

(a) Effective CINRs (dB) of subchannels for each user

Subchannels \ Order	1st	2nd	3rd
ch_1	u_3	u_2	u_1
ch_2	u_3	u_2	u_1
ch_3	u_2	u_3	u_1
ch_4	u_3	u_2	u_1
ch_5	u_3	u_2	u_1

(b) Choice lists of each subchannel according to effective CINR

Users \ Order	1st	2nd	3rd	4th	5th
u_1	ch_5	ch_4	ch_3	ch_2	ch_1
u_2	ch_5	ch_3	ch_1	ch_2	ch_4
u_3	ch_2	ch_1	ch_5	ch_4	ch_3

(c) Choice lists of each user according to effective CINR

Users \ Subchannels	ch_1	ch_2	ch_3	ch_4	ch_5
u_1	5.1	5.3	■5.5	■5.7	5.9
u_2	11.5	10.7	12.5	10.1	■13.1
u_3	■13.5	■13.7	10.7	12.5	13.3

(d) Assignment outcome

Figure 4.3: An example of the stable assignment with deferred acceptance algorithm. The number of users is $K = 3$, and the number of subchannels is $N = 5$. The maximum allowable number of subchannels for each user is $Q = \{q_{i,1}, q_{i,2}, q_{i,3}\} = [2, 1, 2]$.

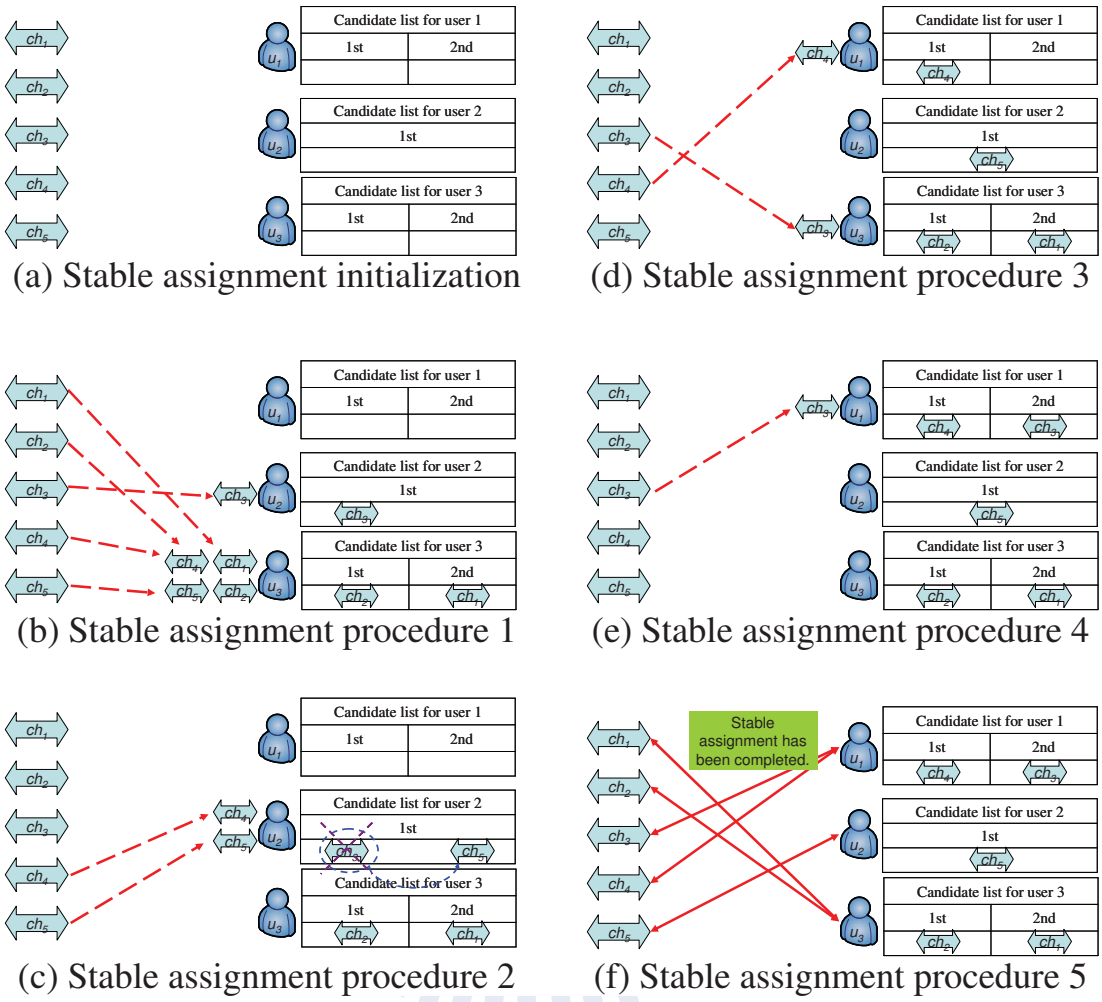

Figure 4.4: The procedures of the stable assignment with deferred acceptance algorithm for the example in Fig. 4.3. In each procedure, each subchannel firstly chooses a user according to its choice list, and then each user decides whether to tentatively accept or to reject depended on the user's choice list. The deferred acceptance procedures are finished when every subchannel is assigned to users or every subchannel has been rejected by every user in the choice list. Meanwhile, each user admits all held subchannels in the candidate list, and the system outputs the assignment outcome.

and β and two users A and B such that

1. Assign subchannel α to user A,

2. Assign subchannel β to user B,

3. In user A's choice list, the priority of subchannel β is higher than that of subchannel α,

4. In subchannel β's choice list, the priority of user A is higher than that of user B.

Definition 2. *An assignment is called stable if there is not any unstable assignment exists.*

An stable subchannel assignment implies that it can achieve the optimal femtocell throughput, and even arbitrarily exchange the matching does not have more throughput than the stable assignment. The procedure of the stable subchannel assignment with the deferred acceptance algorithm is depicted as fellows [12].

- **Initialization**

  1 A set of subchannels $CH = \{ch_1, \ldots, ch_N\}$.

  2 A set of users $U = \{u_1, \ldots, u_K\}$, with the maximum allowable number of used subchannels $Q = \{q_{i,1}, \ldots, q_{i,K}\}$, where $q_{i,k} = N \times (\alpha_k / \sum_{k=1}^{K} \alpha_k) \times QF, \forall i, \forall k$, and $\alpha_k > 0$, $k = 1, \cdots, K$, are selected weights to characterize the desired quality of service. Besides, QF is an adjustable factor to allow more subchannels assigned to users.

  3 N sets of subchannels' choice lists $P_{ch,n} = \{p_{ch,n,1}, \ldots, p_{ch,n,K}\}$, $n = \{1, \ldots, N\}$ in which all users are sorted in decreasing order of effective CINR.

  4 K sets of users' choice lists $P_{u,k} = \{p_{u,k,1}, \ldots, p_{u,k,N}\}$, $k = \{1, \ldots, K\}$ in which all subchannels are sorted in decreasing order of effective CINR.

  5 K empty sets of users' candidate lists for temporarily accepting the matching with subchannels.

- **Deferred Acceptance**

1 Each subchannel is assigned to the first user in its choice list.

2 Each user tentatively accepts the top $q_{i,k}$ subchannels in the choice list, then place on the candidate list. Any remaining subchannels are rejected.

3 The rejected subchannels are assigned to the next user in their choice lists.

4 Each user tentatively accepts the top $q_{i,k}$ in the choice list from among the new and held subchannels, and place on the candidate list. The other subchannels are rejected.

5 **if** every subchannel is assighed to users or every subchannel has been rejected by every user in the choice list,

6 each user admits all held subchannels in the

candidate list and return the assignment outcome.

// the stable assignment has been completed.

7 **else** go to step 3.

We explain these steps by the example in Figs. 4.3 and 4.4. In Fig. 4.3(a), there are $K = 3$ users and $N = 5$ subchannels, and the corresponding effective CINRs are presented. The maximum allowable number of subchannels for each user is $Q = \{q_{i,1}, q_{i,2}, q_{i,3}\} = [2, 1, 2]$. The choice lists for all subchannels and users are sorted in decreasing order of the effective CINRs, as shown in Fig. 4.3(b) and 4.3(c). After the stable assignment is finished, the outcome is output as shown in Fig. 4.3(d). Figure 4.4 shows the procedures of the stable assignment with deferred acceptance algorithm for the example in Fig. 4.3. The procedures are described as follows:

(a) Stable assignment initialization:

- A set of subchannels $CH = \{ch_1, ch_2, ch_3, ch_4, ch_5\}$.
- A set of users $U = \{u_1, u_2, u_3\}$, with the maximum allowable number of used subchannels $Q = \{q_{i,1}, q_{i,2}, q_{i,3}\} = [2, 1, 2]$.
- Five sets of subchannels' choice lists are shown in Fig. 4.3(b).

- Three sets of users' choice lists are shown in Fig. 4.3(c).
- Three empty sets of users' candidate lists for temporarily accepting the matching with subchannels.

(b) Stable assignment procedure 1:

- ch_1 chooses u_3, ch_2 chooses u_3, ch_3 chooses u_2, ch_4 chooses u_3, and ch_5 chooses u_3.
- u_2 accepts ch_3.
- u_3 accepts ch_2 and ch_4, then rejects ch_1, and ch_5.

(c) Stable assignment procedure 2:

- ch_4 chooses u_2, and ch_5 chooses u_2.
- u_2 accepts ch_5, then rejects ch_3 and ch_4.

(d) Stable assignment procedure 3:

- ch_3 chooses u_3, and ch_4 chooses u_1.
- u_1 accepts ch_4.
- u_3 still accepts ch_2 and ch_4, then rejects ch_3.

(e) Stable assignment procedure 4:

- ch_3 chooses u_1.
- u_1 accepts ch_3.

(f) Stable assignment procedure 5: Because every subchannel is assigned to users, each user admits all held subchannels in the candidate list, and the procedure terminates. The assignment outcome is stable and shown in Fig. 4.3(d).

Table 4.1: **The multi-beam OFDMA femtocell system parameters**

Downlink OFDMA Parameters	**Values**
Carrier frequency	2.0 GHz
Macrocell BS (mBS) transmit power	46 dBm
Femtocell BS (fBS) transmit power	20 dBm
Macrocell BS antenna gain $G(\theta)$	14 dB
Macrocell radius (R_m)	500 m
Noise figure (mBS/fBS/UE)	5 dB / 5 dB / 9 dB
System bandwidth (B)	10 MHz
Sampling frequency	11.2 MHz
FFT size (M)	1024
Subcarrier bandwidth	10.9375 kHz
Number of null subcarriers	184
Number of pilot subcarriers	120
Number of data subcarriers (N_{ds})	720
Number of data subchannels (N)	40
Number of subcarriers for each data subchannel (N_d)	18
Guard Fraction (G)	1/8

4.6 Simulation Results

In this section, we investigate the system throughput, fairness index, and delay performance of the different subchannel allocation schemes for the OFDMA-based femtocell system. We compare the switched multi-beam directional antenna system and the 0-dB omnidirectional antenna system. We consider the femtocell sytem as shown in Fig. 4.1. A group of 25 femtocells is uniformly distributed in a macrocell with the coverage radius $R_m = 500$ m. There are 24 femtocells around the considered femtocell. The separation distance between two nearest femtocells is $d_{sf} = 20$ m. We assume that the femtocell base station provides the service for the K authorized users within the house. In each femtocell, $N = 40$ subchannels are allocated to these K femtocell users, and assume that the adjustable factor of the stable subchannel allocation scheme is $QF = 1.5$. We consider the shared spectrum allocation scheme for the femtocell sytem. In addition, we assume a fully-loaded macrocell system, where the macrocell users use all the subcarriers and thus the femtocell user is interfered by the macrocell system. The nominal system parameters for the considered OFDMA-based femtocell are listed in Table 4.1 [59].

4.6.1 Impacts of Subchannel Allocation and Directional Antenna on Femtocell Throughput

Figure 4.5 shows the femtocell throughput against the total number K of indoor users in each femtocell. From the figure, we have the following observations.

1) When the number of users increases, the average femtocell throughput improves because of the multi-user diversity gain. In the omnidirectional antenna system, compared to that at $K = 1$, the average femtocell throughput at $K = 6$ can be improved by 54%, 40%, 37%, 37%, 33%, and 10% for the channel-oriented, proportional fair, exponential rule, queue-based exponential rule, stable, and user-oriented subchannel allocation schemes, respectively.

2) The channel-oriented subchannel allocation scheme has the best throughput,

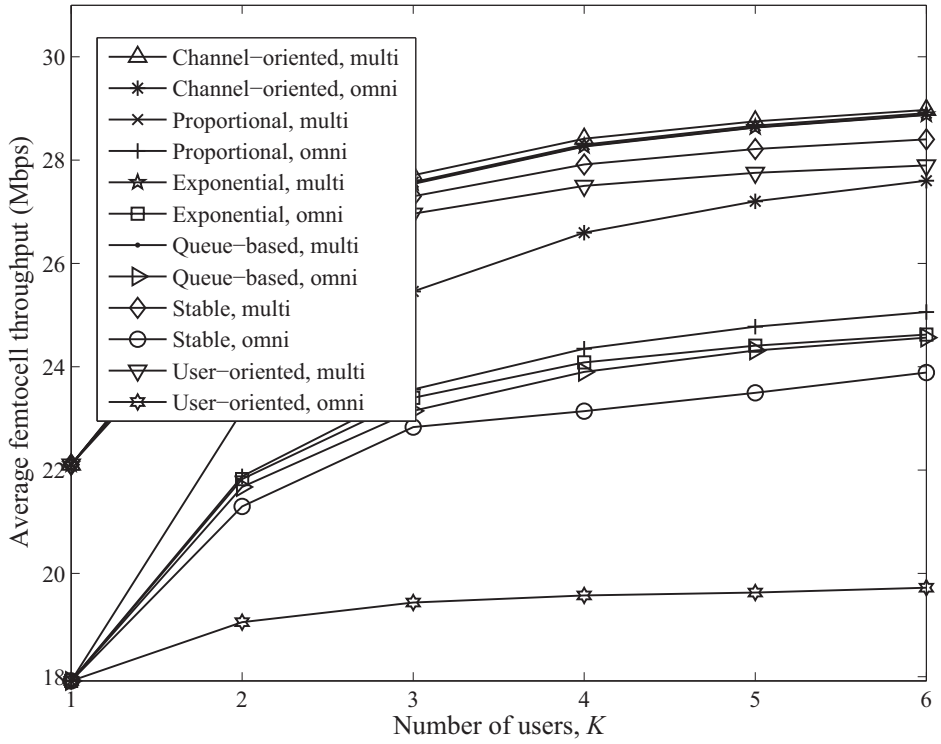

Figure 4.5: Average femtocell throughput versus number of users K.

while the user-oriented subchannel allocation scheme has the lowest throughput for both the switched multi-beam antenna and the omnidirectional antenna systems. In addition, our proposed stable subchannel allocation scheme approximately performs as well as the other three subchannel allocation schemes, and the throughput performances of them are between that of the channel-oriented subchannel allocation scheme and that of user-oriented subchannel allocation scheme. For the omnidirectional antenna system, the stable subchannel allocation scheme can improve the average femtocell throughput by 21%, compared to the user-oriented subchannel allocation scheme when $K = 6$.

3) Thanks to the advantages of the higher antenna gain to enhance the signal strength and narrow beam pattern to reduce the femto-to-femto interference, the switched multi-beam antenna system can further improve the throughput compared to the omnidirectional antenna system. In this example, compared to the omnidirectional antenna at $K = 6$, the switched multi-beam antenna can improve the average femtocell throughput by 5%, 15%, 17%, 18%, 20%, and 42% for the channel-oriented, proportional fair, exponential rule, queue-based exponential rule, stable, and user-oriented subchannel allocation schemes, respectively. Therefore, the switched multi-beam antenna diminishes the difference of the throughput performance for all subchannel allocation schemes. For example, the largest difference in throughput among the six schemes is 4% and 40% for the switched multi-beam antenna system and for the omnidirectional antenna system, respectively.

4.6.2 Impacts of Subchannel Allocation and Directional Antenna on Fairness

Figure 4.6 shows the average Jain's fairness index against the total number K of indoor users in each femtocell. The Jain's fairness index can indicate how fair the system is from the long-term viewpoint. From the figure, we have the following observations.

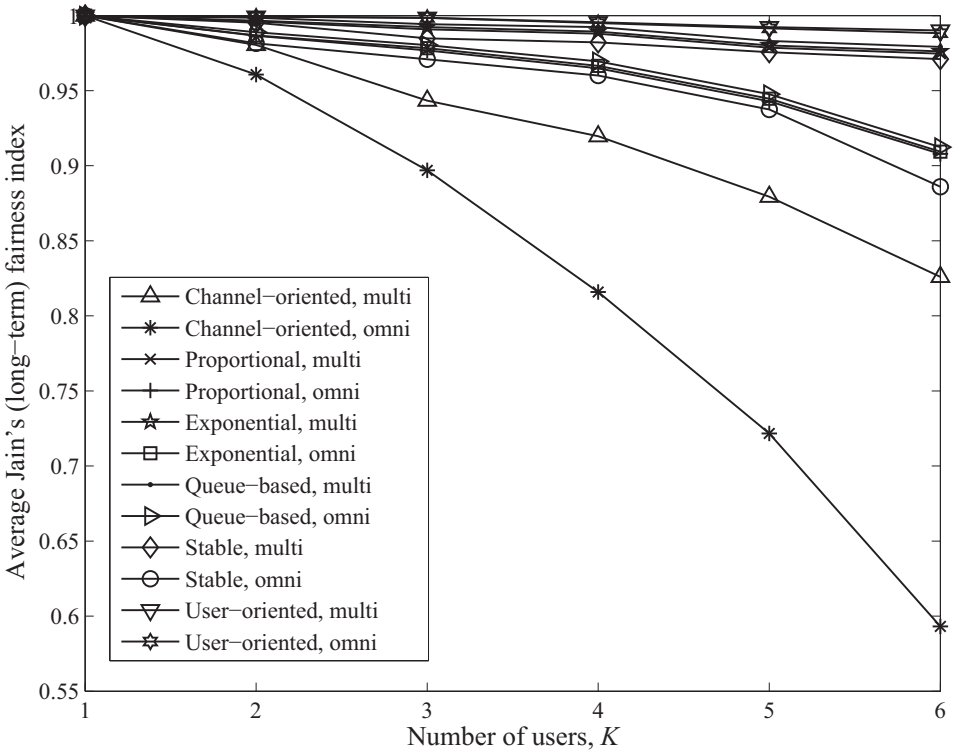

Figure 4.6: Average Jain's fairness (long-term) index versus number of users K.

1) From the long-term standpoint, the user-oriented subchannel allocation scheme can achieve the fairest allocation among active users, while the channel-oriented subchannel allocation scheme has the worst fairness index. In addition, the stable subchannel allocation scheme has similar fairness performance with the exponential rule, the queue-based exponential rule and the proportional fair subchannel allocation schemes. In this figure, compared to the channel-oriented subchannel allocation scheme at $K = 6$, the stable subchannel allocation scheme can raise the Jain's fairness index by 49% and 18% for the omnidirectional antenna system and for the switched multi-beam antenna system, respectively.

2) Interestingly, the switched multi-beam antenna system is fairer than the omnidirectional antenna system form the long-term standpoint. It implies that the switched multi-beam antenna is more effective than the omnidirectional antenna in improving the long-term fairness. For example, compared to the omnidirectional antenna system at $K = 6$, the switched multi-beam antenna can achieve 39% and 10% higher Jain's fairness index for the channel-oriented subchannel allocation scheme and the stable subchannel allocation scheme, respectively.

Figure 4.7 shows the average Wang's fairness index against the total number K of indoor users in each femtocell. The Wang's fairness index can tell how fair the system is from the short-term viewpoint. Based on (4.10), the smaller the Wang's fairness index, the fairer is the system. Actually, the short-term fairness implies the long-term fairness. Nevertheless, the long-term fairness may not be short-term fair even if the subchannel allocation scheme in the system has achieved long-term fairness. We have the following observations from the figure.

1) From the short-term perspective, the queue-based exponential rule subchannel allocation scheme has the fairest allocation for the active users, while the channel-oriented subchannel allocation scheme has the worst Wang's fairness index. Moreover, the stable subchannel allocation scheme can achieve better

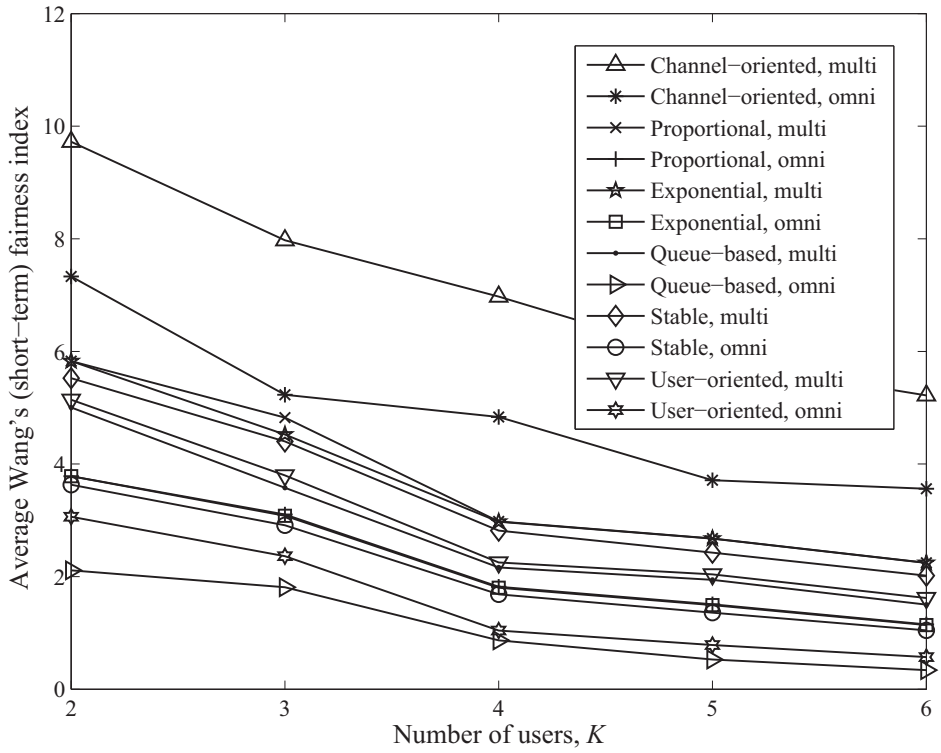

Figure 4.7: Average Wang's (short-term) fairness index versus number of users K.

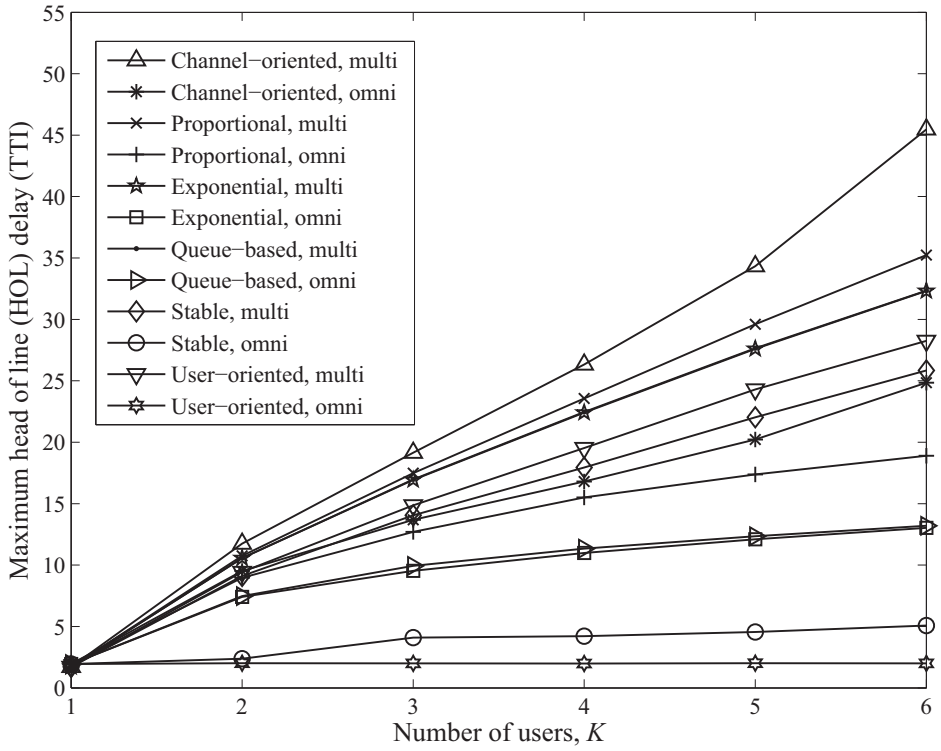

Figure 4.8: Maximum head of line (HOL) delay versus number of users K.

fairness index than the exponential rule and the proportional fair subchannel allocation schemes.

2) Note that the omnidirectional antenna system can achieve better short-term fairness then the switched multi-beam antenna system for active users. This is because the switched multi-beam antenna system only serves the active user in the coverage of antenna beam pattern, but not all the femtocell users in the house. However, the switched multi-beam antenna system can achieve better throughput than the omnidirectional antenna system, as shown in Fig. 4.5.

4.6.3 Impacts of Subchannel Allocation and Directional Antenna on Delay

Figure 4.8 shows the delay performance in terms of maximum HOL delay for the waiting period of users from the time of receiving service to the next time of receiving service. From the figure, we have the following observations.

1) The HOL delay increases as the number of users increases because of the higher traffic load caused by more active users. Moreover, the channel-oriented subchannel allocation scheme has the worst HOL delay performance.

2) Noteworthy, the user-oriented subchannel allocation scheme and the stable subchannel allocation scheme has the best HOL delay performance in the omnidirectional antenna system and in the switched multi-beam antenna system, respectively.

3) Both the queue-based exponential rule subchannel allocation scheme and the exponential rule subchannel allocation scheme have the same HOL delay performance, and perform better than the proportional fair subchannel allocation scheme. Nevertheless, the stable subchannel allocation scheme has better HOL delay performance than the exponential rule, the queue-based exponential rule and the proportional fair subchannel allocation scheme.

4.6.4 Summary

Figures 4.5, 4.6, 4.7, and 4.8 clarify that the stable subchannel allocation scheme well achieves the tradeoff between throughput and throughput fairness, and has the best HOL delay performance compared to the other schemes. In general, the channel-oriented subchannel allocation scheme assigns a subchannel to the user which can achieve the best CINR for the subchannel, thereby enhancing the throughput. On the contrary, in the user-oriented subchannel allocation scheme, the users select the subchannel with the best CINR by turns. The selection sequence for users significantly affects the femtocell throughput because the subchannel selected by the

preceding user can not be reassigned to another user, even if the overall throughput may be improved after rearrangement. Therefore, the user-oriented subchannel allocation scheme sacrifices the overall throughput to achieve better throughput fairness. Different from the traditional allocation methods, we can limit the maximum allowable number of subchannels used by a user in the stable subchannel allocation method to improve the fairness and HOL delay performance. Besides, with the deferred acceptance algorithm to *repeatedly* rearrange the channel allocation, the proposed stable subchannel allocation method can improve the overall throughput. Consequently, the goals of throughput improvement, fairness and delay performance can be fulfilled by using the developed stable subchannel allocation method.

Table 4.2 shows the comparison of subchannel allocation schemes for the OFDMA femtocells in terms of the throughput, fairness, and HOL delay performance. As summarized in Table 4.2, the proposed stable subchannel allocation scheme outperforms all the existing schemes in terms of HOL delay performance.

Table 4.2: **Comparison of various subchannel allocation schemes for OFDMA femtocells**

Subchannel allocation schemes	Femtocell throughput	Long-term fairness	Short-term fairness	HOL delay performance
Channel-oriented, omni	Good	Poor	Poor	Good
User-oriented, omni	Poor	Excellent	Good	Excellent
Proportional fair, omni	Acceptable	Good	Good	Good
Exponential rule, omni	Acceptable	Good	Good	Good
Queue-based exponential rule, omni	Acceptable	Good	Excellent	Good
Stable, omni	Acceptable	Good	Good	Excellent
Channel-oriented, multi	Excellent	Poor	Poor	Poor
User-oriented, multi	Good	Excellent	Good	Good
Proportional fair, multi	Excellent	Good	Acceptable	Acceptable
Exponential rule, multi	Excellent	Good	Acceptable	Acceptable
Queue-based exponential rule, multi	Excellent	Good	Good	Acceptable
Stable, multi	Excellent	Good	Good	Good

Comparison level: excellent > good > acceptable > poor

Chapter 5

Overload Control for Machine Type Communications (MTC) Femtocell Networks

In this chapter, we propose a group-based time control mechanism to solve the CN congestion problem in the MTC femtocell network. We divide the MTC devices into several groups, and dedicate each group with a granted time interval. In a granted time interval, only MTC devices in the corresponding group can access the network. Therefore, the group-based time control method can spread the traffic load of MTC devices over the time to reduce the traffic peak, and mitigate both CN and RAN overload. However, if the number of group is large (i.e., smaller group size), the overall message delay may increase due to the longer cycle time. Therefore, we investigate the impacts of arrival rate and group size (group number) on the RAN overload probability, CN overload probability, successful transmission probability and message delay. We also develop an adaptive joint access probability adjustment and group rearrangement method to implement the proposed group-based time control mechanism. Numerical results show that our group-based time control mechanism can control both CN and RAN overload, and improve the successful transmission probability and message delay of MTC devices.

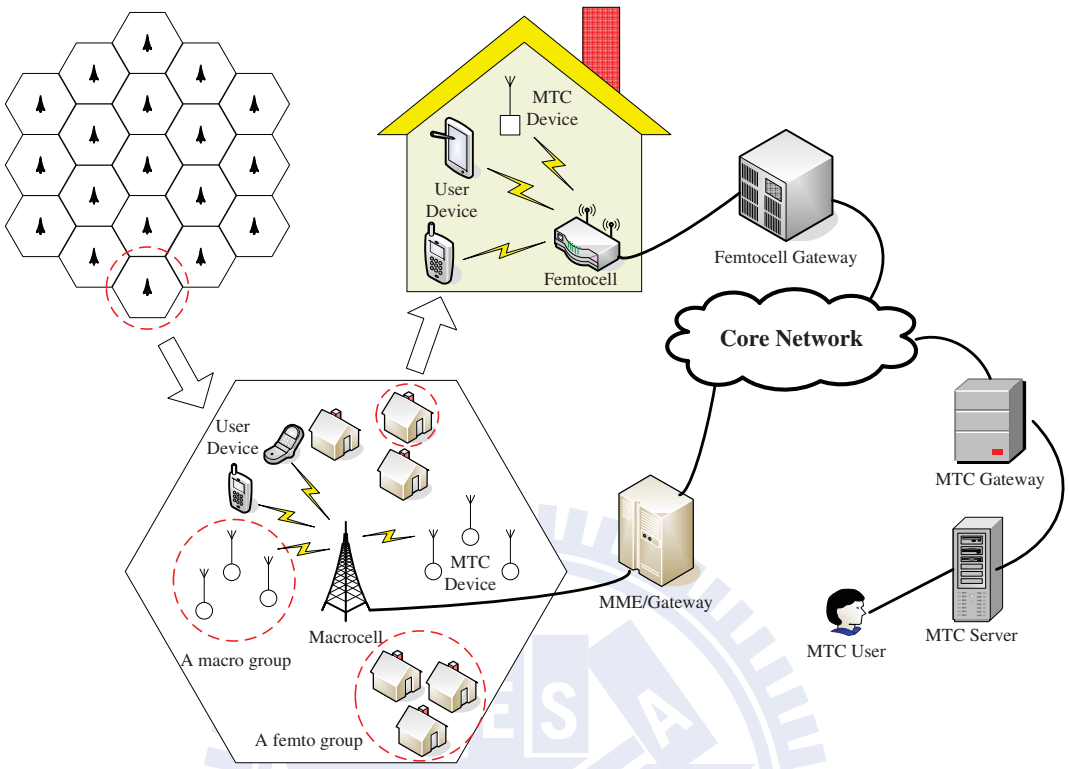

Figure 5.1: Femtocell-based machine type communications (MTC) network architecture.

5.1 System Model

5.1.1 System Architecture

The femtocell-based machine type communications (MTC) network is considered as shown in Fig. 5.1. We assume that $N_{MTC,tot}$ MTC devices are distributed over the N_{Macro} macrocell coverages and served by the same MTC server. For each macrocell coverage, there are N_{Femto} houses, that is, $N_{Macro} \times N_{Femto}$ femtocell base stations are overlaid with the macrocell. Moreover, $N_{MD,M}$ outdoor MTC devices are deployed in each macrocell coverage, and $N_{MD,F}$ indoor MTC devices are deployed in each house.

Both the outdoor and indoor MTC devices collect the information and send to the MTC server cyclically. For the outdoor environment, the MTC devices can

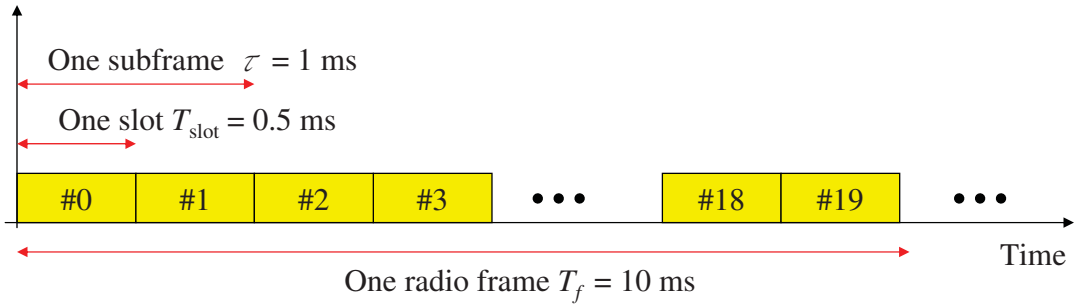

Figure 5.2: Radio Frame Structure.

access to the serving macrocell base station and connect to the core network so that the desired information can arrival in the MTC server. Similarly, the indoor MTC devices can connect to the core network by the access to the femtocell base station. Therefore, all the information from indoor and outdoor MTC devices can be reliably transferred to the MTC server except for the network congestion.

5.1.2 Random Access Resource

We consider the radio frame structure provided by 3GPP [64] as shown in Fig. 5.2. Each radio frame has the duration of 10 ms, and consists of 20 time slots of length $T_{slot} = 0.5$ ms. Two consecutive time slots comprise a subframe.

The random access procedure consists of two parts: preamble and message parts [65]. In the preamble part, the device transmits a preamble in the random-access window (i.e., the first subframe of the radio frame). Then, if the preamble can be detected, the base station transmits a respond to indicate the uplink resource allocation used for the transmission in the message part. If the preamble can not be detected by the base station, the device will not receive any respond for a period, and need to transmit a new preamble in the next random-access window. In the message part, the device builds the radio resource control (RRC) connection setup according to the assigned resource, and transmits the message.

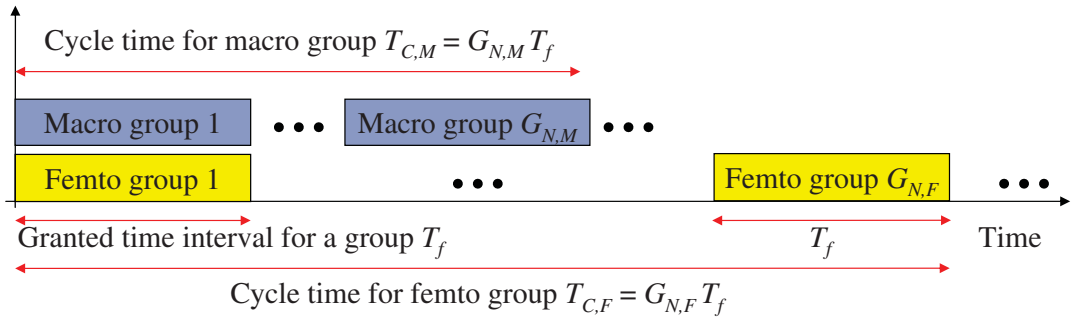

Figure 5.3: Group-based Time Control Mechanism in Femtocell-based MTC Network.

5.2 Overload Control in Femtocell-based MTC Networks

5.2.1 Grouping

In the femtocell-based MTC network, we assume that all the MTC devices can be categorized into two groups: macro groups and femto groups, as shown in Fig. 5.1. All MTC devices served by macrocells are partitioned into macro groups, and all MTC devices served by femtocells are partitioned into femto groups. Moreover, MTC devices in a femtocell are grouped into the same femto group, to reduce total signaling overhead. In each macrocell coverage, each macro group consists of $G_{S,M}$ MTC devices, and each femto group comprises $G_{S,F}$ femtocell base stations. Correspondingly, there are total $G_{N,M}$ macro groups and $G_{N,F}$ femto groups in the femtocell-based MTC network.

5.2.2 Group-Based Time Control Mechanism

Figure 5.3 shows the conception of the group-based time control mechanism in the femtocell-based MTC network. As shown in Fig. 5.3, all the MTC devices are divided into $G_{N,M}$ macro groups and $G_{N,F}$ femto groups, respectively. The CN

only allows the accesses of a group of MTC devices within an allocated time period (i.e., granted time interval). For the convenience, we assume that all groups have the same granted time interval T_f, and we align the granted time interval for the groups. Let all the macro/femto groups have their granted time interval in sequence. Therefore, in the specified granted time interval, the active MTC device can select a random-access preamble to send the connection request.

The granted time interval of each macro/femto group is repeatedly allocated in every cycle time. The cycle time of macro groups and femto groups are defined as $T_{C,M} = G_{N,M} \times T_f$ and $T_{C,F} = G_{N,F} \times T_f$, respectively. Thus, the MTC device can cyclically send the connection request if the MTC device has the message to transmit. However, the transmission may be failure when RAN or CN congestion occurs. If the transmission is failure, the MTC device needs to wait at least a cycle time for it's granted time interval, and sends the connection request again. The MTC device sends the connection request *repeatedly* and *cyclically* until the transmission is successful. If a new message generates, the MTC device only transmits the last message to the MTC server.

5.3 Analysis of Overload Probability and Message Delay

Network congestion occurs because a large number of MTC devices generate the information and forward to the MTC server simultaneously. In general, there are radio access network (RAN) congestion and core network (CN) congestion for the femtocell-based MTC network. The RAN congestion usually happens in a specific base stations as a large number of outdoor/indoor MTC devices access the same macrocell/femtocell base station. However, the CN congestion may occur in the core network or on the link between the core network and the MTC server when a high number of outdoor/indoor MTC devices transfer information from the numerous cell coverage to the single MTC server. The serious CN congection may cause the intolerable delays, packet loss, or even service unavailability. In the following, we

analyze the overload probability and the message delay in the femtocell-based MTC systems.

5.3.1 Overload Probability

Assume that the message generation for a MTC device is Poisson arrival, and the interarrival time of the message generation is exponential distribution with mean $1/\lambda$. For the small λ, assume that at most one message is generated in a cycle time, and only one message is transmitted in each granted time interval T_f. Due to the "small data transmissions feature" of MTC, we assume that a message can be transmitted completely in a granted time interval T_f, and each connection period is T_f. Let $p_{t,M}$ and $p_{t,F}$ be the transmission probability of each MTC device for the macro group and for the femto group, respectively. Then, $p_{t,M}$ and $p_{t,F}$ can be expressed as

$$p_{t,M} = 1 - p_{0,M}(T_{C,M} = G_{N,M}T_f) = 1 - e^{-\lambda G_{N,M}T_f} \tag{5.1}$$

$$p_{t,F} = 1 - p_{0,F}(T_{C,F} = G_{N,F}T_f) = 1 - e^{-\lambda G_{N,F}T_f} \tag{5.2}$$

where $p_{0,M}$ and $p_{0,F}$ are the probability that there are no message generated in the period of the cycle time for the MTC device in the macro group and femto group, respectively.

The probability that x MTC devices connect to the macrocell base station in one macro group can be expressed as

$$p_X(x) = \begin{pmatrix} G_{S,M} \\ x \end{pmatrix} p_{t,M}^x (1 - p_{t,M})^{G_{S,M}-x} \tag{5.3}$$

where $x = 0, \ldots, G_{S,M}$.

For a macrocell base station, as the RAN overload occurs, only $C_{RAN,M}$ MTC devices can send their messages. Therefore, macrocell base station can handle at most $C_{RAN,M}$ connection requests in the RAN overload situation, or at most $G_{S,M}$ connection requests if the RAN is not overloaded. For each macrocell base station, the probability set that there are x MTC devices connect to the CN can be express

as

$$P_{M,\alpha} = \begin{cases} [p_X(0), \ldots, p_X(C_{eNB}-1), \sum_{x=C_{eNB}}^{G_{S,M}} p_X(x)], \\ \qquad\qquad \text{if} \quad \mathrm{G_{S,M}} > \mathrm{C_{eNB}} \\ [p_X(0), \ldots, p_X(G_{S,M}-1), p_X(G_{S,M})], \\ \qquad\qquad \text{if} \quad \mathrm{G_{S,M}} \leq \mathrm{C_{eNB}} \end{cases} \tag{5.4}$$

where $\alpha = 1, \ldots, N_{Macro}$.

In the CN, there are at most $N_{Macro} \times C_{RAN,M}$ connection requests from the macrocell base stations. Therefore, the probability that there are 1 to $N_{Macro} \times C_{RAN,M}$ MTC devices connect to the CN in the macro group can be expressed as

$$P_M = P_{M,1} * P_{M,2} * \cdots * P_{M,N_{Macro}} \tag{5.5}$$

where $*$ is the convolution operator.

It is assumed that the RAN overload does not occur in the femtocell because the number of MTC devices in each house is limited. Therefore, there are at most $N_{Macro} \times G_{S,F} \times N_{MD,F}$ connection requests come to the CN from all the femtocell base stations. The probability that y MTC devices send connect requests to the CN in one femto group can be expressed as

$$p_Y(y) = \begin{pmatrix} \beta \\ y \end{pmatrix} p_{t,F}^{y} (1 - p_{t,F})^{\beta - y} \tag{5.6}$$

where $\beta = N_{Macro} \times G_{S,F} \times N_{MD,F}$, and $y = 0, \ldots, \beta$.

Similarly, the probability set that there are 1 to β MTC devices connect to the CN in the femto group can be expressed as

$$p_F = [p_Y(0), \ldots, p_Y(\beta - 1), p_Y(\beta)] \tag{5.7}$$

For the CN, all the connection requests come from all the macrocell and femtocell base stations. Therefore, the probability set that each number of connection requests from all the macrocell and femtocell base stations can be express as

$$p_Z = p_M * p_F \tag{5.8}$$

Let the capacity of one macrocell base station, that of one femtocell base station, and that of the MTC server be C_{eNB}, C_{HeNB}, and C_{MTC}, respectively. To minimize the impact on human-to-human (H2H) communications, assume that only $\mu\%$ of C_{eNB}, $\nu\%$ of C_{HeNB}, and $\eta\%$ of C_{MTC} can be used in the MTC network. Then, we define the RAN overload and CN overload as follows.

Definition 3. *RAN overload: if the number of random-access requests received by the macrocell/femtocell base station in a granted time interval is larger than the capacity threshold of macrocell/femtocell base station for the MTC network. In this situation, only ($C_{RAN,M} = C_{eNB} \times \mu\%$) and ($C_{RAN,F} = C_{HeNB} \times \nu\%$) MTC devices can send their messages through the macrocell and femtocell base stations, respectively.*

Definition 4. *CN overload: if total number of connection requests from all MTC devices to the MTC server in a granted time interval is larger than the capacity threshold of the MTC server. Meanwhile, only ($C_{CN} = C_{MTC} \times \eta\%$) MTC connections can be handled by the MTC server.*

According to the Definitions 3 and 4, the macrocell RAN overload probability $P_{RAN,M}$ and the CN overload probability P_{CN} are given as

$$P_{RAN,M} = 1 - \sum_{x=0}^{C_{RAN,M}} p_X(x) \tag{5.9}$$

$$P_{CN,M} = 1 - \sum_{z=0}^{C_{CN}} p_Z(z) \tag{5.10}$$

5.3.2 Message Delay

The message delay is defined as the elapsed time from the instant of the message generation to that of the message reception at the MTC server. Therefore, the delay includes the time of waiting for the granted time interval and the access delay. Moreover, the average waiting time for the granted time interval are $T_{C,M}/2$ and $T_{C,F}/2$ for the macro groups and for the femto groups, respectively.

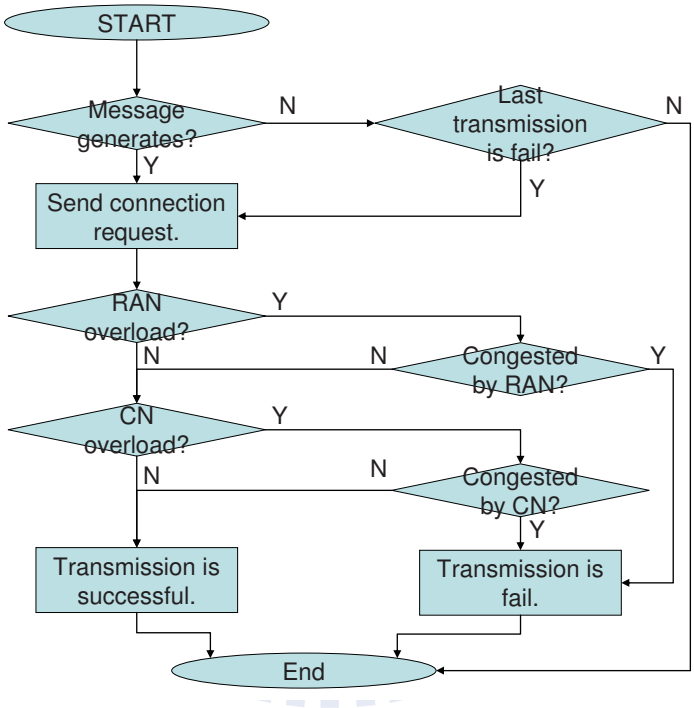

Figure 5.4: The procedure for a single MTC device to transmit the message to the MTC server in the granted time interval.

Figure 5.4 shows the procedure that a MTC device accesses the network and transmits the message to the MTC server in the granted time interval. If a message is generated, the MTC device will send the connection request in the granted time interval of it's group. If the RAN overload or CN overload occurs, the access may be failure. For macrocell RAN overload, only $C_{RAN,M}$ MTC devices can send their messages, while only C_{CN} MTC devices' messages can be handled by the MTC server for CN overload. Then, the redundant connection requests are dropped by the RAN or CN, and the transmission is failure. If the transmission is failure, the MTC device must wait a cycle time period ($T_{C,M}$ or $T_{C,F}$) for sending the connection request again.

For the convenience to determine the access delay, we define some parameters as follows.

- $P_{CFP,RAN}$: The connection failure probability on the condition of RAN overload.
- $P_{CFP,CN}$: The connection failure probability on the condition of CN overload.
- $\gamma_{RAN,M}$: The average number of failure connections in a macrocell base station because of macro RAN congestion.
- $\gamma_{CN,M}$: The average number of failure connections in a macrocell base station because of CN congestion.
- $\gamma_{CN,F}$: The average number of failure connections in a femtocell base station because of CN congestion

According the above definitions, we have the following three equations.

$$\gamma_{RAN,M} = \max\{0, (G_{S,M} - \gamma_{RAN,M} - \gamma_{CN,M})p_{t,M} + \gamma_{RAN,M} + \gamma_{CN,M} - C_{CN}\} \tag{5.11}$$

$$N_{Macro}\gamma_{CN,M} + N_{Macro}G_{S,F}\gamma_{CN,F} = \max\{0, N_{Macro}X + N_{Macro}G_{S,F}Y - C_{CN}\} \tag{5.12}$$

$$N_{Macro}\gamma_{CN,M} : N_{Macro}G_{S,F}\gamma_{CN,F} = N_{Macro}X : N_{Macro}G_{S,F}Y \tag{5.13}$$

where

$$\begin{cases} X = (G_{S,M} - \gamma_{RAN,M} - \gamma_{CN,M})p_{t,M} + \gamma_{CN,M} \\ Y = (N_{MD,F} - \gamma_{RAN,F} - \gamma_{CN,F})p_{t,F} + \gamma_{CN,F} \end{cases} \tag{5.14}$$

By iterative operation, we can obtain $\gamma_{RAN,M}$, $\gamma_{CN,M}$, and $\gamma_{CN,F}$. Therefore, the connection failure probability $P_{CFP,RAN}$ and $P_{CFP,CN}$ can be given by

$$P_{CFP,RAN} = \frac{\max\{0, X + \gamma_{RAN,M} - C_{CN}\}}{X + \gamma_{RAN,M}} \tag{5.15}$$

$$P_{CFP,CN} = \frac{\max\{0, N_{Macro}X + N_{Macro}G_{S,F}Y - C_{CN}\}}{N_{Macro}X + N_{Macro}G_{S,F}Y} \tag{5.16}$$

Let $T_{A,M}$ and $T_{A,F}$ be the access time for the MTC device of the macro group and that of the femto group, respectively. Therefore, we can determine the the access time $T_{A,M}$ and $T_{A,F}$ according to the connection failure probability $P_{CFP,RAN}$ and $P_{CFP,CN}$.

$$T_{A,M} = \frac{1 - P_{S,M}}{P_{S,M}}T_{C,M} + T_f \tag{5.17}$$

$$T_{A,F} = \frac{1 - P_{S,F}}{P_{S,F}}T_{C,F} + T_f \tag{5.18}$$

where

$$P_{S,M} = 1 - (P_{RAN,M}P_{CFP,RAN} + P_{CN}P_{CFP,CN} - P_{RAN,M}P_{CFP,RAN}P_{CN}P_{CFP,CN}) \tag{5.19}$$

$$P_{S,F} = 1 - (P_{CN}P_{CFP,CN}) \tag{5.20}$$

$P_{S,M}$ and $P_{S,F}$ are the successful transmission probability for MTC devices of macro groups and femto groups, respectively. Finally, the average message delay of the macro group D_M and that of the femto group D_F are given by

$$D_M = \frac{T_{C,M}}{2} + T_{A,M} \tag{5.21}$$

$$D_F = \frac{T_{C,F}}{2} + T_{A,F} \tag{5.22}$$

5.4 Adaptive Joint Access Probability Adjustment and Group Rearrangement Method

In this section, we develop a adaptive joint access probability adjustment and group rearrangement mechanism to implement the overload control in the femtocell-based MTC networks. The mechanism contains two part: adaptive access probability adjustment and adaptive group rearrangement. We detail the method as follows.

5.4.1 Adaptive Access Probability Adjustment

In the part of the adaptive access probability adjustment, we assume that the MTC devices can autonomously adjust the access probability to decrease the RAN collision and CN congestion. From Fig. 5.4, the message transmission from a MTC device to the MTC server may fail due to the RAN congestion or CN congestion. As the transmission is fail, the MTC device needs to send the connection request again. However, the re-transmission is possibly fail again since the RAN or CN is still overload. Therefore, MTC devices can adaptively adjust the access probability to mitigate the RAN and CN overload. The access probability $P_{a,j}$ can be divided into J levels, where $P_{a,1} > P_{a,2} > \cdots > P_{a,J}$. $P_{a,1}$ is the maximum access probability, and $P_{a,J}$ is the minimum access probability. If the transmission is fail, the MTC device adjusts the access probability $P_{a,j}$ to $P_{a,j+1}$. Otherwise, the MTC device adjusts the access probability $P_{a,j}$ to $P_{a,j-1}$ as the transmission is successful. By adaptively

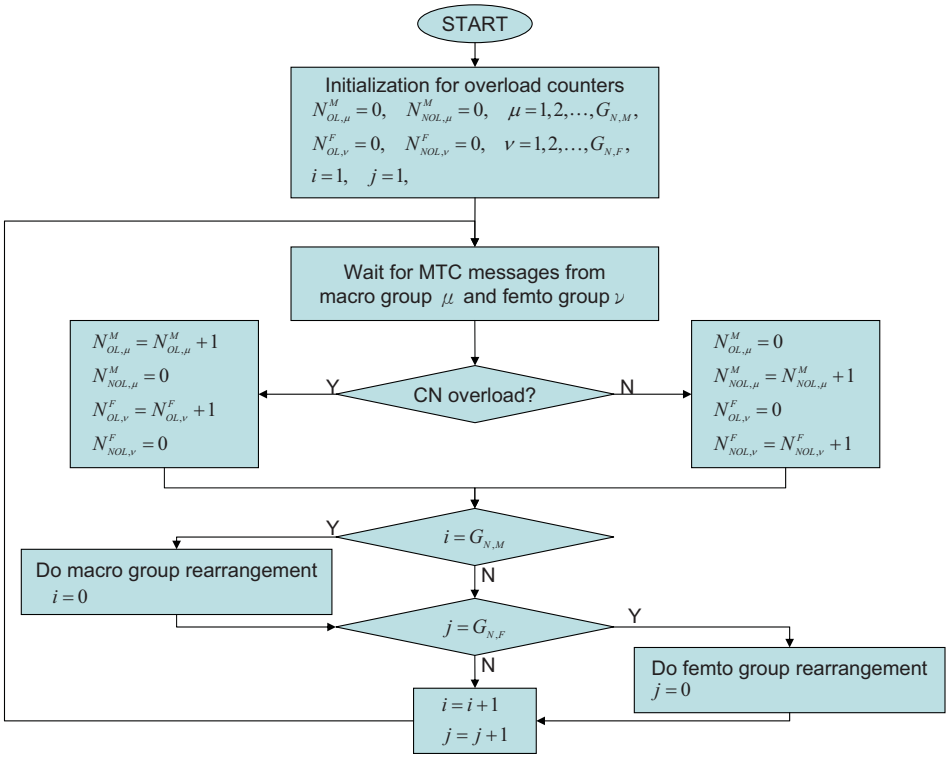

Figure 5.5: The mechanism for the MTC server to rearrange the groups in the adaptive joint access probability adjustment and group rearrangement method.

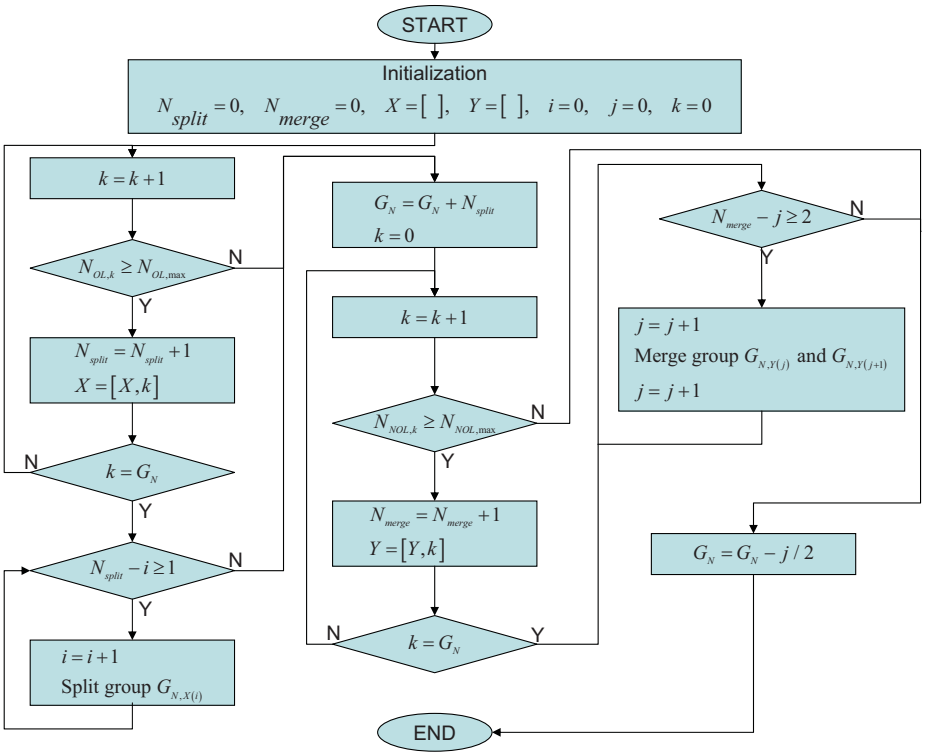

Figure 5.6: The procedure of the group rearrangement in the adaptive joint access probability adjustment and group rearrangement method. Both group splitting and group merging are considered in the group rearrangement procedure.

adjusting the access probability, the RAN and CN congestions can be eased from the MTC device's standpoint.

5.4.2 Adaptive Group Rearrangement

In the part of the adaptive group rearrangement, we assume that the MTC server can adaptively arrange the grouping for macro and femto groups to control the CN congestion based on the present traffic in the CN. Figure 5.5 illustrates the procedure of the adaptive group rearrangement mechanism for the MTC server. We assume that the MTC server have two counters for each group to count the number of cycles that the CN overload consecutively occurs or not. $N^M_{OL,\mu}$ and $N^F_{OL,\nu}$ denote the number of cycles that the CN overload occurs *consecutively* for the μth macro group and the νth femto group, respectively. $N^M_{NOL,\mu}$ and $N^F_{NOL,\nu}$ represent the number of cycles that the CN overload does NOT occur consecutively for the μth macro group and the νth femto group, respectively. During a granted time interval, the MTC devices in the μth macro group and the νth femto group may send the connection requests to the MTC server through the CN. Therefore, the CN overload may occur due to the massive concurrent transmissions. If CN overload occurs, we add one to the overload counters $N^M_{OL,\mu}$ and $N^F_{OL,\nu}$, and the non-overload counters $N^M_{NOL,\mu}$ and $N^F_{NOL,\nu}$ are modified to zero, and vice versa. Based on the outcome of the overload counters at the end of each group cycle time, the MTC server executes the group rearrangement procedure, as shown in Fig. 5.6.

The group rearrangement procedure in Fig. 5.6 includes the group splitting and group merging processes. The MTC server decides whether to split a group or to merge groups based on the outcome of the overload counters for each groups and the predefined count thresholds $N_{OL,\max}$ and $N_{NOL,\max}$. For a given group μ, if the times of the consecutive CN overload occurrences are more than the predefined overload count threshold, i.e., $N_{OL,\mu} \geq N_{OL,\max}$, the MTC server divides equally the group μ into two groups with the half the original group size. Similarly, for two given groups μ and ν, if the times of the consecutive CN non-overload occurrences are more than the predefined non-overload count threshold, i.e., $N_{NOL,\mu} \geq N_{NOL,\max}$

and $N_{NOL,\nu} \geq N_{NOL,\max}$, the MTC server combines the group μ with the group ν to be a new group. By adaptively rearrange the macro and femto groups, the MTC server can effectively control the CN overload.

5.5 Numerical Results

In this section, we show performance improvements of the group-based time control mechanism for the femtocell-based MTC network systems subject to the massive concurrent transmissions from the MTC devices to a single MTC server. We investigate the effect of femtocells on macrocell's RAN congestion. The impact of the arrival rate is also discussed. Moreover, we apply the developed adaptive joint access probability adjustment and group rearrangement method to implement the overload control of the MTC femtocell network. The simulation results of the developed method are shown in terms of the group size, successful transmission probability and message delay.

We consider the femtocell-based MTC network as shown in Fig. 5.1. Total $N_{MTC,tot} = 30000 \times 19 = 570000$ MTC devices are distributed over the $N_{Macro} = 19$ macrocell coverages and served by the same MTC server. For each macrocell coverage, $N_{Femto} = 5000$ femtocell base stations are overlaid with the macrocell. In addition, there are $N_{MD,M} = 5000$ outdoor MTC devices in each macrocell coverage, and $N_{MD,F} = 5$ indoor MTC devices deployed in each house, respectively. All results are simulated by MATLAB. The nominal system parameters for the considered femtocell-based MTC network are listed in Table 5.1. The overload probability threshold and the minimum successful transmission reliability requirement are 0.1 and 0.9, respectively.

5.5.1 Impacts of Group-Based Time Control

Figure 5.7 shows the overload probability against the arrival rate λ. In this case, we assume that each macro group consists of $G_{S,M} = 50$ MTC devices, and each femto group comprises $G_{S,F} = 40$ femtocell base stations in each macrocell cover-

Table 5.1: **MTC femtocell network system parameters**

Parameters	**Values**
Number of macrocell coverages, N_{Macro}	19
Number of total MTC devices, $N_{MD,tot}$	570000
Number of femtocell in each macrocell coverage, N_{Femto}	5000
Number of outdoor MTC devices in each macrocell coverage, $N_{MD,M}$	5000
Number of indoor MTC devices in each house, $N_{MD,F}$	5
Capacity of one macrocell base station, C_{eNB}	800 connections
Capacity of one femtocell base station, C_{HeNB}	200 connections
Capacity of the MTC server, C_{MTC}	15200 connections
Ratios of available capacity for macrocell base staion, femtocell base station, and MTC server, $\mu/\nu/\eta$	0.25
Overload probability threshold	0.1
Minimum transmission reliability requirement	0.9
Predefined overload count threshold, $N_{OL,\max}$	5
Predefined non-overload count threshold, $N_{NOL,\max}$	30

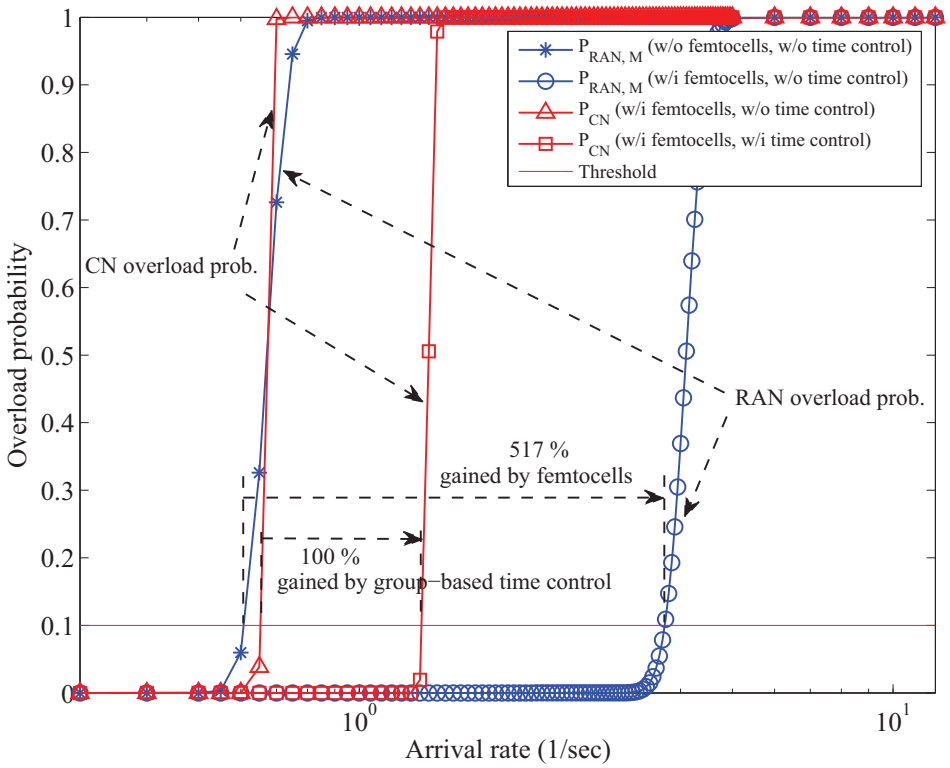

Figure 5.7: Overload probability versus arrival rate, where 950 MTC device in each macro group and 760 femtocell base stations in each femto group are considered for the femtocell-based MTC network.

age. Namely, for the femtocell-based MTC network, each macro group has $G_{S,M} \times N_{Macro} = 950$ MTC devices, and each femto group has $G_{S,F} \times N_{Macro} = 760$ femtocell base stations. Therefore, there are total $G_{N,M} = 100$ macro groups and $G_{N,F} = 125$ femto groups in the femtocell-based MTC network. From the figure, we have the following observations.

1) Femtocells are helpful to solve the RAN congestion for macrocell base stations. Under the overload probability threshold requirement, the macrocell with femtocells can support 517% higher arrival rate, compared to the macrocell without femtocells.

2) The group-based time control mechanism can mitigate the CN congestion for the femtocell-based MTC network. Under the overload probability threshold requirement, the femtocell-based MTC network with group-based time control mechanism can support 100% higher arrival rate, compared to the femtocell-based MTC network without group-based time control mechanism.

Figure 5.8 shows the CN overload probability against the femto group size, where there are 950 MTC device in each macro group. From the figure, we have the following observations.

1) It is shown that the CN overload probability increases as the femto group size increases. To mitigate the CN congestion, it is important to control the group size to limit the CN traffic load. Under the overload probability threshold requirement, the largest permissible femto group size is about 500 femtocells, 1050 femtocells, and 3000 femtocells for $\lambda = 5$ (1/sec), $\lambda = 1$ (1/sec), and $\lambda = 0.75$ (1/sec), respectively.

2) The higher the arrival rate increases, the severer the CN congestion becomes. For a given femto group size, such as 1000 femtocells in a femto group, the maximum allowable arrival rate is $\lambda = 1$ (1/sec). When the arrival rate increases to $\lambda > 1$ (1/sec), the CN congestion may occur because the CN overload probability increases rapidly.

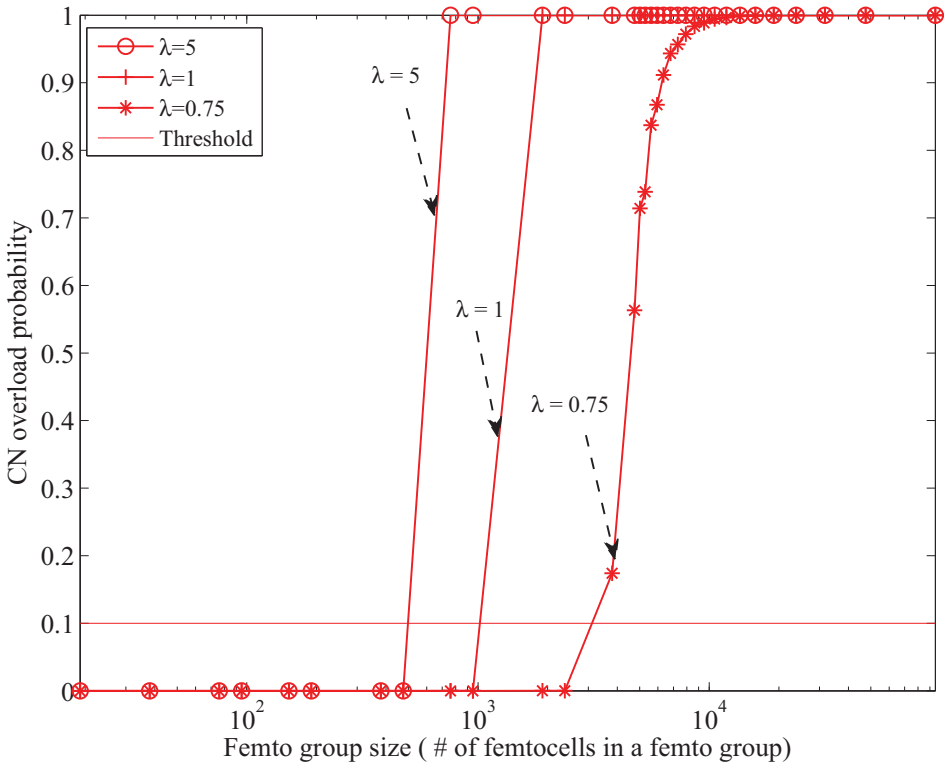

Figure 5.8: CN overload probability versus femto group size, where 950 MTC device in each macro group is considered for the femtocell-based MTC network.

Figure 5.9 shows the average successful transmission probability of MTC devices against the femto group size, where there are 950 MTC device in each macro group. From the figure, we have the following observations.

1) It is shown that the curve of the macro group is overlaid with that of the femto group for the same arrival rate. This is because the RAN overload does not occur for macro and femto groups in the case, and the network congestion may occur only in the CN. In the case with 950 MTC devices in the macro group over the $N_{Macro} = 19$ macrocell coverages, each macrocell base station serves mere $950/19 = 50$ MTC devices. However, the available capacity is $C_{eNB} \times \mu = 800 \times 0.25 = 200$ MTC devices for macrocell base station, and it means that the RAN overload does not occur. Similarly, the RAN overload does not occur for femtocells, because each femtoce base station serves only 5 MTC devices. Therefore, the curves only react to the CN traffic load.

2) To achieve the reliable transmission for MTC devices, the group-based time control mechanism can adjust the group size for macro and femto groups. In the case, with the minimum transmission reliability requirement, the largest permissible femto group size is about 620 femtocells, 1300 femtocells, and 6300 femtocells for $\lambda = 5$ (1/sec), $\lambda = 1$ (1/sec), and $\lambda = 0.75$ (1/sec), respectively.

3) The arrival rate also significantly affects the successful transmission probability of MTC devices for a given group size. In the case, for the given group size with 1300 femtocells, the maximum allowable arrival rate is $\lambda = 1$ (1/sec), under the minimum transmission reliability requirement. When the arrival rate exceeds the maximum allowable arrival rate, i.e., $\lambda > 1$ (1/sec), the successful transmission probability decreases rapidly, and the service quality may degrade.

Figure 5.10 shows the average message delay against the femto group size. From the figure, we have the following observations.

1) The message delay is significantly affected by the group size. The large group size may result in the CN congestion, and therefore the message delay in-

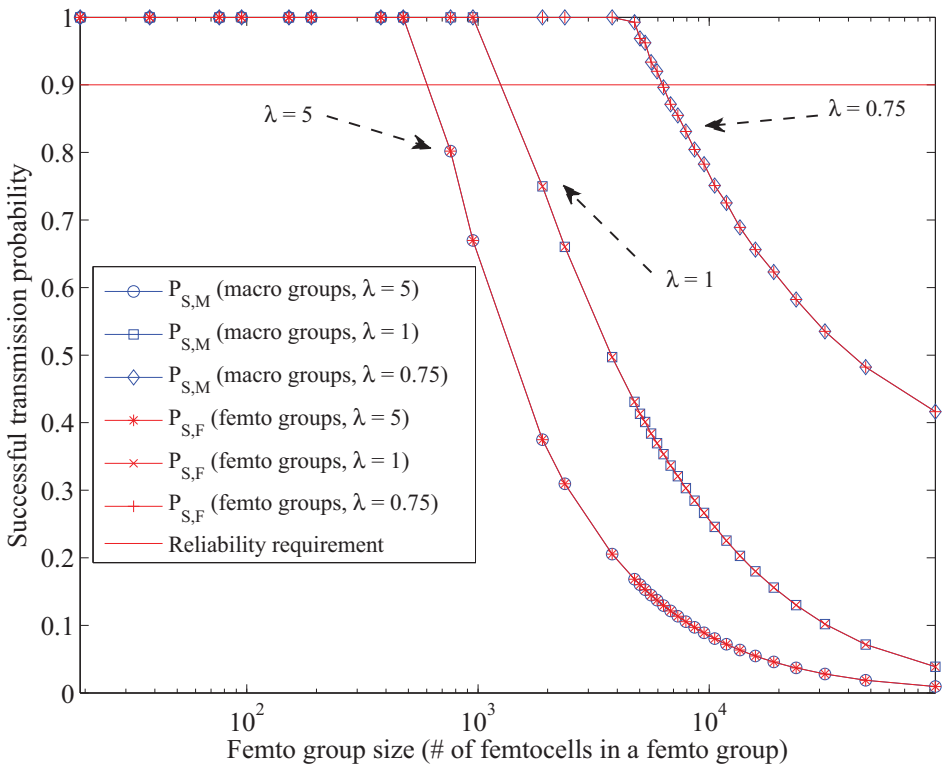

Figure 5.9: Average successful transmission probability versus femto group size, where 950 MTC device in each macro group is considered for the femtocell-based MTC network.

creases. However, the small group size may extend the group cycle time to increase the message delay. Consequently, for optimizing the message delay performance, the group size is neither too large nor too small. In the case, when the femto group size increases from 1 femtocell to about 1000 femtocells, the average message delay of the femto group decreases from about 25 seconds to about 1 second and 0.5 second for $\lambda = 5$ (1/sec) and $\lambda = 1$ (1/sec), respectively. As the femto group size keeps increasing to about 10000 femtocells, the average message delay of the macro group increases to about 105 second and 25 second for $\lambda = 5$ (1/sec) and $\lambda = 1$ (1/sec), respectively. Thus, the optimal femto group size in the case is about 1000 femtocells to achieve the tradeoff between the CN overload and group cycle time.

2) It is shown that the arrival rate significantly affects the message delay only when the CN congestion occurs. If the group size is sufficiently small, the total traffic load is limited to the available capacity of CN. Hence, the CN congestion does not occur even though the arrival rate increases. However, if the group size is too large to limit the traffic load to the available capacity of CN, the CN congestion may occur. In the circumstance, the message delay increases as well as the arrival rate. For example, for a given femto group size with 1000 femtocells, the femto group with $\lambda = 5$ increases 97% more message delay time than that with $\lambda = 1$ (1/sec). If the femto group size increases to 10000 femtocells, the femto group with $\lambda = 5$ increases 223% more message delay time than that with $\lambda = 1$ (1/sec).

5.5.2 Impacts of Adaptive Joint Access Probability Adjustment and Group Rearrangement Method

Figures 5.11, 5.12, and 5.13 shows the group size rearrangement, successful transmission probability, and message delay against the processing time, respectively. The results are simulated by the developed adaptive joint access probability adjustment and group rearrangement method. The initial macro group size and femto group

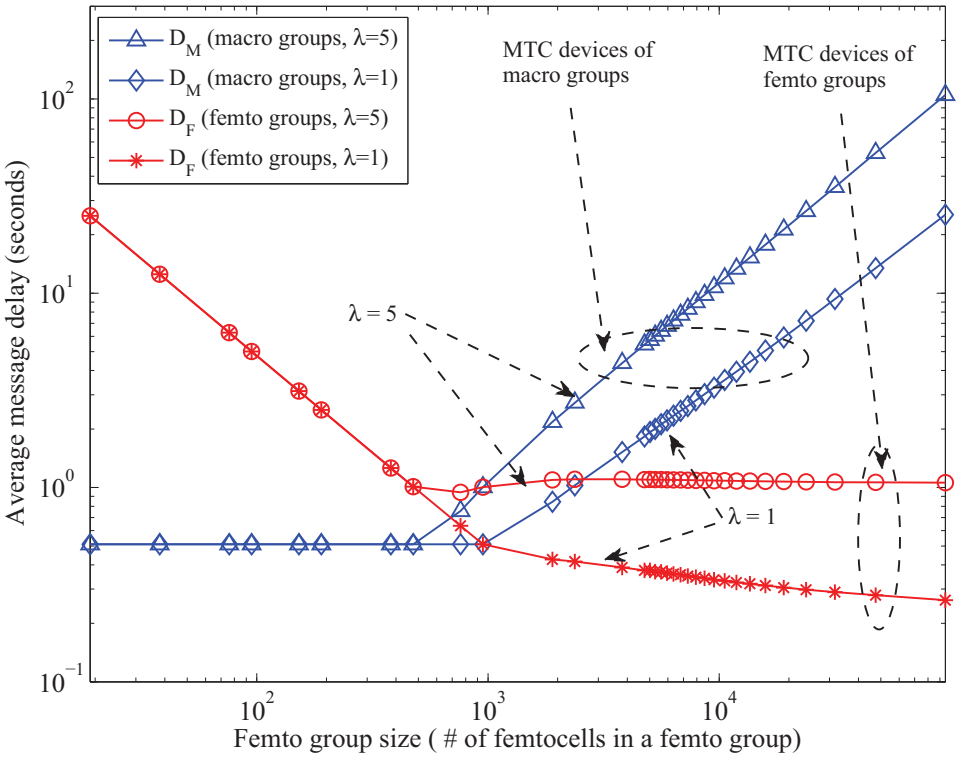

Figure 5.10: Average message delay versus femto group size, where 950 MTC device in each macro group is considered for the femtocell-based MTC network.

size are 47500 MTC devices and 19000 femtocells over the $N_{Macro} = 19$ macrocell coverages, respectively. The predefined overload count threshold and predefined non-overload count threshold are $N_{OL,\max} = 5$ and $N_{NOL,\max} = 30$, respectively. The assumption of $N_{NOL,\max} > N_{OL,\max}$ is for that CN overload can be mitigated rapidly.

From Fig. 5.11, we have the following observations.

1) In the beginning, the MTC server rearranges the group size by equally splitting because too large group size results in the CN overload. When CN congestion is released, the MTC server stops slitting the group. In the case, the macro group size and the femto group size are 47500 MTC devices and 19000 femtocells in the beginning. After 8 seconds, the MTC server stops slitting the group, and the size become 750 MTC devices and 600 femtocells for the macro group and the femto group, respectively.

2) The group size can significantly affect the CN overload, while the effect of the arrival rate is minor. In the case, after the MTC stops slitting the group, the macro group size and the femto group size are 750 MTC devices and 600 femtocells. It implies that total $750 + 600 \times 5 = 3750$ MTC devices are granted to send the connection request in a granted time interval. However, the available capacity for MTC server is $C_{MTC} \times \eta = 15200 \times 0.25 = 3800$ MTC devices. Therefore, the MTC server can guarantee that the CN congestion does not occur.

From Fig. 5.12, we have the following observations.

1) As time goes on, the successful transmission probability can be improved by the develop adaptive joint access probability adjustment and group rearrangement method. In the case, the successful transmission probability is below 0.2 for all MTC devices at the first second. However, the successful transmission probability is improved to 1 after the 8th second.

2) As mentioned above, the improvement of the arrival rate for the successful transmission probability is also minor. Nevertheless, splitting the group is the

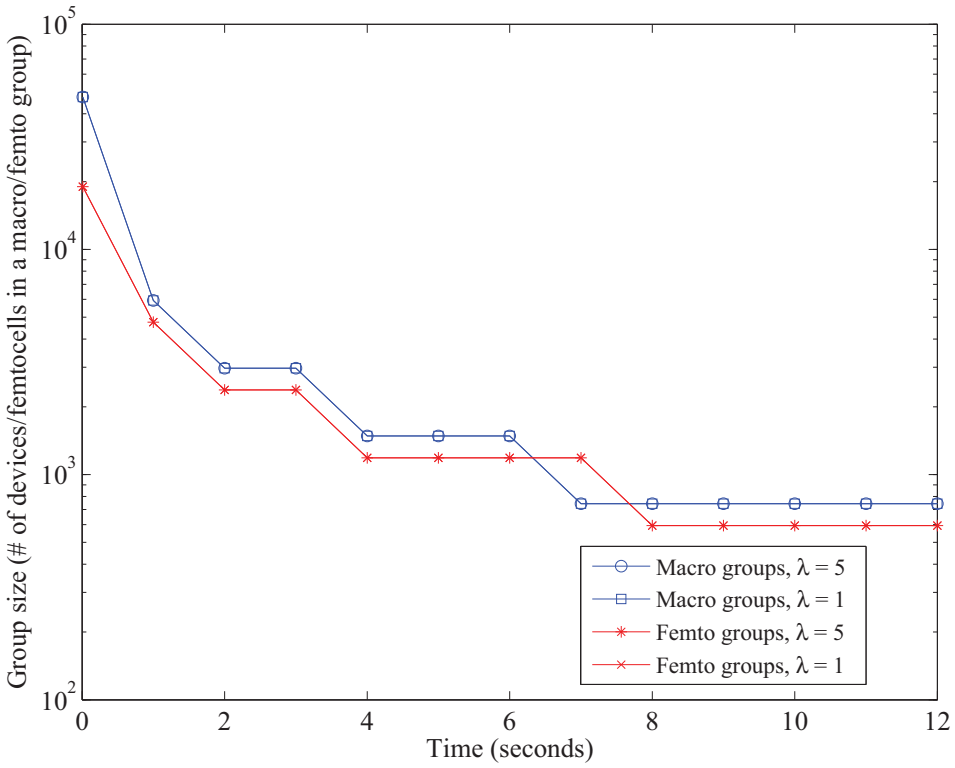

Figure 5.11: Group size versus processing time. The group size is adjusted by the adaptive joint access probability adjustment and group rearrangement method.

better way than decreasing the arrival rate to improve the successful transmission probability for MTC devices.

From Fig. 5.13, we have the following observations.

1) The average message delay can be improved by the developed adaptive joint access probability adjustment and group rearrangement method. In the case, when the processing time beyond the 8th second, the average message time can be adjusted to 0.65 seconds and 0.81 seconds for macro groups and femto groups, respectively.

2) Decreasing the arrival rate can improve the average message delay for MTC devices when the CN congestion is quite severe. However, the impact of the arrival rate becomes insignificant when the traffic load of the CN is gradually alleviated.

5.5.3 Summary

The proposed group-based time control mechanism aims to help decide the suitable group size to control the RAN and CN overload and guarantee the message delay performance of MTC devices. In addition, the developed adaptive joint access probability adjustment and group rearrangement method can help the proposed mechanism to implement. Actually, without grouping, all the MTC devices may transmit their message at the same time, and the network congestion may happen due to the massive concurrent data transmission from the MTC devices. The simplest way is to increase the capacity of the CN or the MTC server to tolerate the maximum traffic load from all the MTC devices. However, the utility is inefficient because the traffic load is not always full, and the cost for sufficient capacity expansion is quite expensive. On the contrary, if grouping is available, the maximum traffic can be limited into the network so that the traffic can be uniformly spread over the time to decrease the traffic peak. Therefore, the network congestion can be improved. Nevertheless, the message delay may increase because of the long cycle

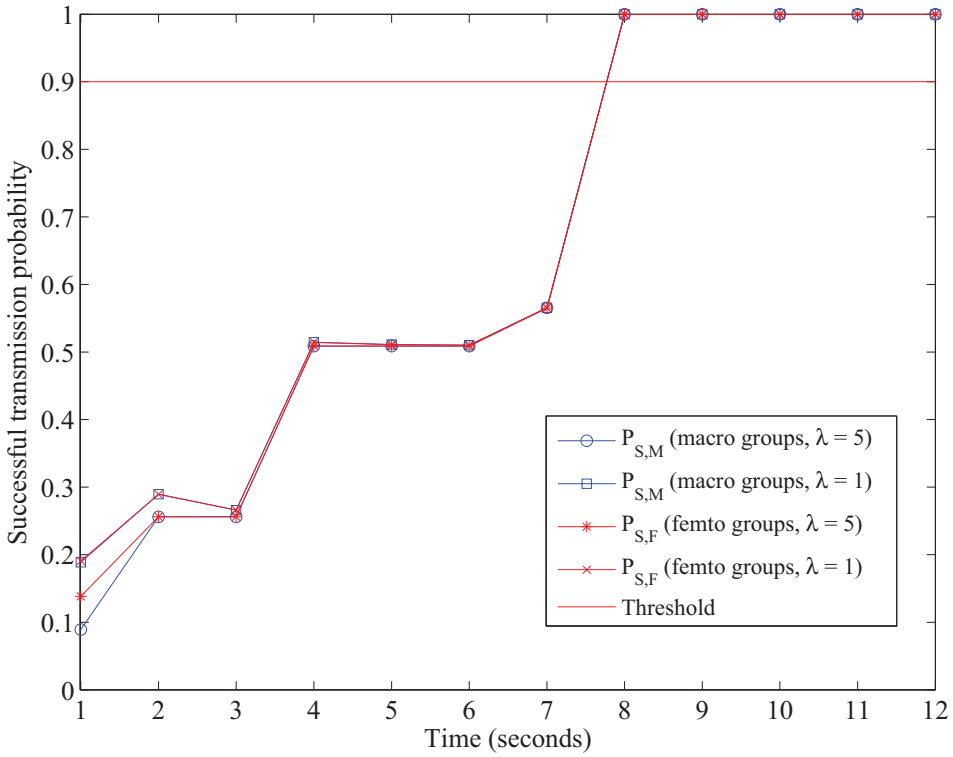

Figure 5.12: Successful transmission probability of MTC devices versus processing time. The probability is resulted from the adaptive joint access probability adjustment and group rearrangement method.

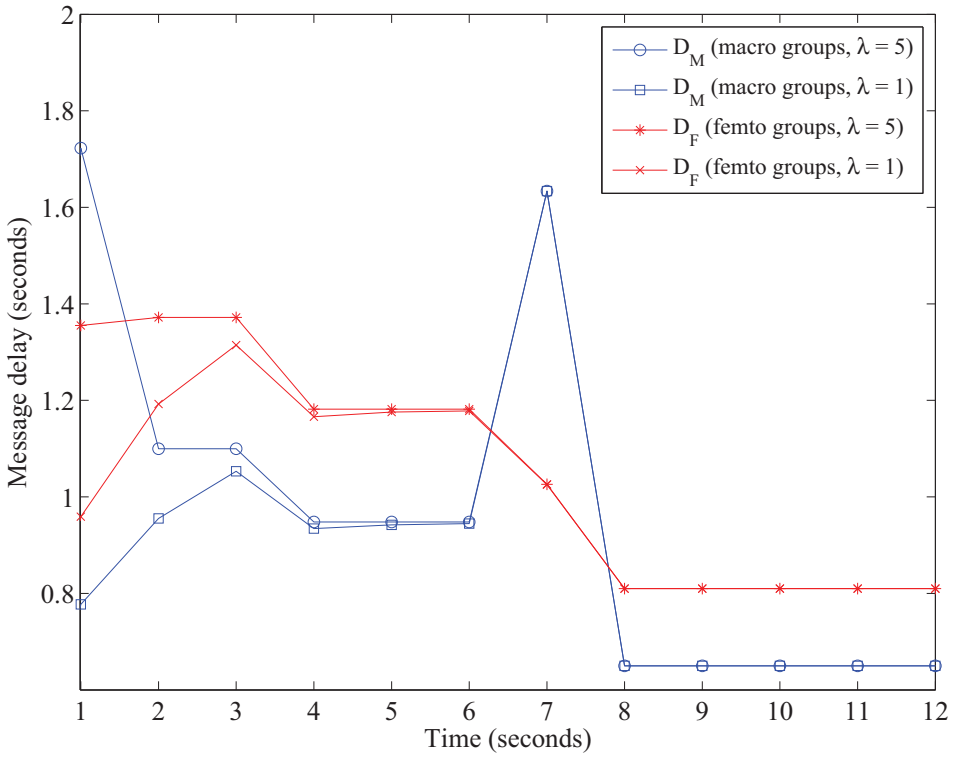

Figure 5.13: Average message delay versus processing time. As time goes on, the average message delay is shorten by the adaptive joint access probability adjustment and group rearrangement method.

time resulted from the excessive grouping. Consequently, the appropriate choice of the group size can achieve the tradeoff between the network congestion and delay time, and the suitable group size can be determined by the analysis in the chapter. If the tradeoff is impossible, it implies the demand for more capacity of network.

Chapter 6

Intelligent Resource Management for Device-to-Device (D2D) Femtocell Networks

In this chapter, we propose the network-assisted device-controlled resource management to enhance the system throughput and service quality for D2D femtocell systems. Based on the information of the maximum interference tolerance (MIT) broadcast by macrocell base station (MBS) and femtocell base station (FBS), the D2D pairs can effectively and autonomously manage their resource blocks to avoid the complicated three-tier interference, which improves the system throughput. In addition to system throughput, we take the link reliability of all users into account. Consequently, the proposed method can allocate the optimum resource blocks for D2D pairs, and guarantee the service quality for macrocell users (MUEs) and femtocell users (FUEs).

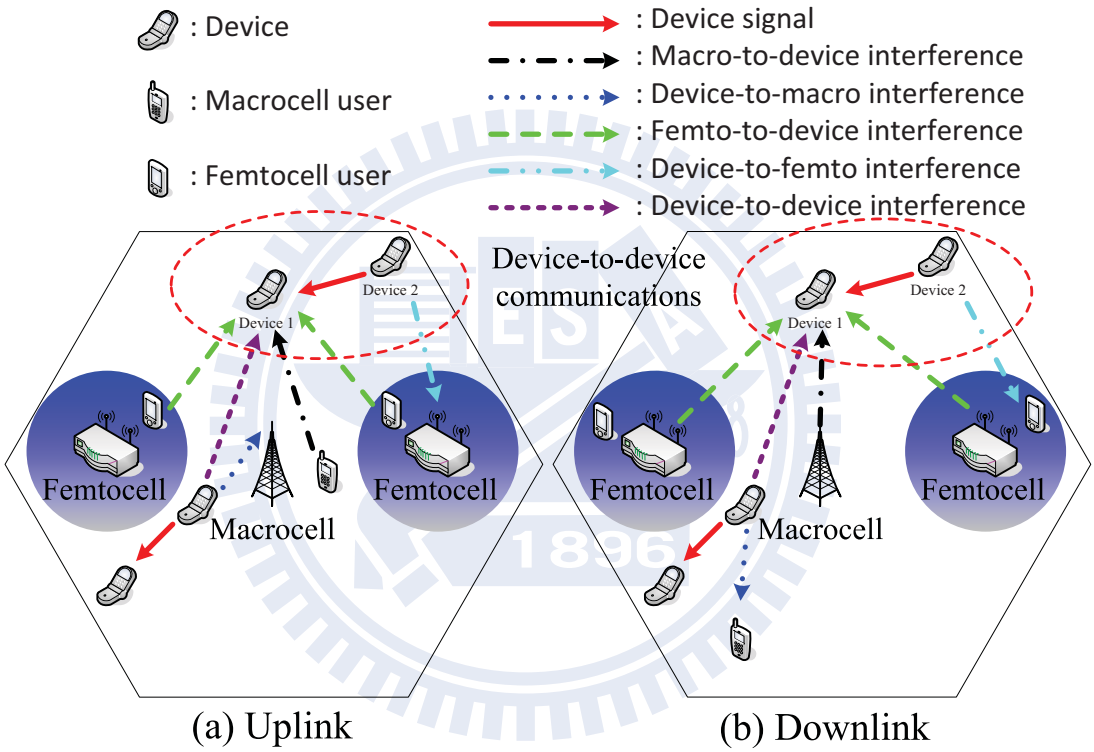

Figure 6.1: The concept of device-to-device (D2D) communications femtocell networks with the three-tier interference in the uplink and downlink.

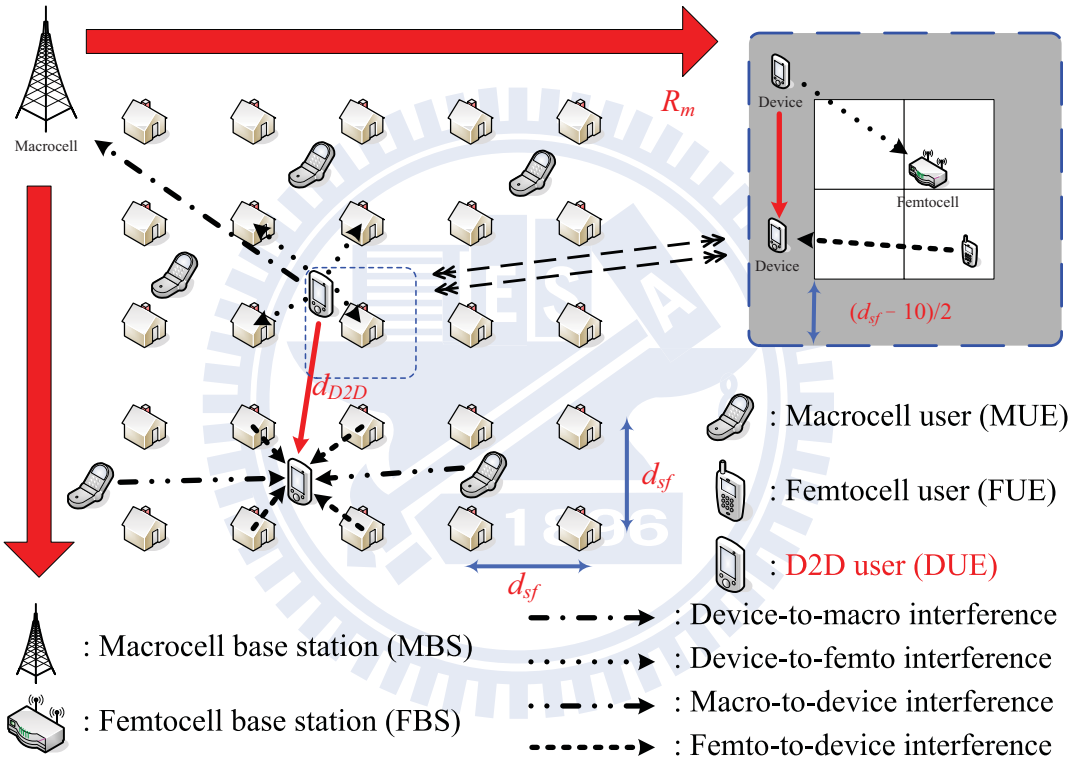

Figure 6.2: Heterogeneous Macro/Femto/D2D networks.

6.1 System Model

6.1.1 System Architecture

We consider the uplink of the OFDMA-based Macro/Femto/D2D system in the campus/community environment, as shown in Fig. 6.2. We assume that a cluster of 25 femtocells is uniformly distributed in a macrocell with a radius of R_m (m). Each house covers an area of 100 square meters and has four 5 m-by-5 m rooms. The FBS is deployed at the center of the house with a shift of (0.1 m, 0.1 m). The separation distance between two neighboring FBSs is d_{sf} (m). Each femtocell serves one indoor user, and the femtocell user's locations are uniformly distributed within the house. One pair of outdoor D2D users (DUEs) are around the considered femtocell. The D2D transmitted user (DTUE) is located in the shadowed region with width of $(d_{sf} - 10)/2$ (m) surrounding the house, and the D2D received user (DRUE) is in the proximity of the DTUE with a distance of d_{D2D} (m), as shown in Fig. 6.2.

Spectrum allocation schemes can significantly affect the spectrum efficiency. Generally, there are exclusive spectrum allocation scheme and shared spectrum allocation scheme for heterogeneous Macro/Femto/D2D systems. The former scheme allocates different frequency bands to the macrocell, femtocell and D2D systems, and the later scheme allows the same spectrum shared by all the systems. Since the macrocell, femtocell and D2D systems are allocated with different spectrum, the exclusive spectrum allocation scheme can eliminate the mutual interference, but may have lower spectrum efficiency. By contrast, with the same spectrum allocated for the macrocell, femtocell and D2D systems, the shared spectrum allocation scheme can increase the spectrum efficiency at the cost of higher three-tier interference. In this chapter, we consider the shared spectrum allocation scheme, and we propose an intelligent resource management method to deal with the three-tier interference.

6.1.2 Channel Models

We consider the following radio propagation effects, including path loss, wall penetration loss, shadowing, and frequency-selective multipath fading, to evaluate the three-tier interference in the OFDMA-based hybrid macrocell, femtocell and D2D systems.

Path Loss

For macrocell and femtocell systems, as the transmitter and the receiver are in the same house, the path loss between the transmitter and the receiver with the propagation distance d (km) is defined as [61]

$$L(d)\ (\text{dB}) = 127 + 30\log_{10}(d)\ . \tag{6.1}$$

As the transmitter and the receiver are not in the same house, the path loss is defined as

$$L(d)\ (\text{dB}) = 128.1 + 37.6\log_{10}(d)\ . \tag{6.2}$$

For D2D systems, the path loss is defined as [66]

$$L(d)\ (\text{dB}) = 148 + 40\log_{10}(d)\ . \tag{6.3}$$

Wall Penetration Loss

We assume that the penetration attenuation is 20 dB per wall for outdoor-to-indoor links [61]. In addition, let $W_{M2F,k}$ be the total penetration loss between the k-th MUE and the considered FBS, $W_{F2M,j}$ be that between the FUE of the j-th FBS and the MBS, $W_{F2F,j}$ be that between the FUE of the j-th FBS and the considered FBS, $W_{F2DR,j}$ be that between the FUE of the j-th FBS and the DRUE, and W_{DT2F} be that between the DTUE and the considered FBS.

Shadowing

Shadowing is modelled by a log-normal random variable $10^{\xi/10}$, where ξ is a Gaussian distributed random variable with zero mean. The shadowing standard deviation for

the indoor links is $\sigma = 10$ dB; that for the links between the FUE of neighboring femtocells and the considered FBS is $\sigma = 8$ dB; that for the outdoor-to-indoor and indoor-to-outdoor links between macrocells and femtocells is $\sigma = 8$ dB; that for the cellular links is $\sigma = 8$ dB; that for the D2D links is $\sigma = 8$ dB [61].

Frequency-Selective Multipath Fading

We take the frequency-selective fading channel into account. The multipath fading is described by the Stanford University interim-3 (SUI-3) channel model assuming 3 taps with non-uniform delays [55].

6.1.3 Effective Carrier to Interference-and-noise Ratio (CINR)

The effective CINR for a resource block (RB) comprising multiple subcarriers in the OFDMA-based Macro/Femto/D2D system can be evaluated as follows. In the uplink phase, the MUEs, FUEs and DTUE transmit signal power to the MBS, FBSs, and DRUE, respectively. Denote $S^{UL}_{M,\ell,k}$, $S^{UL}_{F,\ell,i}$, and $S_{D2D,\ell}$ as the received signal power of the ℓ-th subcarrier for the MBS from the k-th MUE in the uplink phase, that for the considered i-th FBS from the FUE in the uplink phase, and that for the DRUE from the DTUE, respectively. The received signal power $S^{UL}_{M,\ell,k}$, $S^{UL}_{F,\ell,i}$, and $S_{D2D,\ell}$ can be expressed as

$$S^{UL}_{M,\ell,k} = \frac{P^{UL}_{M,\ell,k} \cdot 10^{\frac{\xi_{M,k}}{10}} |h_{M,\ell,k}|^2}{10^{\frac{L\left(d_{M,k}\right)}{10}}} , \tag{6.4}$$

$$S^{UL}_{F,\ell,i} = \frac{P^{UL}_{F,\ell,i} \cdot 10^{\frac{\xi_{F,i}}{10}} |h_{F,\ell,i}|^2}{10^{\frac{L\left(d_{F,i}\right)}{10}}} , \tag{6.5}$$

and

$$S_{D2D,\ell} = \frac{P_{D2D,\ell} \cdot 10^{\frac{\xi_{D2D}}{10}} |h_{D2D,\ell}|^2}{10^{\frac{L(d_{D2D})}{10}}} . \tag{6.6}$$

$P^{UL}_{M,\ell,k}$ is the transmission power of the k-th MUE for the subcarrier ℓ; $P^{UL}_{F,\ell,i}$ is that of the FUE in the considered i-th FBS for the subcarrier ℓ; $P_{D2D,\ell}$ is that of the DTUE for the subcarrier ℓ. $\xi_{M,k}$ is the shadowing between the k-th MUE and the MBS; $\xi_{F,i}$ is that between the FUE of the considered i-th FBS and the considered i-th FBS; ξ_{D2D} is that between the D2D pair. $|h_{M,\ell,k}|^2$ represents the link gain between the k-th MUE and the MBS on the subcarrier ℓ; $|h_{F,\ell,i}|^2$ represents that between the FUE of the considered i-th FBS and the considered i-th FBS on the subcarrier ℓ; $|h_{D2D,\ell}|^2$ represents that between the D2D pair on the subcarrier ℓ. $d_{M,k}$ is the separation distance from the k-th MUE to the MBS; $d_{F,i}$ is that from FUE of the considered i-th FBS to the considered i-th FBS; d_{D2D} is that between the D2D pair.

The MBS, FBSs, and DRUE are interfered in the uplink phase. For the MBS, the interference comes from femtocell and the D2D systems. On the subcarrier ℓ of the MBS, the interference from the j-th FBS is $I^{UL}_{F2M,\ell,j}$, and that from the DTUE is $I_{DT2M,\ell}$. The interference power $I^{UL}_{F2M,\ell,j}$, and $I_{DT2M,\ell}$ can be expressed as

$$I^{UL}_{F2M,\ell,j} = \frac{P^{UL}_{F,\ell,j} \cdot 10^{\frac{\xi_{F2M,j}}{10}} |h_{F2M,\ell,j}|^2}{10^{\frac{L\left(d_{F2M,j}\right)+W_{F2M,j}}{10}}} \tag{6.7}$$

and

$$I_{DT2M,\ell} = \frac{P_{D2D,\ell} \cdot 10^{\frac{\xi_{DT2M}}{10}} |h_{DT2M,\ell}|^2}{10^{\frac{L(d_{DT2M})}{10}}} \ . \tag{6.8}$$

$\xi_{F2M,j}$, $|h_{F2M,\ell,j}|^2$, and $d_{F2M,j}$ are the shadowing between the FUE of the j-th FBS and the MBS, the link gain between the FUE of the j-th FBS and the MBS on the subcarrier ℓ, and the separation distance from the FUE of the j-th FBS to the MBS, respectively. ξ_{DT2M}, $|h_{DT2M,\ell}|^2$, and d_{DT2M} are the shadowing between the DTUE and the MBS, the link gain between the DTUE and the MBS on the subcarrier ℓ, and the separation distance from the DTUE to the MBS, respectively.

For the FBS, the interference comes from the MBS, the other neighboring FBSs and the DTUE. On the subcarrier ℓ of the FBS, the interference from the MBS is $I^{UL}_{M2F,\ell,k}$, that from the j-th FBS is $I^{UL}_{F2F,\ell,j}$, and that from the DTUE is $I_{DT2F,\ell}$. The

interference power $I^{UL}_{M2F,\ell,k}$, $I^{UL}_{F2F,\ell,j}$, and $I_{DT2F,\ell}$ can be expressed as

$$I^{UL}_{M2F,\ell,k} = \frac{P^{UL}_{M,\ell,k} \cdot 10^{\frac{\xi_{M2F,k}}{10}} |h_{M2F,\ell,k}|^2}{10^{\frac{L\left(d_{M2F,k}\right)+W_{M2F,k}}{10}}} \tag{6.9}$$

$$I^{UL}_{F2F,\ell,j} = \frac{P^{UL}_{F,\ell,j} \cdot 10^{\frac{\xi_{F2F,j}}{10}} |h_{F2F,\ell,j}|^2}{10^{\frac{L\left(d_{F2F,j}\right)+W_{F2F,j}}{10}}} \tag{6.10}$$

$$I_{DT2F,\ell} = \frac{P_{D2D,\ell} \cdot 10^{\frac{\xi_{DT2F}}{10}} |h_{DT2F,\ell}|^2}{10^{\frac{L(d_{DT2F})+W_{DT2F}}{10}}} \tag{6.11}$$

$\xi_{M2F,k}$, $|h_{M2F,\ell,k}|^2$, and $d_{M2F,k}$ are the shadowing between the k-th MUE and the considered i-th FBS, the link gain between the k-th MUE and the considered i-th FBS on the subcarrier ℓ, and the separation distance from the k-th MUE to the considered i-th FBS, respectively. $\xi_{F2F,j}$, $|h_{F2F,\ell,j}|^2$, and $d_{F2F,j}$ are the shadowing between the FUE of the j-th FBS and the considered i-th FBS, the link gain between the FUE of the j-th FBS and the considered i-th FBS on the subcarrier ℓ, and the separation distance from the FUE of the j-th FBS to the considered i-th FBS, respectively. ξ_{DT2F}, $|h_{DT2F,\ell}|^2$, and d_{DT2F} are the shadowing between the DTUE and the considered i-th FBS, the link gain between the DTUE and the considered i-th FBS on the subcarrier ℓ, and the separation distance from the DTUE to the considered i-th FBS, respectively.

For the DRUE, the interference comes from both the macrocell and femtocell systems. On the subcarrier ℓ of the DRUE, the interference from the MBS is $I^{UL}_{M2DR,\ell,k}$, and that from the j-th FBS is $I^{UL}_{F2DR,\ell,j}$. The interference power $I^{UL}_{M2DR,\ell,k}$ and $I^{UL}_{F2DR,\ell,j}$ can be expressed as

$$I^{UL}_{M2DR,\ell,k} = \frac{P^{UL}_{M,\ell,k} \cdot 10^{\frac{\xi_{M2DR,k}}{10}} |h_{M2DR,\ell,k}|^2}{10^{\frac{L\left(d_{M2DR,k}\right)}{10}}} \tag{6.12}$$

$$I^{UL}_{F2DR,\ell,j} = \frac{P^{UL}_{F,\ell,j} \cdot 10^{\frac{\xi_{F2DR,j}}{10}} |h_{F2DR,\ell,j}|^2}{10^{\frac{L\left(d_{F2DR,j}\right)+W_{F2DR,j}}{10}}} \tag{6.13}$$

$\xi_{M2DR,k}$, $|h_{M2DR,\ell,k}|^2$, and $d_{M2DR,k}$ are the shadowing between the k-th MUE and the DRUE, the link gain between the k-th MUE and the DRUE on the subcarrier ℓ, and the separation distance from the k-th MUE to the DRUE, respectively. $\xi_{F2DR,j}$, $|h_{F2DR,\ell,j}|^2$, and $d_{F2DR,j}$ are the shadowing between the FUE of the j-th FBS and the DRUE, the link gain between the FUE of the j-th FBS and the DRUE on the subcarrier ℓ, and the separation distance from the FUE of the j-th FBS to the DRUE, respectively.

Consequently, in the heterogeneous macro/femto/D2D network, the uplink CINR of the ℓ-th subcarrier for the MBS, FBS and D2D can be defined as $\gamma^{UL}_{M,\ell,k}$, $\gamma^{UL}_{F,\ell,i}$, and $\gamma_{D2D,\ell}$, respectively. $\gamma^{UL}_{M,\ell,k}$, $\gamma^{UL}_{F,\ell,i}$, and $\gamma_{D2D,\ell}$ are expressed as

$$\gamma^{UL}_{M,\ell,k} = \frac{S^{UL}_{M,\ell,k}}{\sum_{j=1}^{N_F} I^{UL}_{F2M,\ell,j} + I_{DT2M,\ell} + N_0} \tag{6.14}$$

$$\gamma^{UL}_{F,\ell,i} = \frac{S^{UL}_{F,\ell,i}}{\sum_{k=1}^{K} I^{UL}_{M2F,\ell,k} + \sum_{j=1,j\neq i}^{N_F} I^{UL}_{F2F,\ell,j} + I_{DT2F,\ell} + N_0} \tag{6.15}$$

$$\gamma_{D2D,\ell} = \frac{S_{D2D,\ell}}{I^{UL}_{M2DR,\ell,k} + \sum_{j=1}^{N_F} I^{UL}_{F2DR,\ell,j} + N_0} \tag{6.16}$$

N_F is the total number of FBSs, and K is the total number of MUEs. N_0 is the power spectrum density of AWGN.

To investigate the effects of D2D, we compare the Macro/Femto/D2D system with the Macro/Femto system. Accordingly, for the heterogeneous macro/femto network, the uplink CINR of the ℓ-th subcarrier for the MBS and FBS can be defined as $\gamma^{UL,\Theta}_{M,\ell,k}$, and $\gamma^{UL,\Theta}_{F,\ell,i}$, respectively. We express $\gamma^{UL,\Theta}_{M,\ell,k}$, and $\gamma^{UL,\Theta}_{F,\ell,i}$ as

$$\gamma^{UL,\Theta}_{M,\ell,k} = \frac{S^{UL}_{M,\ell,k}}{\sum_{j=1}^{N_F} I^{UL}_{F2M,\ell,j} + N_0} \tag{6.17}$$

and

$$\gamma^{UL,\Theta}_{F,\ell,i} = \frac{S^{UL}_{F,\ell,i}}{\sum_{k=1}^{K} I^{UL}_{M2F,\ell,k} + \sum_{j=1,j\neq i}^{N_F} I^{UL}_{F2F,\ell,j} + N_0} \ . \tag{6.18}$$

We can map a vector of CINRs for multiple subcarriers of a RB to a single effective CINR based on the exponential effective SIR mapping (EESM) method [56]. Suppose that a RB includes N_d subcarriers, and the corresponding CINR for each subcarrier is γ_ℓ, $\ell = 1, 2, \ldots, N_d$. Then, the effective CINR of the RB can be calculated by

$$\gamma_{eff}(\gamma_1, \gamma_2, ..., \gamma_{N_d}) = -\beta \cdot \ln(\frac{1}{N_d} \sum_{\ell=1}^{N_d} \exp[-\gamma_\ell/\beta]) \ , \tag{6.19}$$

where β is the calibration factor for the selected modulation coding scheme (MCS) [56]. Table 3.1 lists the considered MCSs, the corresponding effective CINR thresholds, and the EESM parameter β. As obtaining the effective CINR of the n-th RB, based on Table 3.1, we can determine the MCS and the corresponding theoretical spectrum efficiency $\eta_{M,n}$, $\eta_{F,n}$, and $\eta_{D,n}$ for the macrocell, femtocell, and D2D systems, respectively.

6.1.4 Link Reliability and Throughput

In this chapter, we consider the link reliability and throughput as the performance metrics. The link reliability P_{rel} is defined as the probability that the effective CINR is higher than a predefined effective CINR threshold γ_{th}, that is,

$$P_{rel} = \Pr[\gamma_{eff} \geq \gamma_{th}] \ . \tag{6.20}$$

The achieved macrocell throughput C_M, femtocell throughput C_F, and D2D throughput C_D are defined as

$$C_M = \sum_{n=1}^{N_{RB}} B_{RB} \cdot \eta_{M,n} \ , \tag{6.21}$$

$$C_F = \sum_{n=1}^{N_{RB}} B_{RB} \cdot \eta_{F,n} \ , \tag{6.22}$$

and

$$C_D = \sum_{n=1}^{N_{RB}} B_{RB} \cdot \eta_{D,n} \ . \tag{6.23}$$

N_{RB} is the total number of RBs, and B_{RB} is the bandwidth of a single RB.

6.2 Network-Assisted Interference Management

Assume that the MBS and FBS can provide the maximum interference tolerance (MIT) information of each RB for D2D pair to manage the resource. Based on the MIT information of each RB, the D2D pair can determine the maximum allowable transmission power. On the other hand, the D2D pair can estimate the minimum power on each RB for reliable transmission by the negotiation with each other. By properly selecting the RBs and adjusting the transmission power on the selected RBs, the D2D pair can effectively and autonomously manage the resource to avoid the interference to MBS and FBS.

6.2.1 Maximum Allowable Transmission Power from MIT

For the Macro/Femto network, if the up transmission on the RB n is reliable, the effective CINRs $\gamma_{eff,M,n,k}^{UL,\Theta}$ and $\gamma_{eff,F,n,i}^{UL,\Theta}$ should be higher than the predefined effective CINR threshold γ_{th}, and it can be expressed as

$$\gamma_{eff,M,n,k}^{UL,\Theta} = \frac{S_{M,n,k}^{UL}}{\sum_{j=1}^{N_F} I_{F2M,n,j}^{UL} + N_0} \geq \gamma_{th} \ , \tag{6.24}$$

$$\gamma_{eff,F,n,i}^{UL,\Theta} = \frac{S_{F,n,i}^{UL}}{\sum_{k=1}^{K} I_{M2F,n,k}^{UL} + \sum_{j=1,j\neq i}^{N_F} I_{F2F,n,j}^{UL} + N_0} \geq \gamma_{th} \ . \tag{6.25}$$

To maintain the link reliability of the macrocell and femtocell systems, it is assumed that the effective CINR is at least equivalent to the predefined effective CINR threshold γ_{th} in the Macro/Femto/D2D systems, even if the interference from the DTUE is involved. Therefore, we rewrite the above equations as

$$\frac{S_{M,n,k}^{UL}}{\sum_{j=1}^{N_F} I_{F2M,n,j}^{UL} + I_{DT2M,n}^{MIT} + N_0} = \gamma_{th} \tag{6.26}$$

$$\frac{S_{F,n,i}^{UL}}{\sum_{k=1}^{K} I_{M2F,n,k}^{UL} + \sum_{j=1,j\neq i}^{N_F} I_{F2F,n,j}^{UL} + I_{DT2F,n}^{MIT} + N_0} = \gamma_{th} \ . \tag{6.27}$$

$I^{MIT}_{DT2M,n}$ and $I^{MIT}_{DT2F,n}$ are the maximum allowable interference from DTUE to the MBS and FBS, respectively. Then, the MIT of each RB for the MBS and the considered FBS can be obtained by

$$I^{MIT}_{DT2M,n} = \frac{S^{UL}_{M,n,k} \cdot \left(\gamma^{UL,\Theta}_{eff,M,n,k} - \gamma_{th}\right)}{\gamma^{UL,\Theta}_{eff,M,n,k} \cdot \gamma_{th}} \tag{6.28}$$

$$I^{MIT}_{DT2F,n} = \frac{S^{UL}_{F,n,i} \cdot \left(\gamma^{UL,\Theta}_{eff,F,n,i} - \gamma_{th}\right)}{\gamma^{UL,\Theta}_{eff,F,n,i} \cdot \gamma_{th}} \tag{6.29}$$

The maximum allowable interference power for the MBS and the considered FBS are $P^{MIT,M}_{D2D,n}$ and $P^{MIT,F}_{D2D,n}$, respectively. As the D2D pair obtain the MIT information from the MBS and the considered FBS, $P^{MIT,M}_{D2D,n}$ and $P^{MIT,F}_{D2D,n}$ can be calculated by

$$P^{MIT,M}_{D2D,n} = \frac{I^{MIT}_{DT2M,n} \cdot 10^{\frac{L(d_{D2M})}{10}}}{10^{\frac{\xi_{D2M}}{10}} |h_{D2M,n}|^2} \tag{6.30}$$

$$P^{MIT,F}_{D2D,n} = \frac{I^{MIT}_{DT2F,n} \cdot 10^{\frac{L(d_{D2F})+W_{D2F}}{10}}}{10^{\frac{\xi_{D2F}}{10}} |h_{D2F,n}|^2} \tag{6.31}$$

Hence, the maximum allowable transmission power $P^{MIT}_{D2D,n}$ for the DTUE can be obtained by

$$P^{MIT}_{D2D,n} = \min\left(P^{MIT,M}_{D2D,n}, P^{MIT,F}_{D2D,n}\right) \tag{6.32}$$

6.2.2 Minimum Transmission Power Criterion

To have the reliable transmission for the D2D communications, the effective CINR of each RB n should be higher than the predefined effective CINR threshold γ_{th}, and we have the following equation.

$$\begin{aligned}\gamma_{D2D,n} =& \frac{P_{D2D,n} \cdot 10^{\frac{\xi_{D2D}}{10}} |h_{D2D,n}|^2 / 10^{\frac{L(d_{D2D})}{10}}}{I^{UL}_{M2DR,n,k} + \sum_{j=1}^{N_F} I^{UL}_{F2DR,n,j} + N_0} \\ =& \frac{P_{D2D,n} \cdot \Gamma}{\mathrm{Z}} \geq \gamma_{th} \ ,\end{aligned} \tag{6.33}$$

where

$$\begin{cases} \Gamma = 10^{\frac{\xi_{D2D}}{10}} |h_{D2D,n}|^2 / 10^{\frac{L(d_{D2D})}{10}} \\ \mathrm{Z} = I^{UL}_{M2DR,n,k} + \sum_{j=1}^{N_F} I^{UL}_{F2DR,n,j} + N_0 \end{cases} \tag{6.34}$$

Therefore, the minimum transmission power criterion $P^{Criterion}_{D2D,n}$ for the reliable D2D transmission can be expressed as

$$P^{Criterion}_{D2D,n} \geq \frac{\gamma_{th}}{\Gamma} \mathrm{Z} \tag{6.35}$$

6.2.3 Intelligent Resource Management

With the information of the maximum allowable transmission power and minimum transmission power criterion, the DTUE can effectively select the suitable RBs and adjust the power on the selected RBs to eliminate the harmful interference to the MBS and FBS, while have the reliable transmission quality. The intelligent resource management for the D2D communications can be achieved by the joint resource block selection and power adjustment method. The procedures of the joint resource block selection and power adjustment method are described in the following:

1 The D2D pair collect all the MIT information from MBS and FBS.

2 Determine the maximum allowable transmission power $P^{MIT}_{D2D,n}$ based on the MIT information.

3 Determine the minimum transmission power criterion $P^{Criterion}_{D2D,n}$.

4 **For** $n = 1$ to N_{RB}

5 **If** $P^{MIT}_{D2D,n} \geq P^{Criterion}_{D2D,n}$

6 The RB n is selected, and the transmission power on the RB n is adjusted to $P^{MIT}_{D2D,n}$.

7 **end**

8 **end**

6.3 Simulation Results

In this section, we show performance improvements of the intelligent resource management for the OFDMA-based heterogeneous Macro/Femto/D2D network systems subject to the complicated three-tier interference. We compare the conventional Macro/Femto systems with the Macro/Femto/D2D systems in the shared spectrum allocation schemes. In addition, we compare the proposed joint resource block selection and power adjustment method with the full-load scheme, in which DTUE use all the RBs and maximum power for transmission. The macrocell system is assumed to be fully-loaded, i.e., all the RBs are occupied by the MUEs.

Our simulation environment is shown in Fig. 6.2, where a group of 25 femtocells are separated by $d_{sf} = 20$ m, and covered by a macrocell with a radius of $R_m = 500$ m. One femtocell serves one indoor user uniformly distributed within the house. The DTUE is located in the shadowed region with width of $(d_{sf} - 10)/2 = 5$ (m) surrounding the central house. The DRUE is in the proximity of the DTUE with a distance of d_{D2D} (m), as shown in Fig. 6.2. Table 6.1 lists the related system parameters for the considered OFDMA-based Macro/Femto/D2D systems, including the predefined effective CINR threshold $\gamma_{th} = -2.5$ dB, link reliability requirement $P_{rel} = 90\%$, etc. The total number of RBs for the use of data payload is $N_{RB} = 50$. Each RB consists of 12 subcarries, and comprises B_{RB} =180 KHz bandwidth. We assume that femtocells can appropriately adjust the number of used RBs to lower the interference. Denote N_{data} as the number of used RBs and define the resource block usage ratio as $\rho_F = \frac{N_{data}}{N_{RB}}$ for femtocells.

6.3.1 Impacts of Intelligent Resource Management

Figure 6.3 shows the link reliability performance of macrocell, femtocell and D2D users with a distance $d_{D2D} = 10$ (m) against the resource block usage ratio ρ_F of the femtocells in the shared spectrum allocation scheme. We consider three scenarios. Scenarios I represents the the conventional Macro/Femto systems without D2D. Scenarios II represents the situation that the D2D pair intelligently manage the

Table 6.1: **The OFDMA heterogeneous Macro/Femto/D2D network system parameters**

Parameters	**Values**
Macrocell radius (R_m)	500 m
Carrier Frequency	2.0 GHz
System bandwidth (B)	10 MHz
FFT size (N_{FFT})	1024
Number of RBs (N_{RB})	50
Number of data subcarriers (N_{SC})	600
RB bandwidth (B_{RB})	180 KHz
Number of MUEs (K)	50
Transmit power (MUE/FUE/DUE)	23 dBm
Noise figure (MBS/FBS/UE)	5 dB / 5 dB / 7 dB
Predefined effective CINR threshold for link reliability requirement (γ_{th})	-2.5 dB
Minimum link reliability requirement	$P_{rel} = 90\%$

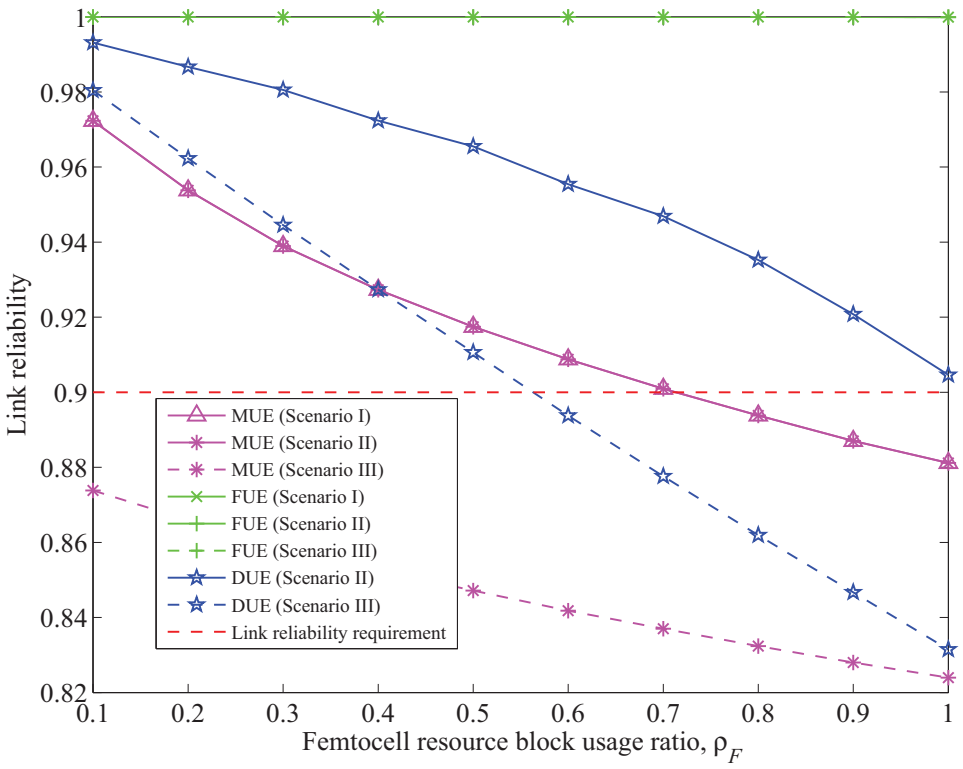

Figure 6.3: Link reliability of macrocell, femtocell and D2D users versus the resource block usage ratio ρ_F of the femtocells, where $d_{D2D} = 10$ (m). Scenario I: the conventional Macro/Femto systems without D2D; Scenario II: the D2D pair intelligently manage the resource with the joint resource block selection and power adjustment method in the Macro/Femto/D2D systems; Scenario III: the D2D pair use all the RBs and maximum power for transmission in the Macro/Femto/D2D systems.

resource with the joint resource block selection and power adjustment method in the Macro/Femto/D2D systems. Scenarios III represents the situation that the D2D pair use all the RBs and maximum power for transmission in the Macro/Femto/D2D systems. From the figure, we have the following observations:

1) The proposed joint resource block selection and power adjustment method (Scenarios II) can intelligently manage the resource for the D2D pair to achieve higher link reliability than the full-load scheme (Scenarios III), even if the the D2D pair use all the RBs and maximum power for transmission.

2) The proposed method (Scenarios II) can guarantee the macrocell and femtocell users against any degradation of link reliability, while the full-load scheme (Scenarios III) substantially degrades the link reliability of macrocell users.

3) The link reliability of femtocell users is not affected by macrocell, the other neighboring femtocells and D2D users due to the higher wall-penetration loss.

Figure 6.4 shows the throughput performance of macrocell, femtocell and D2D systems against the resource block usage ratio $\rho_{_F}$ of the femtocells in the shared spectrum allocation scheme, with the D2D distance $d_{D2D} = 10$ (m). From the figure, we have the following observations:

1) The throughput of macrocell and femtocell in Scenarios II is not influenced by the D2D communications because the D2D users intelligently select the RBs and adjust the power for transmission.

2) In Scenario III, the throughput of macrocell is degraded compared to that in Scenario I. This is because the D2D users use the whole RBs with the maximum transmission power, and it causes the strong interference to macrocells.

3) Although the throughput of macrocell and D2D decreases as the resource block usage ratio of femtocells increases, the total system throughput still increases as the ratio increases. It implies that femtocells can help improve the total system throughput.

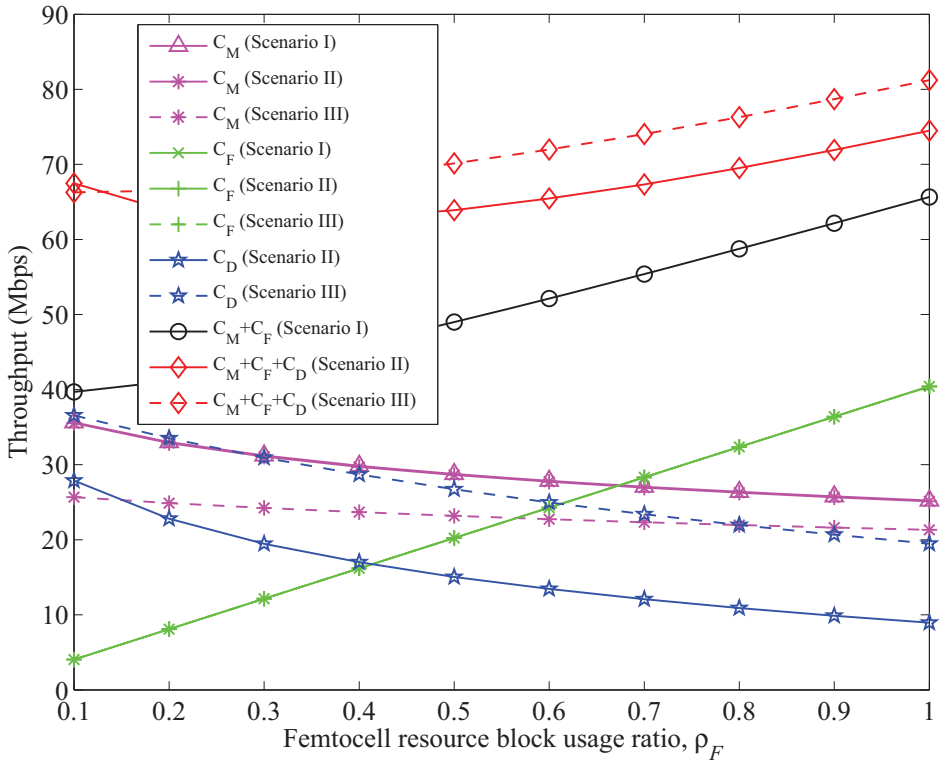

Figure 6.4: Throughput of macrocell, femtocell and D2D systems versus the resource block usage ratio ρ_F of the femtocells, where $d_{D2D} = 10$ (m).

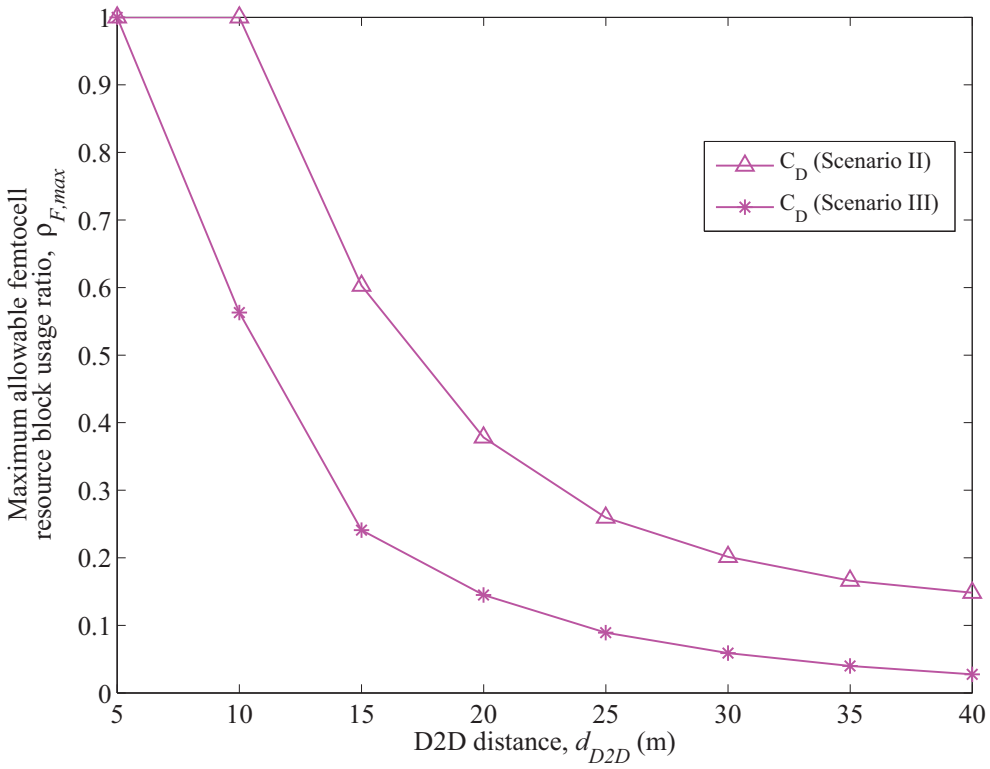

Figure 6.5: Maximum allowable resource block usage ratio of femtocells versus the D2D distance in the shared spectrum allocation scheme subject to the link reliability requirement $P_{rel} \geq 90\%$.

6.3.2 Tradeoff between Femtocell Resource Block Usage Ratio and D2D Distance

Figure 6.5 shows the maximum allowable resource block usage ratio of femtocells against the D2D distance in the shared spectrum allocation scheme with the link reliability requirement $P_{rel} \geq 90\%$. From the figure, we have the following observations:

1) With the link reliability requirement $P_{rel} \geq 90\%$, the maximum allowable resource block usage ratio $\rho_{F,max}$ of femtocells decreases as the D2D distance d_{D2D} increases. Moreover, the maximum allowable D2D distance $d_{D2D,max}$ is significantly affected by the femtocell resource block usage ratio ρ_F. Under

the link reliability requirement $P_{rel} \geq 90\%$, as the femtocells use the whole resource blocks (i.e., $\rho_{_F} = 100\%$) for transmission, the largest D2D distance d_{D2D} is 10 (m) and 5 (m) for Scenario II and Scenario III, respectively.

2) For a given D2D distance d_{D2D}, femtocells in Scenario II can use more resource block than femtocells in Scenario III. In the case with $d_{D2D} = 15$ (m), femtocells in Scenario II can use 150% more resource blocks than femtocells in Scenario III, under the link reliability requirement $P_{rel} \geq 90\%$.

6.3.3 Summary

Figures 6.3, 6.4 and 6.5 can determine the largest permeable femtocell resource block usage ratio, the maximum allowable D2D distance and the optimum system throughput, if the service quality of all users must be guaranteed. For Scenario II, with the link reliability requirement $P_{rel} \geq 90\%$, the largest femtocell resource block usage ratio should be 0.7 according to Fig. 6.3. Hence, the total system throughput is 67.34 Mbps based on Fig. 6.4. Consequently, the D2D distance can not exceed 14 meters for the reliable proximity communications from Fig. 6.5.

Chapter 7

Conclusions

7.1 Dissertation Summary

In this dissertation, we have investigated the interference management issues and proposed the distributed interference control for heterogeneous wireless networks, including the OFDMA-based femtocell system, the MTC femtocell network, and the D2D femtocell network. In the OFDMA-based femtocell systems, we proposed the location-aware capability combined with our switched-beam directional antenna to improve the spectrum efficiency. In addition, we proposed the stable subchannel allocation scheme to achieve the tradeoff between the system capacity, users' fairness, and head of line (HOL) delay for the OFDMA femtocell systems. In the MTC femtocell networks, the proposed group-based time control method was able to control the RAN and CN congestion problems, and improved the service delay for MTC devices. In the heterogeneous Macro/Femto/D2D networks, the network-assisted power control method was proposed to enhance the system capacity and guarantee the service quality for all users. This dissertation includes the following research topics, and the contributions from this research are listed as follows.

1. Capacity evaluation for OFDMA femtocells by location awareness and directional antennas:

(a) We provided a useful principle for femtocell network planning to select the appropriate spectrum allocation scheme and access method to improve spectrum efficiency.

(b) We found that the location awareness capability is essential to the success of improving the femtocell spectrum efficiency because using the directional antenna is not enough to guarantee the link reliability of all indoor and outdoor users.

(c) The impacts of spectrum allocation, access method, femtocell density, and directional antenna on link reliability and spectrum efficiency of OFDMA femtocells are investigated, and has some important observations. For example, we found that the shared spectrum scheme may not always have better spectrum efficiency than the exclusive spectrum scheme under the link reliability requirement.

2. Subchannel allocation for multi-beam OFDMA femtocells:

(a) We proposed the joint subchannel allocation and antenna pattern selection algorithm, by which femtocells can distributedly select the antenna patterns and allocate the subchannels for multiple users.

(b) We proposed the stable subchannel allocation scheme to achieve a better tradeoff among the femtocell capacity, the users' fairness, and the HOL delay.

3. Overload control for machine type communications (MTC) femtocell networks:

(a) We provided an analyzable model of the group-based time control mechanism for MTC femtocell network planning to arrange the suitable macro group and femto group sizes to avoid the network congestion and achieve the optimal message delay.

(b) We found that the adaptive joint access probability adjustment and group rearrangement method was helpful for networks to mitigate the overload and reduce the message delay of devices.

(c) The impacts of arrival rate and group size on the overload probability, successful transmission probability, and the message delay of MTC femtocells were investigated, and had some important observations. For example, we found that the group size and arrival rate can significantly affect the message delay in the heavy CN overload, while in the light CN overload, the improvement of the arrival rate is minor for message delay.

4. Intelligent resource management for device-to-device (D2D) femtocell networks:

   (a) We provided a practical principle for the Macro/Femto/D2D network planning to determine the suitable D2D distance to enter the D2D mode, and select the optimal resource utility rate of femtocells to improve the system throughput with the link reliability requirement.

   (b) We found that the proposed intelligent resource management mechanism was essential to the success of improving the total system throughput because the mechanism could effectively avoid the link reliability degradation of macrocell and femtocell systems.

   (c) The impacts of the joint resource block selection and power adjustment method, femtocell resource block usage ratio, and D2D distance on link reliability and system throughput of heterogeneous Macro/Femto/D2D network were investigated, and had some important observations. For example, we found that the full utility of resource blocks and maximum transmission power scheme does not significantly improve the link reliability, and further, the scheme degrades the link reliability of macrocells below the link reliability requirement.

In the following, we summarize the results from the above contributions.

7.1.1 Capacity Evaluation for OFDMA Femtocells by Location Awareness and Directional Antennas

In this part, we evaluated the throughput of the OFDMA femtocell system with the directional antenna by applying three techniques to reduce the interference between macrocells and femtocells. Firstly, the low-cost four-sector switched-beam antenna is employed to mitigate the interference because of the narrow-beam pattern. Secondly, the partial usage of subcarriers approach can ensure the link reliability of all users by adjusting the number of OFDMA subcarriers used by a femtocell. Thirdly, the location awareness is applied to the femtocell systems for improving spectrum efficiency. Combining these elements, a location-aware femtocell can achieve higher spectrum efficiency than the conventional femtocells using the directional antennas, under the link reliability requirement. In summary, the design principles provided in this part can help decide the suitable spectrum allocation and access method for the femtocells.

7.1.2 Subchannel Allocation for Multi-beam OFDMA Femtocells

In this part, we investigated the joint subchannel allocation and antenna pattern selection in the OFDMA-based femtocell systems with the switched multi-beam directional antenna in terms of throughput, fairness, and HOL delay performance. We proposed the stable subchannel allocation scheme to achieve a better tradeoff among the femtocell throughput, the fairness, and the HOL delay, by limiting the maximum allowable number of subchannels used by one user. In addition, adopting the switched multi-beam directional antenna in the femtocell systems can improve the overall throughput. We summarized the results in Table 4.2. It is shown that the stable subchannel allocation scheme with the switched multi-beam antenna can achieve better femtocell throughput and guarantee the fairness and HOL delay compared to the existing methods.

7.1.3 Overload Control for Machine Type Communications (MTC) Femtocell Networks

In this part, we proposed the group-based time control mechanism to improve the RAN overload, CN overload, and message delay of MTC femtocell networks. We categorized all the MTC devices into macro groups and femto groups, and assumed that the MTC devices in a femtocell are grouped into the same femto group to reduce the total signaling overhead. By grouping, the MTC server can limit the maximum traffic pumped into the CN to avoid the overload. With the time control of groups, the total MTC traffic can be spread over the time, and the message delay can be controlled well if the group sizes are arranged carefully. Therefore, we analyzed the overload probability and message delay of the group-based time control mechanism to achieve the tradeoff between the group size and message delay. Moreover, we developed the adaptive joint access probability adjustment and group rearrangement method to rapidly and repeatedly rearrange the suitable group size of MTC devices to mitigate the CN overload and perform the shortest message delay.

7.1.4 Intelligent Resource Management for Device-to-Device (D2D) Femtocell Networks

In this part, we proposed the network-assisted device-controlled resource management mechanism to improve the system throughput and guarantee the service quality of all users for the heterogeneous Macro/Femto/D2D systems. The complicated three-tier interference can be reduced by applying three techniques. First, the MIT (maximum interference tolerance) information of each resource block from macrocell and femtocell base stations could help the D2D pair limit the maximum allowable transmission power to avoid the harmful interference to macrocell and femtocell systems. Second, the minimum transmission power criterion of reliable link measured by the D2D pair could be employed to judge whether the resource block can be selected for the D2D communications. A resource block can provide reliable D2D communications without the harmful interference to macrocell and

femtocell systems if the maximum allowable transmission power is higher than the minimum transmission power criterion. Third, the partial usage of resource blocks could ensure the link reliability of all users by adjusting the utility rate of resource blocks for the OFDMA femtocells. Combining these elements, the heterogeneous Macro/Femto/D2D network achieved higher system throughput than the conventional Macro/Femto network, under the link reliability requirement.

7.2 Suggestions for Future Research

Possible interesting research topics that can be extended from this dissertation are listed as follows:

- For the OFDMA femtocell systems
    1. Design a low-complexity power allocation method to reduce the two-tier interference.
    2. Design the algorithm to combine the power control with the switched-beam directional antenna.
- For the MTC femtocell systems
    1. Develop an adaptive group-based time control method to achieve the fairness according to the network overload situations.
    2. Analyze the overhaed of the control signaling.
- For the D2D femtocell systems
    1. To investigate the various spectrum allocation schemes for proximity communications.
    2. To investigate the impacts of multiple D2D pairs.

Bibliography

[1] H. Claussen, L. T. W. Ho, and L. G. Samuel, "An overview of the femtocell concept," *Bell Labs Technical Journal*, vol. 13, no. 1, pp. 221–246, 2008.

[2] V. Chandrasekhar and J. G. Andrews, "Femtocell networks: A survey," *IEEE Communications Magazine*, vol. 46, no. 9, pp. 59–67, Sep. 2008.

[3] S.-P. Yeh, S. Talwar, S.-C. Lee, and H. Kim, "WiMAX femtocells: A perspective on network architecture, capacity, and coverage," *IEEE Communications Magazine*, vol. 46, no. 10, pp. 58–65, Oct. 2008.

[4] D. López-Pérez, A. Valcarce, G. de la Roche, and J. Zhang, "OFDMA femtocells: A roadmap on interference avoidance," *IEEE Communications Magazine*, vol. 47, no. 9, pp. 41–48, Sep. 2009.

[5] 3GPP, "Service requirements for machine-type communications (MTC); stage 1," 3GPP, Tech. Rep. TS 22.368 V10.2.0, Sep. 2010.

[6] K.-R. Jung, A. Park, and S. Lee, "Machine-type-communication (MTC) device grouping algorithm for congestion avoidance of MTC oriented LTE network," in *Security-Enriched Urban Computing and Smart Grid*, ser. Communications in Computer and Information Science, T.-h. Kim, A. Stoica, and R.-S. Chang, Eds. Springer Berlin Heidelberg, vol. 78, pp. 167–178, 2010.

[7] 3GPP, "Study on RAN improvements for machine-type communications," 3GPP, Tech. Rep. TR 37.868 V0.6.3, Oct. 2010.

[8] ——, "Feasibility study for proximity services (prose)," 3GPP, Tech. Rep. TR 22.803 V0.2.0, Feb. 2012.

[9] R. Y. Kim, J. S. Kwak, and K. Etemad, "WiMAX femtocell: Requirements, challenges, and solutions," *IEEE Communications Magazine*, vol. 47, no. 9, pp. 84–91, Sep. 2009.

[10] L.-C. Wang and C.-J. Yeh, "Adaptive joint subchannel and power allocation for multi-user MIMO-OFDM systems," in *Proc. IEEE International Symposium on Personal, Indoor and Mobile Radio Communications (PIMRC)*, pp. 1–5, Sep. 2008.

[11] D. Gale and L. S. Shapley, "College admissions and the stability of marriage," *The American Mathematical Monthly*, vol. 69, no. 1, pp. 9–15, Jan. 1962.

[12] R. A. Brualdi, *Introductory Combinatorics*. Prentice Hall, 2009.

[13] 3GPP, "System improvements for machine-type communications," 3GPP, Tech. Rep. TR 23.888 V1.0.0, Jul. 2010.

[14] V. Chandrasekhar, J. G. Andrews, T. Muharemovic, Z. Shen, and A. Gatherer, "Power control in two-tier femtocell networks," *IEEE Transactions on Wireless Communications*, vol. 8, no. 8, pp. 4316–4328, Aug. 2009.

[15] G. de la Roche, A. Valcarce, D. López-Pérez, and J. Zhang, "Access control mechanisms for femtocells," *IEEE Communications Magazine*, vol. 48, no. 1, pp. 33–39, Jan. 2010.

[16] P. Xia, V. Chandrasekhar, and J. G. Andrews, "Open vs. closed access femtocell in the uplink," *IEEE Transactions on Wireless Communications*, vol. 9, no. 12, pp. 3798–3809, Dec. 2010.

[17] H. Zeng, C. Zhu, and W.-P. Chen, "System performance of self-organizing network algorithm in WiMAX femtocells," in *Proc. International Wireless Internet Conference (WICON)*, Nov. 2008.

[18] V. Chandrasekhar and J. G. Andrews, "Spectrum allocation in tiered cellular networks," *IEEE Transactions on Communications*, vol. 57, no. 10, pp. 3059–3068, Oct. 2009.

[19] C. Lee, J.-H. Huang, and L.-C. Wang, "Distributed channel selection principles for femtocells with two-tier interference," in *Proc. IEEE Vehicular Technology Conference (VTC-Spring)*, pp. 1–5, May 2010.

[20] C.-H. Ko and H.-Y. Wei, "On-demand resource-sharing mechanism design in two-tier ofdma femtocell networks," *IEEE Transactions on Vehicular Technology*, vol. 60, no. 3, pp. 1059–1071, Mar. 2011.

[21] S.-Y. Lien, C.-C. Tseng, K.-C. Chen, and C.-W. Su, "Cognitive radio resource management for QoS guarantees in autonomous femtocell networks," in *Proc. IEEE International Conference on Communications (ICC)*, pp. 1–6, May 2010.

[22] S.-Y. Lien, Y.-Y. Lin, and K.-C. Chen, "Cognitive and game-theoretical radio resource management for autonomous femtocells with QoS guarantees," *IEEE Transactions on Wireless Communications*, vol. 10, no. 7, pp. 2196 –2206, Jul. 2011.

[23] V. Chandrasekhar and J. G. Andrews, "Uplink capacity and interference avoidance for two-tier femtocell networks," *IEEE Transactions on Wireless Communications*, vol. 8, no. 7, pp. 3498–3509, Jul. 2009.

[24] H. Claussen, F. Pivit, and L. T. W. Ho, "Self-optimization of femtocell coverage to minimize the increase in core network mobility signalling," *Bell Labs Technical Journal*, vol. 14, no. 2, pp. 155–184, 2009.

[25] S.-G. Josep and W. H. Chin, "Performance of an LTE femtocell base station employing uplink antenna selection," in *Proc. Wireless Advanced (WiAd)*, pp. 224 –229, Jun. 2011.

[26] N.-D. Dào, Y. Sun, and W. H. Chin, "Receive antenna selection techniques for femtocell uplink interference mitigation," in *Proc. IEEE International Sym-*

posium on Personal, Indoor and Mobile Radio Communications Workshops (PIMRC Workshops), pp. 180 –184, Sep. 2010.

[27] Y. Jeong, H. Kim, B.-S. Kim, and H. Choo, "Avoidance of co-channel interference using switched parasitic array antenna in femtocell networks," in *Proc. International Conference on Computational Science and Its Applications (ICCSA)*, ser. Lecture Notes in Computer Science. Springer Berlin Heidelberg, vol. 6018, pp. 158–167, 2010.

[28] A.-H. Tsai, J.-H. Huang, L.-C. Wang, and R.-B. Hwang, "High capacity femtocells with directional antennas," in *Proc. IEEE Wireless Communications and Networking Conference (WCNC)*, pp. 1–6, Apr. 2010.

[29] F. Cao and Z. Fan, "Power loading and resource allocation for femtocells," in *Proc. IEEE Vehicular Technology Conference (VTC-Spring)*, pp. 1–5, May 2011.

[30] J. Zhang, Z. Zhang, K. Wu, and A. Huang, "Optimal distributed subchannel, rate and power allocation algorithm in OFDM-based two-tier femtocell networks," in *Proc. IEEE Vehicular Technology Conference (VTC-Spring)*, pp. 1–5, May 2010.

[31] D.-C. Oh, H.-C. Lee, and Y.-H. Lee, "Cognitive radio based femtocell resource allocation," in *Proc. International Conference on Information and Communication Technology Convergence (ICTC)*, pp. 274–279, Nov. 2010.

[32] K. Sundaresan and S. Rangarajan, "Efficient resource management in OFDMA femto cells," in *Proc. ACM International Symposium on Mobile Ad Hoc Networking and Computing*, ser. MobiHoc'09, pp. 33–42, May 2009.

[33] R. K. Saha and P. Saengudomlert, "Novel resource scheduling for spectral efficiency in LTE-advanced systems with macrocells and femtocells," in *Proc. International Conference on Electrical Engineering/Electronics, Com-*

puter, Telecommunications and Information Technology (ECTI-CON), pp. 340–343, May 2011.

[34] M. C. Ertürk, H. Aki, İsmail Güvenc, and H. Arslan, "Fair and QoS-oriented spectrum splitting in macrocell-femtocell networks," in *Proc. IEEE Global Telecommunications Conference (Globecom)*, pp. 1–6, Dec. 2010.

[35] K. Lee, O. Jo, and D.-H. Cho, "Cooperative resource allocation for guaranteeing intercell fairness in femtocell networks," *IEEE Communications Letters*, vol. 15, no. 2, pp. 214–216, Feb. 2011.

[36] G. Wang, X. Zhong, S. Mei, and J. Wang, "An adaptive medium access control mechanism for cellular based machine to machine (M2M) communication," in *Proc. 2010 IEEE International Conference on Wireless Information Technology and Systems (ICWITS)*, pp. 1–4, Sep. 2010.

[37] D. Niyato, L. Xiao, and P. Wang, "Machine-to-machine communications for home energy management system in smart grid," *IEEE Communications Magazine*, vol. 49, no. 4, pp. 53–59, Apr. 2011.

[38] S.-Y. Lien and K.-C. Chen, "Massive access management for QoS guarantees in 3GPP machine-to-machine communications," *IEEE Communications Letters*, vol. 15, no. 3, pp. 311–313, Mar. 2011.

[39] S.-Y. Lien, K.-C. Chen, and Y. Lin, "Toward ubiquitous massive accesses in 3GPP machine-to-machine communications," *IEEE Communications Magazine*, vol. 49, no. 4, pp. 66–74, Apr. 2011.

[40] K. Doppler, M. P. Rinne, P. Jänis, C. Ribeiro, and K. Hugl, "Device-to-device communications; functional prospects for lte-advanced networks," in *Proc. IEEE International Conference on Communications Workshops (ICC Workshops)*, pp. 1–6, Jun. 2009.

[41] K. Doppler, M. Rinne, C. Wijting, C. B. Ribeiro, and K. Hugl, "Device-to-device communication as an underlay to LTE-Advanced networks," *IEEE Communications Magazine*, vol. 47, no. 12, pp. 42–49, Dec. 2009.

[42] M. S. Corson, R. Laroia, J. Li, V. Park, T. Richardson, and G. Tsirtsis, "Toward proximity-aware internetworking," *IEEE Wireless Communications*, vol. 17, no. 6, pp. 26–33, DEC. 2010.

[43] F. Baccelli, N. Khude, R. Laroia, J. Li, T. Richardson, S. Shakkottai, S. Tavildar, and X. Wu, "On the design of device-to-device autonomous discovery," in *Proc. Fourth International Conference on Communication Systems and Networks (COMSNETS)*, pp. 1–9, 2012.

[44] G. Fodor, E. Dahlman, G. Mildh, S. Parkvall, N. Reider, G. Miklós, and Z. Turányi, "Design aspects of network assisted device-to-device communications," *IEEE Communications Magazine*, vol. 50, no. 3, pp. 107–177, Mar. 2012.

[45] K. Doppler, C. B. Ribeiro, and J. Kneckt, "Advances in D2D communications: Energy efficient service and device discovery radio," in *Proc. International Conference on Wireless Communication, Vehicular Technology, Information Theory and Aerospace Electronic Systems Technology (Wireless VITAE)*, pp. 1–6, 2011.

[46] J. Lee, J. Gu, S. J. Bae, and M. Y. Chung, "A session setup mechanism based on selective scanning for device-to-device communication in cellular networks," in *Proc. Asia-Pacific Conference on Communications (APCC)*, pp. 677–681, 2011.

[47] C.-H. Yu, O. Tirkkonen, K. Doppler, and C. Ribeiro, "Power optimization of device-to-device communication underlaying cellular communication," in *Proc. IEEE International Conference on Communications (ICC)*, pp. 1–5, 2009.

[48] K. Doppler, C.-H. Yu, C. B. Ribeiro, and P. Jänis, "Mode selection for device-to-device communication underlaying an LTE-Advanced network," in *Proc. IEEE Wireless Communications and Networking Conference (WCNC)*, pp. 1–6, 2010.

[49] C.-H. Yu, K. Doppler, C. B. Ribeiro, and O. Tirkkonen, "Resource sharing optimization for device-to-device communication underlaying cellular networks," *IEEE Transactions on Wireless Communications*, vol. 10, no. 8, pp. 2752–2763, Aug. 2011.

[50] M. Zulhasnine, C. Huang, and A. Srinivasan, "Efficient resource allocation for device-to-device communication underlaying LTE network," in *Proc. International Conference on Wireless and Mobile Computing, Networking and Communications (WiMob)*, pp. 368–375, 2010.

[51] B. Wang, L. Chen, X. Chen, X. Zhang, and D. Yang, "Resource allocation optimization for device-to-device communication underlaying cellular networks," in *Proc. IEEE Vehicular Technology Conference (VTC-Spring)*, pp. 1–6, 2011.

[52] H. S. Chae, J. Gu, B.-G. Choi, and M. Y. Chung, "Radio resource allocation scheme for device-to-device communication in cellular networks using fractional frequency reuse," in *Proc. Asia-Pacific Conference on Communications (APCC)*, pp. 58–62, 2011.

[53] R. Srinivasan and S. Hamiti, "IEEE 802.16m system description document (SDD)," IEEE, Tech. Rep. 802.16m-09/0034r2, Sep. 2009.

[54] V. Erceg, L. Schumacher, P. Kyritsi, A. Molisch, D. S. Baum, A. Y. Gorokhov, C. Oestges, C. Lanzl, V. J. Rhodes, J. Medbo, D. Michelson, M. Webster, E. Jacobsen, D. Cheung, Q. Li, C. Prettie, M. Ho, S. Howard, B. Bjerke, K. Yu, L. Jengx, A. Jagannatham, N. Tal, S. Valle, and A. Poloni, "Indoor MIMO WLAN channel models," IEEE, Tech. Rep. 802.11-03/871r1, Nov. 2003.

[55] V. Erceg, K. V. S. Hari, M. S. Smith, D. S. Baum, K. P. Sheikh, C. Tappenden, J. M. Costa, C. Bushue, A. Sarajedini, R. Schwartz, D. Branlund, T. Kaitz,

and D. Trinkwon, "Channel models for fixed wireless applications," IEEE, Tech. Rep. 802.16.3c-01/29r4, Jul. 2001.

[56] R. Yaniv, D. Stopler, T. Kaitz, and K. Blum, "CINR measurements using the EESM method," IEEE, Tech. Rep. C802.16e-05/141, Mar. 2005.

[57] J. G. Andrews, A. Ghosh, and R. Muhamed, *Fundamentals of WiMAX*. Englewood Cliffs, NJ: Prentice-Hall, 2007.

[58] R. Srinivasan, J. Zhuang, L. Jalloul, R. Novak, and J. Park, "IEEE 802.16m evaluation methodology document (EMD)," IEEE, Tech. Rep. 802.16m-08/004r4, Nov. 2008.

[59] WiMAX Forum, "WiMAX system evaluation methodology," *Version 2.1*, Jul. 2008.

[60] M. A. Imran et al., "Energy efficiency analysis of the reference systems, areas of improvements and target breakdown," EARTH Project, Tech. Rep. INFSO-ICT-247733 EARTH, Deliverable D2.3, Nov. 2010.

[61] 3GPP, "Further advancements for E-UTRA physical layer aspects," 3GPP, Tech. Rep. TR 36.814 V9.0.0, Mar. 2010.

[62] R. K. Jain, D.-M. W. Chiu, and W. R. Hawe, "A quantitative measure of fairness and discrimination for resource allocation in shared computer systems," Digital Equipment Corporation, Tech. Rep. DEC-TR-301, Sep. 1984.

[63] L.-C. Wang and M.-C. Chen, "Comparisons of link-adaptation-based scheduling algorithms for the WCDMA system with high-speed downlink packet access," *Canadian Journal of Electrical and Computer Engineering*, vol. 29, no. 1/2, pp. 109–116, Jan./Apr. 2004.

[64] 3GPP, "Physical channels and modulation," 3GPP, Tech. Rep. TS 36.211 V8.6.0, Mar. 2009.

[65] Ericsson, "E-UTRA random access," 3GPP, Tech. Rep. R1-060584, Feb. 2006.

[66] 3GPP, “Selection procedures for the choice of radio transmission technologies of the UMTS,” 3GPP, Tech. Rep. TR 30.03U V3.2.0, Mar. 1998.

Vita

Ang-Hsun Tsai (S'09) received the B.S. degree in electrical engineering from the Chung Cheng Institute of Technology, National Defense University, Taoyuan, Taiwan, in 1998, the M.S. degree in electro-optical engineering from the National Sun Yet-sen University, Kaohsiung, Taiwan, in 2005, and the Ph.D degree in communication engineering from the National Chiao Tung University, Hsinchu, Taiwan, in 2012, respectively.

In 2005, Mr. Tsai was elected an Honorary Member of the Phi Tau Phi Scholastic Honor Society of the Republic of China by National Sun Yet-Sen University. His current research interests include femtocell networks, heterogeneous machine-type communications networks, and radio resource management.

Publication List

Journal Paper

1. Ang-Hsun Tsai, Li-Chun Wang, Jane-Hwa Huang, and Ruey-Bing Hwang, "High-Capacity OFDMA Femtocells by Directional Antennas and Location Awareness," *IEEE Systems Journal*, vol. 6, no. 2, pp.329-340, June 2012.

2. Ang-Hsun Tsai, Li-Chun Wang, and Jane-Hwa Huang, "Stable Subchannel Allocation for OFDMA Femtocells with Switched Multi-beam Directional Antennas," to be submitted.

3. Ang-Hsun Tsai, Li-Chun Wang, Jane-Hwa Huang, and Tzu-Ming Lin, "Overload Control for Machine Type Communications with Femtocells," to be submitted.

Conference Paper

1. Ang-Hsun Tsai, Li-Chun Wang, Jane-Hwa Huang, and Tzu-Ming Lin, "Intelligent Resource Management for Device-to-Device (D2D) Communications in Heterogeneous Networks," in *Proc. International Symposium on Wireless Personal Multimedia Communications (WPMC)*, Sep., 2012.

2. Ang-Hsun Tsai, Li-Chun Wang, Jane-Hwa Huang, and Tzu-Ming Lin, "Overload Control for Machine Type Communications with Femtocells," in *Proc. IEEE Vehicular Technology Conference (VTC-Fall)*, Sep., 2012.

3. Ang-Hsun Tsai, Li-Chun Wang, Jane-Hwa Huang, and Ruey-Bing Hwang, "Stable Subchannel Allocation for OFDMA Femtocells with Switched Multi-beam Directional Antennas," in *Proc. IEEE Global Telecommunications Conference (Globecom)*, Dec., 2011.

4. Ang-Hsun Tsai, Li-Chun Wang, Jane-Hwa Huang, and Ruey-Bing Hwang, "Capacity Comparison for CSG and OSG OFDMA Femtocells," in *Proc. IEEE Globecom Workshop on Femtocell Networks (FEMnet)*, Dec., 2010.

5. Ang-Hsun Tsai, Li-Chun Wang, Jane-Hwa Huang, and Ruey-Bing Hwang, "High Capacity Femtocells with Directional Antennas," in *Proc. IEEE Wireless Communications and Networking Conference (WCNC)*, Apr., 2010.